Coordinated Control of Inter-area Oscillations using SMA and LMI

Anamitra Pal

Thesis submitted to the faculty of Virginia Polytechnic Institute & State University in partial fulfillment of the requirements for the degree of

Master of Science
In
Electrical Engineering

James S. Thorp, Committee Chair
Virgilio A. Centeno
Robert P. Broadwater

February 17, 2012
Blacksburg, Virginia

Keywords: Inter-area Oscillations, Linear Matrix Inequality (LMI) Control, Polytopic Model, Selective Modal Analysis (SMA), Wide Area Measurements

Coordinated Control of Inter-area Oscillations using SMA and LMI

Anamitra Pal

(Abstract)

The traditional approach to damp inter-area oscillations is through the installation of Power System Stabilizers (PSSs) which provide damping control action through excitation control systems of the generating units. However, study of recent blackouts has shown that the control action provided by a PSS alone is not sufficient for damping oscillations in modern power systems which operate under stressed conditions. An integrated form of control using remote measurements to coordinate the different control elements present in the system is the need of the hour.

One way of implementing such a coordinated control is through the development of a Linear Matrix Inequality (LMI)-based polytopic model of the system that guarantees pole placement for a variety of operating conditions. The size of the polytopic formulation is an issue for application of LMIs to large systems. The use of Selective Modal Analysis (SMA) alleviates this problem by reducing the size of the system. The previous attempts have used a model containing all the δ and ω modes, with SMA being used to eliminate all the other states. In practical applications the resulting system was still found to be too large to use in a polytopic model. This thesis presents an algorithm to reduce the size of the system to the relevant modes of oscillations.

A 16 machine, 68 bus equivalent model of the New England-New York interconnected power system is used as the test case with DC lines and SVCs acting as the control. The algorithm is then applied to a 127-bus equivalent model of the WECC System. The use of ESDs as a form of control is also demonstrated. The results indicate that the proposed control successfully damps the relevant modes of oscillations without negatively damping the other modes. The control is then transferred to a more detailed 4000+ bus model of the WECC system to realize its performance on real-world systems.

To My Parents: Dipankar Pal and Lopamudra Pal

Acknowledgements

I wish to extend my sincerest gratitude to Dr. James S. Thorp for his help and guidance towards the work contained in this thesis. I have learnt a tremendous amount through the discussions that we have had together. This thesis would not have been what it is without him.

I am very grateful to the rest of the members of my committee namely, Dr. Virgilio Centeno and Dr. Robert P. Broadwater for their invaluable insights and constructive criticisms. I would also like to thank Dr. Jaime De La Ree Lopez and Dr. Arun G. Phadke for their precious inputs from time-to-time. I am also indebted to my fellow graduate students, Shravan Garlapati, Santhosh Sambamoorthy, Gerardo Sanchez, Noah Badayos, Kate Vance, Tong Wang and Peng Zhang for their helpful comments and support.

I am eternally grateful to my parents and my younger brother for their constant motivation and unwavering faith in me. Their love and encouragement has been critical for the successful completion of my degree.

Date: 02/17/2012 Anamitra Pal

Related Reports and Publications

1. Anamitra Pal, and James S. Thorp, "**Co-ordinated control of inter-area oscillations using SMA and LMI**", presented at the *IEEE PES Conference on Innovative Smart Grid Technologies (ISGT 2012),* 16-20 January, Washington D.C., USA.

2. Anamitra Pal, "**Damping low frequency oscillations in the WECC**," *Final Project Report, Public Interest Energy Research (PIER) Program, TRP-08-06*, prepared for California Energy Commission by Virginia Polytechnic Institute and State University, Blacksburg, Virginia, Nov. 2011.

3. Anamitra Pal, James S. Thorp, Santhosh Sambamoorthy, and V. A. Centeno, "**A Robust Control Technique for Damping Low-Frequency Oscillations in the WECC**," submitted to the *IEEE Transactions on Power Systems*.

Table of Contents

List of Figures

List of Tables

Chapter 1 – Introduction

Since its inception in the late 19th Century, the Electric Power Systems has been considered one of the greatest achievements of mankind. Its secure and reliable operation is a tribute to the electrical engineers of the utilities, universities and government organizations who work together to ensure that *when we turn on the switch, our world is enlightened*. This kind of dependability is possible only through continuous progress and in line with this concept; this thesis deliberates upon a small step that has been made in that direction.

The Electric Power System is a dynamic being. For its smooth and stable operation it has to be constantly monitored and its ailments have to be taken care of as promptly as possible. One of the oldest problems that the power system has been plagued with, and still continues to suffer from, is due to small oscillations at low frequencies, collectively termed *"Low Frequency Oscillations (LFOs)"*. These oscillations are primarily related to the small signal stability of the power system and are detrimental to the goals of maximum power transfer and power system security. LFOs are defined by how they are created or where they are located in the power system [1]. Traditionally, LFOs are of four types:

Local Plant Modes of Oscillation

Control Modes of Oscillation

Torsional Modes of Oscillation

Inter-area Modes of Oscillation

Local plant mode oscillation problems are the most commonly encountered among the above and are associated with units at a generating station oscillating with respect to each other or with other machines located in the same area. Such problems are usually caused by the action of the Automatic Voltage Regulators (AVRs) of generating units operating at high-output and feeding into weak-transmission networks. The problem is more pronounced in high-response excitation systems. The local plant oscillations typically have natural frequencies in the range of 1–2 Hz [2]. Their characteristics are well understood and adequate damping can be readily achieved by using supplementary control of excitation systems in the form of Power System Stabilizers (PSSs) [3].

Control mode oscillations are associated with the controls of generating units and other equipment. Poorly tuned controls of excitation systems, prime movers, Static VAR Compensators (SVCs), and HVDC converters are the usual causes of instability of the control modes. Torsional mode oscillations are associated with the turbine-generator rotational (mechanical) components. They have relatively higher frequencies, typically in the range of 10–46 Hz. There have been several instances of torsional mode

instability due to negative interactions within the controls, mainly the generating unit excitation and the prime mover controls. These oscillations can be successfully damped through proper tuning of torsional filters [2].

The most critical of the four LFOs and the primary topic for this thesis are the inter-area modes of oscillations. They are associated with machines in one part of the system oscillating against machines in other parts of the system. Inter-area modes occur when two or more groups of closely coupled machines are interconnected by weak tie-lines. The natural frequency of these oscillations is typically in the range of 0.1–0.8 Hz. The characteristics of inter-area modes of oscillation are complex and in some respects significantly different from the characteristics of the other modes of oscillations [2]. The primary cause for these oscillations is presence of high-gain generator exciters and/or heavy power transfer across weak tie-lines. When present in a power system, this type of oscillation limits the amount of power transferred through the tie-lines between the regions containing the groups of coherent machines [1], [4].

Over the past few decades, attention has been focused on designing controllers to damp the inter-area modes of oscillations. The traditional method of damping these oscillations is through the use of PSSs that control the excitation of generating units. However local PSSs alone cannot guarantee adequate performance of the generator when the operating point changes. In rapidly growing systems, such as the Chinese power system, the limitation of PSSs that are designed for specific modes is more apparent. An inappropriate coordination among the local controllers has caused serious problems [5-9]. The need to frequently retune PSSs has prompted investigation of techniques that can adapt to changing system conditions [10-11].

With the growing implementation of PMUs across the power grids, it is now possible to observe and analyze system wide dynamic phenomena in real-time. PMUs capture dynamic data of power systems through synchronized measurements enabled by GPS satellites. A controller based on such remote signals can enhance damping of inter-area oscillations and improve overall dynamic performance [12]. In recent times, use of HVDC lines, FACTS devices and Energy Storage Devices (ESDs) as potential forms of control have also been investigated. It is therefore desirable to develop an integrated form of control that uses wide-area measurements to coordinate PSSs, DC lines, FACTS devices, and ESDs for stabilizing inter-area oscillations.

This thesis focuses on developing a robust Linear Matrix Inequality (LMI)-based control using PMU measurements and polytopic systems to provide damping to LFOs in general and inter-area modes of oscillations in particular. DC lines, SVCs and ESDs have been used as controls for the systems. An algorithm based on Selective Modal Analysis (SMA) is developed to reduce the size of the systems to the relevant modes of oscillations. It is tested on a reduced-order model of the New England–New York interconnected power system consisting of 16 machines and 68 buses. DC Lines and SVCs are used as the controls for this system. The proposed technique is then applied to a larger and more realistic,

reduced-order model of the WECC system comprising of 29 machines and 127 buses. The control in this system is initially provided through two HVDC lines and one SVC which are already present in the system. The advantage of using ESDs as a form of control is also deliberated upon. The thesis concludes by extending this methodology to the full-order system.

1.1 Inter-area Oscillations

The inter-area modes of oscillations are a system-wide phenomenon observed over a large part of the network. They are associated with weak transmission links and heavy power transfers. They generally involve two coherent groups of generators swinging against each other at frequencies of 0.8 Hz or less. Because of their global nature, they often involve more than one utility and often require the cooperation of all for the most effective and economical solution. The variation in tie-line power corresponding to an inter-area mode of oscillations can be large as shown in Fig. 1.1

Fig. 1.1: Typical example of an Inter-area Oscillation

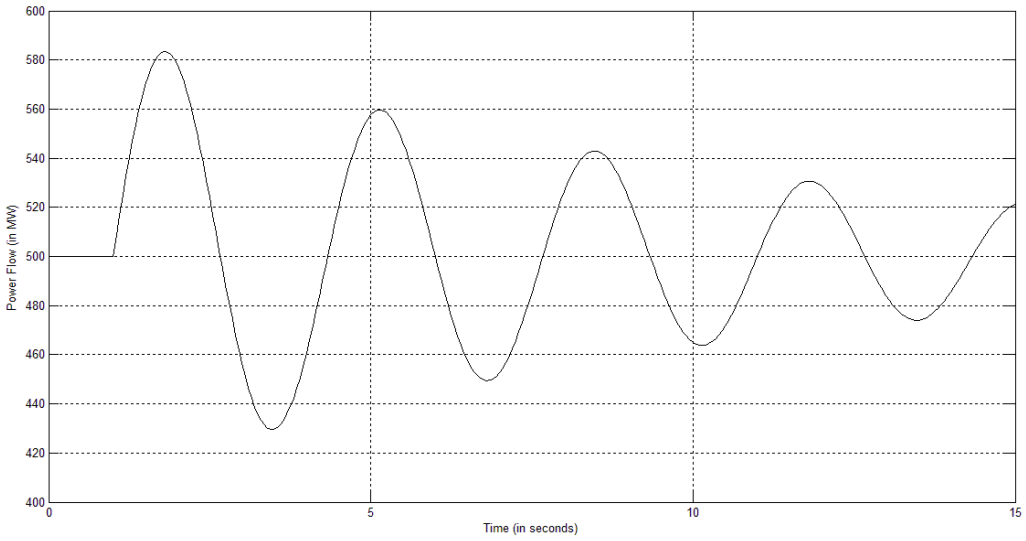

This complex phenomenon involves many components of the power system and has a highly non-linear, dynamic behavior. The damping characteristic of the inter-area modes are dictated by the tie-line strengths, the nature of the loads, the power flow through the interconnections as well as the interaction of the loads with the dynamics of the generators and their associated controls. Inter-area oscillations have led to many system separations and wide-scale blackouts. Table 1.1 summarizes some of the note-worthy incidents attributed to them.

Table 1.1: Blackouts attributed to Oscillations [6-9], [13-14]

Place	Year(s)
Finland – Sweden – Norway – Denmark	1960s
Detroit Edison (DE) – Ontario Hydro (OH) – Hydro Quebec (HQ)	1960s, 1985
Western Electric Coordinating Council (WECC)	1964, 1996
Saskatchewan – Manitoba Hydro – Western Ontario	1966
Mid-continent Area Power Pool (MAPP)	1971, 1972
Italy – Yugoslavia – Austria	1971 – 1974
South-East Australia	1975
Southern Brazil	1975 – 1980, 1984
Scotland – England	1978
Western Australia	1982, 1983
Ghana – Ivory Coast	1985
Taiwan	1985
Hong-Kong Electric Company	1991
China	2003, 2008

Large interconnected systems usually have two distinct forms of inter-area oscillations [1]:

a) A very low frequency mode involving all the generators present in the system. The system is essentially split into two halves with generators in one half swinging against those in the other half. The frequency of this mode of oscillation is in the order of 0.1–0.3 Hz.
b) A relatively higher frequency mode involving sub-groups of generators swinging against one another. The frequency of these oscillations is typically in the range of 0.4–0.8 Hz.

Factors affecting inter-area modes of oscillations: The characteristics of inter-area modes of oscillation are very complex and in some respects significantly different from the characteristics of the other modes of oscillations. Load characteristics, in particular, have a major effect on the stability of the inter-area modes of oscillations. The manner in which the excitation systems affect the inter-area oscillations depends on the types and locations of the exciters, and on the characteristics of the load [15].

Speed-governing systems normally do not have a very significant effect on the inter-area oscillations. However, if they are not properly tuned, they may decrease damping of the oscillations. In extreme situations, in the absence of any other convenient means of increasing the damping, adjustment or blocking of the governors provides relief [16].

A mode of oscillation in one part of the system may also interact with a mode of oscillation in a remote part due to mode coupling. This occurs when the frequencies of the two modes are nearly equal [17-18]. The root causes of these types of inter-area oscillations are the hardest to identify and typically need advanced forms of control.

1.2 Control Techniques

Oscillations are due to the natural modes of the system and therefore cannot be completely eliminated. However, their damping and frequency can be modified. As power systems evolve, the frequency and damping of existing modes change and new modes emerge. The main source of ‘‘negative’’ damping is the power system controls, primarily excitation system AVRs. This section talks about some of the traditional and modern control techniques that have been developed over the years to damp the LFOs in general and the inter-area modes in particular.

Traditional Controls: Power System Stabilizers (PSSs) are the most commonly used devices for enhancing the damping of the inter-area modes of oscillations. A PSS in combination with an AVR uses the auxiliary stabilizing signals for producing a damping torque component which controls the excitation system of the generating units. Commonly used signals for the PSS include changes in shaft speed, terminal frequency and output power. Fig. 1.2 illustrates a typical block diagram of an AVR with a PSS which uses speed deviation for producing the damping torque component [1].

A PSS provides supplemental damping to the oscillation of synchronous machine rotors through the generator excitation. The exciter and the generator usually exhibit frequency dependent phase and gain characteristics; therefore the PSS transfer function $G_{PSS}(s)$ has appropriate phase compensation circuits to compensate for the phase lag between the exciter input and the electrical torque output. In the ideal case, with the phase characteristic of $G_{PSS}(s)$ being an exact inverse of the exciter and generator phase characteristics to be compensated, the PSS would come up with a pure damping torque at all oscillating frequencies. Thus, once the oscillations are damped, the thermal limit of the tie-lines in the system may be approached.

Drawbacks of PSS Control: The supplementary control described previously performs well under normal situations. However, power system instabilities can arise in certain circumstances due to negative damping effects of the PSS on the rotor. The reason for this is that PSSs are tuned around a steady-state operating point. Their damping effect decreases considerably when small excursions occur around the

operating point. If bigger disturbances occur, a PSS may actually cause the generator under its control to lose synchronism in an attempt to control its excitation [19].

Fig. 1.2: Block Diagram representation of an AVR with PSS [1]

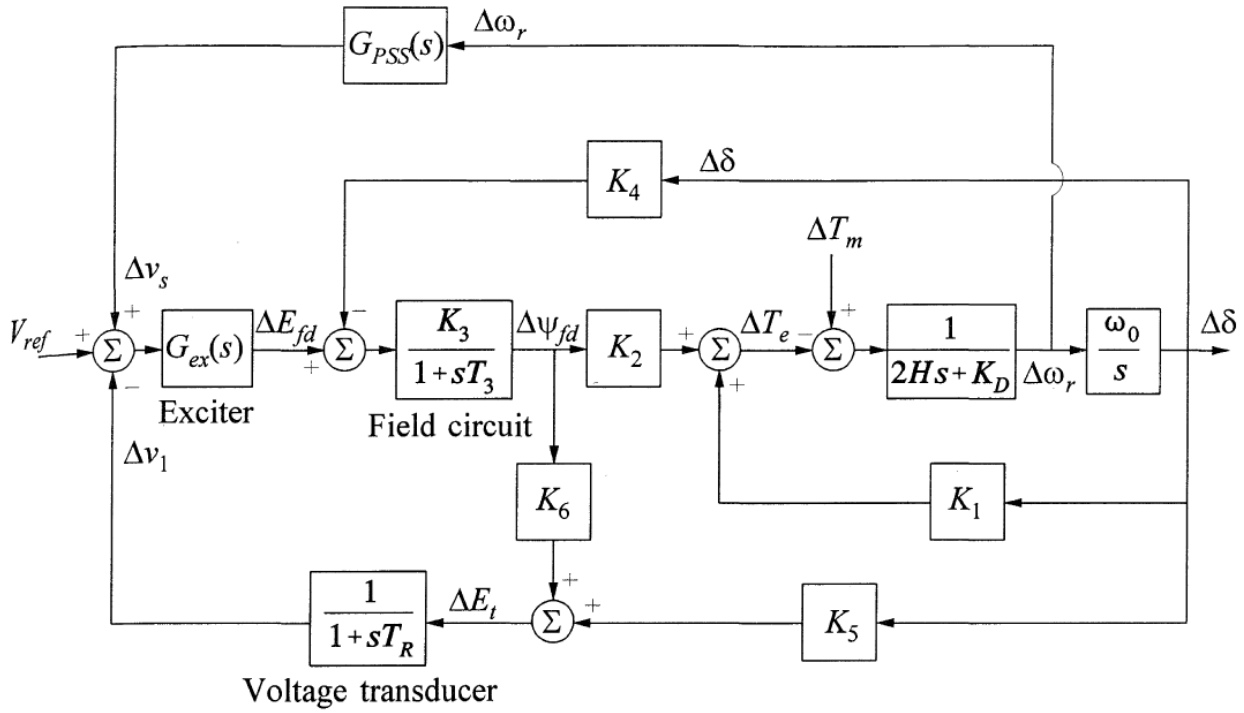

Moreover, a traditional PSS uses local measurements of power and frequency and is tuned to act on a single mode. Therefore, in its efforts to damp a local mode of oscillation, the PSS can negatively damp an inter-area mode of oscillation and vice-versa. It has also been observed that a PSS that is expected to damp oscillations over a broad range of frequencies is not able to sufficiently the critical low frequency modes that might be excited in the system. It therefore becomes obvious that the application of a PSS alone falls short in our goal of damping local and inter-area modes of oscillations over a broad range of operating points.

Modern Controls: The conflicting requirements for stability of local and inter-area modes of oscillations under both small signal and transient conditions have led to many different approaches for the control and tuning of PSSs. However, the most sophisticated digital PSSs [20] still use local measurements of power and frequency and are aimed at a single mode of oscillation. There have also been studies of providing remote measurements to a PSS in a coordinated multi input environment [21-22]. A new PSS using two signals, the first, to damp the local mode in the area and the second, global signal, to damp inter-area modes is proposed in [23]. The need to frequently retune PSSs has prompted investigation of techniques to adapt their operation to changing system conditions [10-11]. The methods investigated include state-space/frequency domain techniques [24-25], residue compensation [23], phase compensation/root locus

of a lead-lag controller [19], [26-27], de-sensitization of a robust controller [28], pole-placement for a PID-type controller [29], sparsity techniques for a lead-lag controller [30] and a strict linearization technique for a linear quadratic controller [31]. The diversity of these approaches can be accounted for by the difficulty of satisfying the conflicting design goals, and each method having its own advantages and disadvantages.

An alternate approach that has been followed for controlling LFOs has been the introduction of passive or active control elements other than PSSs into the power system. These devices include special modulation controls for HVDC-links, Energy Storage Devices (ESDs) and Static VAR Compensators (SVCs) installations in the system, as well as other FACTS devices such as Thyristor-Controlled Series Capacitors (TCSCs), Unified Power Controllers (UPCs) and Thyristor-Controlled Dynamic Brakes [1], [32-33]. Supplementary Damping Controllers (SDCs) for FACTS devices have been found to show great potential in damping inter-area oscillations [34]. It has also been proved that controlling the flow of HVDC lines can help in damping small signal oscillations, increase power transfer capability and improve transient stability of AC/DC hybrid systems [35-36]. Thus, the most ambitious approach for damping low frequency oscillations would be to coordinate PSSs, FACTS devices, and DC lines in stabilizing inter-area oscillations.

Conclusion: The long history of inter-area oscillations in power systems all over the world clearly identifies inadequate/negative damping as the primary factor leading to system separation and eventually blackouts. The amount of damping and the frequency of oscillation vary with system operating conditions. The operating range of a power system is usually very wide, requiring an oscillation damping control strategy that is effective over the whole range. To successfully develop such a control, it is necessary to have comprehensive modeling and analysis techniques of all the components that may interact to produce oscillations. In accordance with this realization, this thesis delves upon the idea of using Linear Matrix Inequalities (LMI) in conjunction with Wide Area Measurements and Selective Modal Analysis (SMA) to come up with a robust control that is effective over a wide range of system conditions.

1.3 Overview of Thesis

This thesis is composed of six chapters. Chapter 1 introduces the concept of Low Frequency Oscillations (LFOs) with special relevance to the inter-area modes of oscillations. It talks about the origin of these oscillations and the effects they have had on power systems worldwide. It goes on to summarize the various control techniques that have been formulated to damp these oscillations starting from the traditional concepts of PSSs to the modern techniques of integrated control. The chapter concludes by outlining the contents of each chapter.

Chapter 2 provides the mathematical basis of the control techniques that are explored in this thesis. It begins with a brief overview of the logic on which Linear Matrix Inequalities (LMIs) operate and its

advantages and disadvantages. Selective Modal Analysis (SMA) is then introduced as a possible method for overcoming the shortcomings of an LMI control. The chapter concludes by describing a small 4 machine – 2 area system to illustrate how the combination of LMI and SMA can be applied to power system problems.

Chapter 3 gives a detailed description of the algorithm that is proposed in this thesis. It starts off by summarizing the assumptions to be satisfied for the successful application of the technique developed herein. It then goes on to describe the steps of the algorithm and caps it off by applying it to a benchmark model of the New England-New York inter-connected power system. The results show that all the low-frequency inter-area modes of oscillations of this system are adequately damped along with most of the local modes. The fact that such a reduced version of the original system is capable of producing such good control is an indication of the robustness of the method developed herein.

Chapter 4 illustrates the results obtained on applying the proposed control on a reduced model of the WECC system. This system is more realistic in the sense that the controls used are actually present in the real world. It then goes on to propose the introduction of new controllers (ESDs) into the system to expand the domain of the proposed control and comes up with optimum locations for their placement. The control is found to be considerably improved through the addition of the three ESDs, thereby justifying their inclusion into the system. The fact that different types of controllers can be integrated together to develop the control is also a compliment to the method developed herein.

Chapter 5 demonstrates how the control developed in one software can be transferred onto another, thereby laying the foundation for making the technique work on larger and more complex systems. An equivalent system, similar to what it is in the real world, is created in PSLF to test the effectiveness of the control developed in Matlab. A hitherto untested contingency is applied on this system and a comparison is made between the time-domain plots obtained with control and those without it. The inter-area modes show considerable damping in their oscillations but the effect on the local modes is not found to be very prominent. Considering the fact that the system which is used to come up with the control is not the same on which it is applied, the decrease in the effectiveness of the control is justified. The inference that is drawn from this analysis is that if the Matlab and the PSLF models are made more compatible to each other, the control results can be made more alike. The proposed control is then applied to the full-order system. The results indicate that the proposed methodology was successful in increasing the damping of all the low frequency inter-area modes present in the system. The implication of this was that the control technique was sufficiently robust to damp oscillations in big systems without becoming computationally too complex.

Chapter 6 summarizes the thesis and suggests possible topics that can be explored in the future.

Chapter 2 – Mathematical Background

As described in the previous chapter, an optimum control for damping Low Frequency Oscillations (LFOs) in general and inter-area modes in particular, can be formulated by using wide area measurements to coordinate PSSs, ESDs, FACTS devices, and DC lines. One way of implementing such an integrated form of control is through the development of an LMI polytopic model of the system where time delays are modeled as uncertain parameters, unmeasured portion of the system are represented by un-modeled dynamics, and LMI techniques are used to design robust controllers [37-40]. The advantage of the polytopic approach being that the span of the model uncertainty is considered within the design itself.

An LMI polytopic model has been used to design PSSs for a single machine [37] and a nine bus, three-machine system [38]. Output feedback for a nine machine system was developed in [39]. A design with either full state feedback or output feedback is formulated through a specification of the closed loop pole locations. This has been used to design a controller for a multi-area load frequency control in [40]. A sequential conic programming approach to design PSSs in a model system is developed in [41]; the conic region being a special case of the general LMI region.

Although the LMI approach appears to give good results for small sized systems, its direct application to bigger systems has been limited due to its computational complexity [42]. The technique proposed in this thesis appears to alleviate this problem by reducing the size of the system to the relevant modes of oscillations. The size of the system is reduced using Selective Modal Analysis (SMA) [43-44]. While there exist a number of other techniques for forming reduced order models to study inter-area modes [45-46], SMA was chosen since it fit the LMI Matlab environment. This chapter provides the mathematical basis of these two techniques. It is to be noted here that in this thesis, LMI and SMA have been used as problem-solving tools; for a more detailed background of LMI and SMA, it is suggested to go through the following [47-51].

2.1 Linear Matrix Inequality (LMI)

LMI techniques have emerged as powerful design tools in the areas of control engineering, system identification and structural design. LMI techniques are very appealing to control engineers for the following reasons [52] –

a) Since efficient LMI solvers are readily available, they can be used to express a variety of design specifications and constraints

b) Once formulated in terms of LMIs, the problem can be solved exactly by efficient convex optimization algorithms; for example, when a control problem is solved as an LMI, then any solution to that problem is a global optimum
c) After a problem has been posed as an LMI, other constraints in the form of LMIs can be added with ease
d) Many problems having multiple constraints or objectives, which lack analytical solution in terms of matrix equations, comply with the LMI framework making it a desirable alternative to "classical" methods

LMI Techniques have been successfully used in the following applications [48]:

a) Specification and manipulation of uncertain dynamical systems (linear-time invariant, polytopic, parameter-dependent etc.)
b) Robustness analysis; various measures of robust stability and performance are implemented, including quadratic stability, techniques based on parameter-dependent Lyapunov functions, analysis and Popov analysis.
c) Multi-model/multi-objective state-feedback design
d) Synthesis of output-feedback H_∞ controllers via Riccati-based and LMI-based techniques, including mixed H_∞/H_2 synthesis with regional pole placement constraints
e) Loop-shaping design
f) Synthesis of robust gain-scheduled controllers for time-varying parameter-dependent systems

An LMI is any constraint of the form:

$$A(p) \coloneqq A_0 + p_1 A_1 + p_2 A_2 + \cdots + p_n A_n < 0 \tag{2.1}$$

Where, $p = p_1, p_2, \ldots p_n$ is an unknown vector comprising of the optimization variables; $A_0, A_1, \ldots A_n$ are known symmetric matrices and < 0 implies "negative definite", i.e. the largest eigenvalue of $A(p)$ is negative. The LMI constraint defined in (2.1) is a convex constraint on p as $A(q) < 0$ and $A(r) < 0$ will imply $A\left(\frac{q+r}{2}\right) < 0$. Moreover, a system of LMI constraints can be thought of as a single LMI problem whose block-diagonal matrix has the system matrices of those individual systems as its diagonal elements.

The pole-placement in LMI regions looks to evaluate the convex sub-sets D described by,

$$D = \{z \in C : L + Mz + M^T z' < 0\} \tag{2.2a}$$

Where M and $L = L^T$ are fixed, real matrices. The characteristic function of this region is given by,

$$f_D(z) \coloneqq L + Mz + M^T z' \tag{2.2b}$$

Reference [48] also provides the option of defining a region of one's choice so as to provide additional constraints on the optimization. Fig. 2.1 depicts a typical LMI region for Pole Placement consisting of a conic section and a vertical barrier. The shaded portion depicts the region where the eigenvalues should lie.

Fig. 2.1: LMI Region for Pole Placement; The Damping ratio of poles lying in the region enclosed by the solid lines is at-least $\cos\theta$

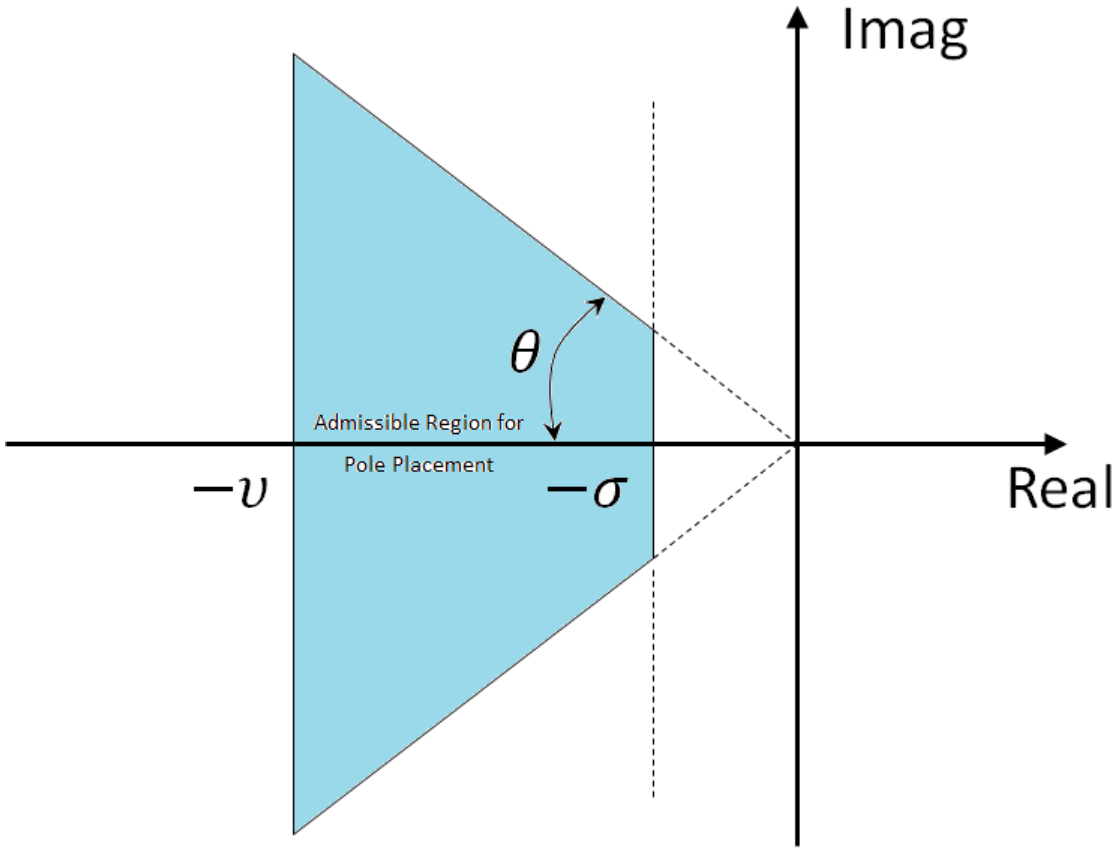

In this thesis, LMIs have been used for developing mixed H_∞/H_2 control design for polytopic systems with regional pole placement constraints. A polytopic system is one whose system matrix varies within a fixed polytope of matrices. The polytopic H_∞/H_2 formulation is posed with state space models of the form,

$$\begin{aligned} \dot{x} &= Ax + B_1\zeta + B_2u \\ z_\infty &= C_1x + D_{11}\zeta + D_{12}u \\ z_2 &= C_2x + D_{22}u \\ y &= C_yx + D_{y1}\zeta + D_{y2}u \end{aligned} \tag{2.3}$$

Where x is the state of the system, u is the control, ζ is a disturbance, z_∞ and z_2 are for the H_∞/H_2 optimizations and y is the output. The cases that would be used to test the robustness of the controller for a power system application such as tie-line outages, load changes, changes in line flows, etc., all have

their own version of the system denoted by (2.3). These systems are then the vertices of the polytope. The k^{th} such system denoted by S_k is of the form:

$$S_k = \begin{bmatrix} A_k & B_{k1} & B_{k2} \\ C_1 & D_{k11} & D_{k12} \\ C_{k2} & 0 & D_{k22} \\ C_{ky} & D_{ky1} & D_{ky2} \end{bmatrix} \tag{2.4}$$

The convex combination of the systems is given by,

$$S\{S_1, S_2, \dots S_k\} = \left\{ \sum_{i=1}^{k} \alpha_i S_i : \sum_i \alpha_i = 1, \alpha_i \geq 0 \right\} \tag{2.5}$$

The non-negative numbers $\alpha_1, \alpha_2, \dots, \alpha_k$ are called the polytopic coordinates of S. Many of the convex combinations in (2.5) have simple explanations. If S_1 is the base case and S_2 represents the outage of a tie-line then $\alpha S_1 + (1-\alpha)S_2$ can be thought of as continuously increasing the impedance of the tie-line until it is open. Figure 2.2 illustrates this concept with a simple example. The three terminals (P, Q and R) represent the base case (no contingency case), an outage of a tie-line and a 10% increase in the loads, whereas the edges represent the trajectory followed by the system for moving from one condition to the other. The points a, b, c, d, and e denote different operating conditions. For example, operating condition 'a' can imply a 2% increase in the loads and a slight decrease in the power flowing through the tie-line. Similarly condition 'b' can denote a larger decrease in tie-line power flow and a 7.5% increase in load and so on. In such scenarios, the LMI control states that all operating conditions lying within the enclosed area (i.e. a, b, c, d, and e) can be simultaneously optimized by a single control law. The application of this technique to a standard power system problem is described in the next sub-section.

Fig. 2.2: LMI Control Design using a Polytopic system having three vertices

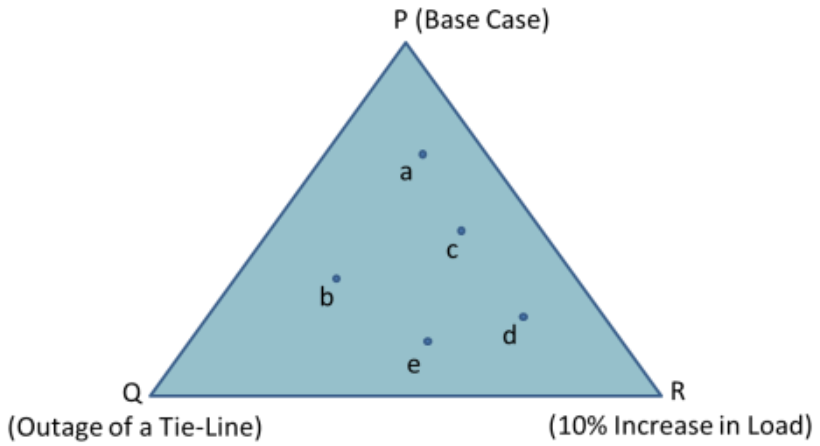

2.1.1 Application of LMI Control on 4 Machine – 2 Area System

Fig. 2.3: A simple four machine – two area system [53]

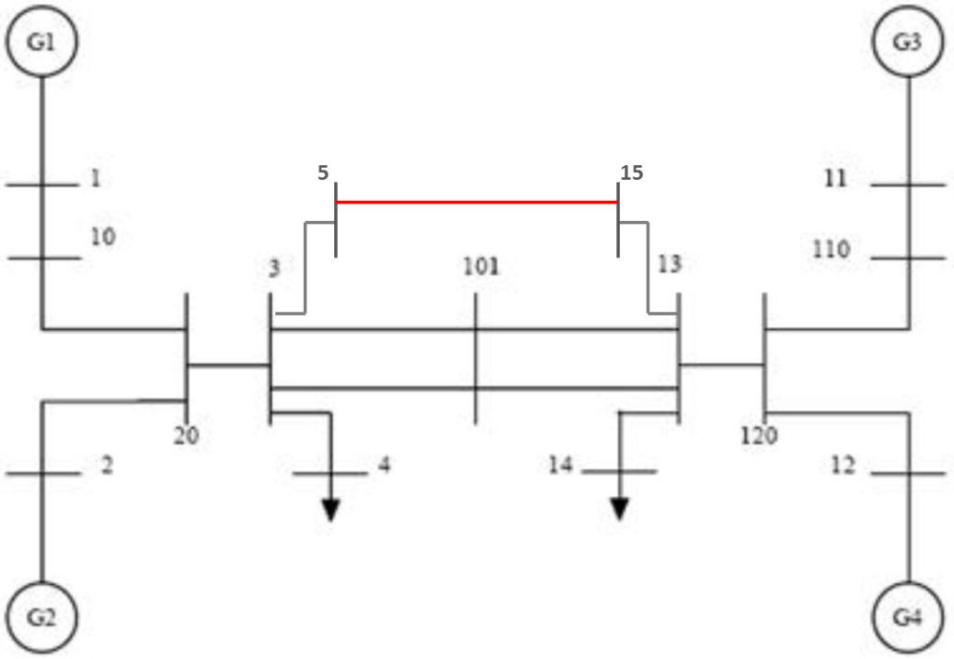

The system consists of two similar areas connected by two long, but weak tie-lines. Each area consists of two identical generating units coupled with one another. The loads are located at buses 4 and 14 with the generator G4 at bus 12 acting as the swing machine. The system has been modeled to operate under heavy stress by increasing the flow through the inter-connecting transmission lines. There are three different electromechanical modes of oscillations present in this system. They are:

a) One inter-area mode of oscillation in which the generators in area 1 (G1 and G2) oscillate against those in area 2 (G3 and G4)
b) Two local modes of oscillation in which G1 oscillates against G2 and G3 oscillates against G4

The analysis of this system is performed by developing a polytopic state space model similar to the one described in (2.3). The Power System Toolbox (PST) of Matlab is used to linearize the system by numerically perturbing each state of the model. Classical Generator models have been assumed for all the machines with exciters and PSSs as described in the system details provided in the appendix. The control action is provided by the DC line (marked in red) which has been added between buses 3 and 13, with buses 5 and 15 acting as dummy buses. It is to be noted here that in PST simulations, DC lines are approximated as active and reactive power injections. Since the test system has four machines with one acting as the swing, the total number of state variables is six. These six state variables correspond to the rotor angles, δ and the frequencies, ω of machines 1-3; machine 4 being the reference.

Matrix formulation: The individual matrices needed for (2.3) for the test system is derived as follows.

A matrix: It has a dimension of 19×19. It has been re-ordered such that the first three rows and columns correspond to the rotor angles (δ) whereas the next three correspond to the frequencies (ω). The rest of the elements refer to the exciters, PSSs and the DC control.

B matrices: The two matrices, B_1 and B_2 correspond to the disturbance and input vectors respectively. For the given system, the disturbance and the inputs being the same, the two matrices are identical. The dimension of each B matrix is 19×1. As the state vector x includes the machine as well as the system states, the relevant portion of the B matrices are the last rows.

C matrices: The two matrices C_1 and C_2 correspond to the H_∞ and H_2 optimizations respectively. They are based on the rotor angle and frequency of the generators. The C_1 matrix is a row matrix of dimension 1×19. It is a row vector because the H_∞ norm only ensures that the norm of the states is less than a set scalar value. The C_2 matrix typically contains of an Identity matrix controlling the frequency.

D matrices: It consists of four matrices, D_{11}, D_{12}, $D_{21}$and D_{22} with its dimension depending on those of B and C matrices. The D_{11} matrix has a dimension of 1×1 and has one as its element corresponding to the disturbance. If a particular component of D_{11} is not 1, then it implies that there is no control for that particular disturbance. The D_{12} matrix corresponds to the input. It is set to 0 because it does not affect the H_∞ synthesis for this system as H_∞ evaluates the tolerance to disturbances and not input values. If it is made non-zero, it only increases the duration of the H_∞ synthesis. D_{21} is a 1×1 Null matrix because otherwise it would feed-forward an error in the H_2 optimization resulting in the system becoming unstable resulting in compilation errors. The D_{22} matrix is a 1×1 Identity matrix implying that the inputs are fed forward in the H_2 synthesis. For compatibility of dimensions, the rest of the elements are zeros.

The complete system matrix in Matlab has a dimension of 24×22 with the number of rows/columns of A matrix being the first element of the last column and negative infinity as the last row and column element. This is done to differentiate the system matrix from other matrices. The complete system matrix for the 4 machine – 2 area system is shown in Fig. 2.4 below with the bold lines indicating A, B, C and D matrices.

Multi-objective Design: The H_∞ analysis is used to evaluate the robustness of the system when exposed to dynamic uncertainties. It minimizes the maximum error and ensures that its norm is less than some pre-specified value. However, when this optimization is performed, the equalizing of the values causes shifts in some of the other values present in the matrix. This results in the H_∞ control becoming computationally complex and time intensive. The H_2 design parameters are tailored towards measuring the control effort and providing disturbance rejection. The combination of the two is therefore a logical choice for a robust control design [22]. An even more desirable pole placement region can be developed by imposing extra damping constraints.

Fig. 2.4: The Complete System Matrix for the 4 machine – 2 area system

0.000	0.000	0.000	376.991	0.000	0.000	0.000	0.000	0.000	0.000	0.000	0.000	0.000	0.000	0.000	0.000	0.000	0.000	0.000	0.000	19.000
0.000	0.000	0.000	0.000	376.991	0.000	0.000	0.000	0.000	0.000	0.000	0.000	0.000	0.000	0.000	0.000	0.000	0.000	0.000	0.000	0.000
0.000	0.000	0.000	0.000	0.000	376.991	0.000	0.000	0.000	0.000	0.000	0.000	0.000	0.000	0.000	0.000	0.000	0.000	0.000	0.000	0.000
-0.103	0.075	-0.028	-0.269	-0.019	-0.019	-0.002	-0.002	-0.002	-0.002	-0.002	-0.002	-0.002	-0.002	-0.002	-0.002	-0.002	-0.002	-0.012	0.000	0.000	0.000
0.120	-0.124	-0.041	-0.017	-0.274	-0.017	-0.002	-0.002	-0.002	-0.002	-0.002	-0.002	-0.002	-0.002	-0.002	-0.002	-0.002	-0.002	-0.013	0.000	0.000	0.000
0.011	0.014	-0.181	-0.002	-0.002	-0.288	0.000	0.000	0.000	0.000	0.000	0.000	0.000	0.000	0.000	0.000	0.000	0.000	0.005	0.000	0.000	0.000
-0.269	15.079	-6.503	0.482	0.482	0.482	-99.953	0.048	0.048	0.048	0.048	0.048	0.048	0.048	0.047	0.048	0.048	0.048	-0.280	0.000	0.000	0.000
0.000	0.000	0.000	0.050	0.000	0.000	0.000	-0.050	0.000	0.000	0.000	0.000	0.000	0.000	0.000	0.000	0.000	0.000	0.000	0.000	0.000	0.000
0.000	0.000	0.000	-187.500	0.000	0.000	0.000	187.500	-25.000	0.000	0.000	0.000	0.000	0.000	0.000	0.000	0.000	0.000	0.000	0.000	0.000	0.000
0.000	0.000	0.000	-562.500	0.000	0.000	0.000	562.500	-25.000	-25.000	0.000	0.000	0.000	0.000	0.000	0.000	0.000	0.000	0.000	0.000	0.000	0.000
-14.248	-5.547	-36.801	-23.557	-23.557	-23.557	-2.287	-2.356	-2.356	-2.356	-102.332	-2.356	-2.356	-2.356	-2.287	-2.356	-2.356	-2.356	-15.206	0.000	0.000	0.000
0.000	0.000	0.000	0.000	0.050	0.000	0.000	0.000	0.000	0.000	0.000	-0.050	0.000	0.000	0.000	0.000	0.000	0.000	0.000	0.000	0.000	0.000
0.000	0.000	0.000	0.000	-187.500	0.000	0.000	0.000	0.000	0.000	0.000	187.500	-25.000	0.000	0.000	0.000	0.000	0.000	0.000	0.000	0.000	0.000
0.000	0.000	0.000	0.000	-562.500	0.000	0.000	0.000	0.000	0.000	0.000	562.500	-25.000	-25.000	0.000	0.000	0.000	0.000	0.000	0.000	0.000	0.000
3.031	18.462	-52.958	-16.640	-16.640	-16.640	-1.616	-1.664	-1.664	-1.664	-1.647	-1.664	-1.664	-1.664	-101.616	-1.664	-1.664	-1.664	-8.909	0.000	0.000	0.000
0.000	0.000	0.000	0.000	0.000	0.050	0.000	0.000	0.000	0.000	0.000	0.000	0.000	0.000	0.000	-0.050	0.000	0.000	0.000	0.000	0.000	0.000
0.000	0.000	0.000	0.000	0.000	-187.500	0.000	0.000	0.000	0.000	0.000	0.000	0.000	0.000	0.000	187.500	-25.000	0.000	0.000	0.000	0.000	0.000
0.000	0.000	0.000	0.000	0.000	-562.500	0.000	0.000	0.000	0.000	0.000	0.000	0.000	0.000	0.000	562.500	-25.000	-25.000	0.000	0.000	0.000	0.000
0.000	0.000	0.000	0.000	0.000	0.000	0.000	0.000	0.000	0.000	0.000	0.000	0.000	0.000	0.000	0.000	0.000	0.000	-43.600	43.600	43.600	0.000
0.895	0.238	0.027	0.051	0.051	0.051	0.005	0.005	0.005	0.005	0.005	0.005	0.005	0.005	0.005	0.005	0.005	0.005	0.044	1.000	0.000	0.000
0.000	0.000	0.000	1.000	0.000	0.000	0.000	0.000	0.000	0.000	0.000	0.000	0.000	0.000	0.000	0.000	0.000	0.000	0.000	0.000	1.000	0.000
0.000	0.000	0.000	0.000	1.000	0.000	0.000	0.000	0.000	0.000	0.000	0.000	0.000	0.000	0.000	0.000	0.000	0.000	0.000	0.000	0.000	0.000
0.000	0.000	0.000	0.000	0.000	1.000	0.000	0.000	0.000	0.000	0.000	0.000	0.000	0.000	0.000	0.000	0.000	0.000	0.000	0.000	0.000	0.000
0.000	0.000	0.000	0.000	0.000	0.000	0.000	0.000	0.000	0.000	0.000	0.000	0.000	0.000	0.000	0.000	0.000	0.000	0.000	0.000	0.000	−∞

The output of the LMI controller is a gain matrix (K) of the form,

$$u = Kx \tag{2.6}$$

Substituting (2.6) in (2.3), for the test system and dropping the output from consideration, one gets,

$$\begin{aligned} \dot{x} &= (A + BK)x + B\zeta \\ z_\infty &= C_1 x + D_{11}\zeta \\ z_2 &= (C_2 + K)x \end{aligned} \tag{2.7}$$

The above equation represents the closed-loop system in the state-space form. The polytopic system can now be formed by creating contingencies in the test system.

Polytopic System: The polytopic system is formed by creating different contingencies within the test system. Typical contingency cases include, increase/decrease in loads, increase/decrease in line flows, tie-line outages etc. These cases form the vertices of the polytope. The list of contingencies performed on the test system is summarized in Table 2.1 below.

Table 2.1: Case Bank for the 4 machine – 2 area system

Case No.	Case Details
1	No Contingency Case
2	Loads decreased to 90% of their original value
3	Loads increased to 102% of their original value
4	Flow in line 3 to 101 increased by 200 MW
5	Flow in line 3 to 101 decreased by 100 MW

We are now in a position to apply the LMI control to the test system. Each of the LMI problems is described by 24×22 LTI system. The collection of the five cases results in a 24×116 polytopic system while the closed loop system has a size of 24×111. For the design of the controller, equal importance was given to the H_∞ and H_2 optimizations. The LMI pole placement region was suitable specified. The outputs of the LMI control were the performances of the $\mathrm{H}_\infty/\mathrm{H}_2$ norms, the closed loop system matrix, and a single feedback-gain matrix for all the different contingencies that had been simulated. Figure 2.5 below shows that all the closed-loop poles lie in the left half of the s-plane and have the requisite damping. The computational time for the LMI optimization was found to be 29.286383 seconds.

Fig. 2.5: Output of the LMI Control for the 4 machine system

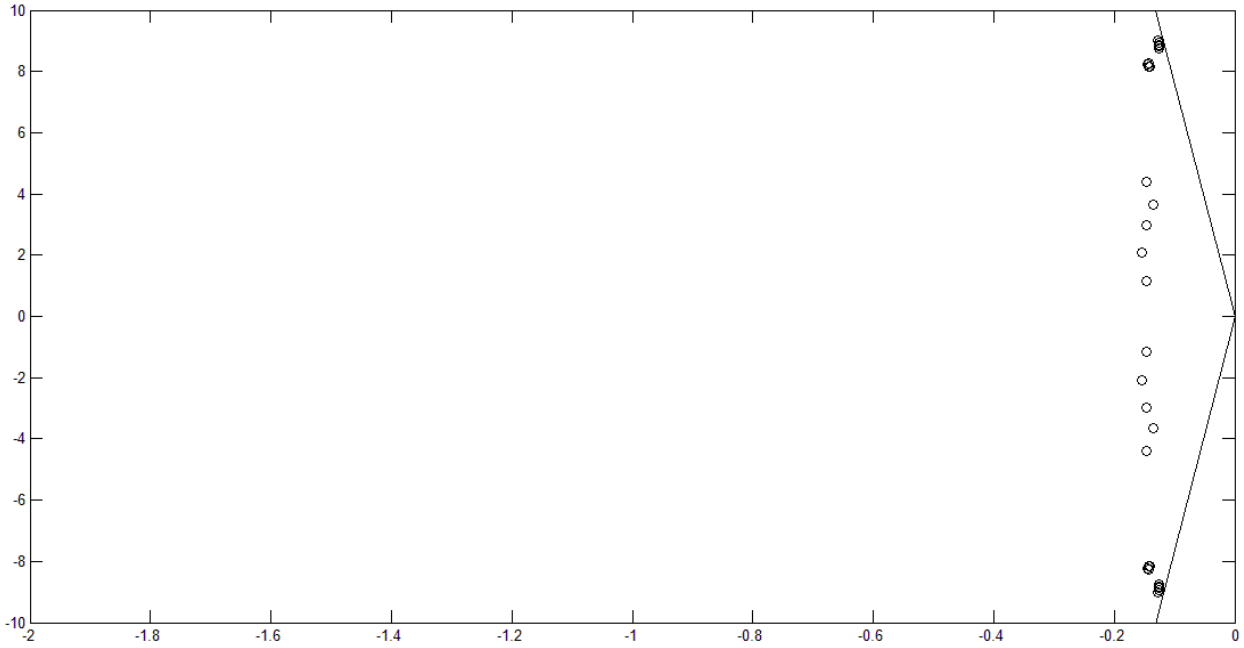

Although LMIs have been successfully used for solving small complex problems in the field of control systems, image processing and signal processing etc., their direct application to large systems has been limited due to the following disadvantages [52] –

a) There is no systematic procedure to build LMIs for a general classes of problems
b) There is no method of knowing whether or not it is possible to reduce a system problem to an LMI without actually doing it
c) A good understanding of LMIs and how the optimization is to be carried out
d) The LMI representation becomes complex due to the transformations via Schur complements

While applying LMI optimizations to a given problem, there is no guarantee that it will work, i.e. there are no conditions which if satisfied, will assure the user that LMIs will work before carrying it out. If for some reason, the optimization fails to converge, it is not very clear as to what the user should do. An alternative is to restate the entire optimization problem in the form used by some particular numerical non-linear optimization solvers. However, since optimizations over matrix functions are inherently not smooth, there is no guarantee of even a local minimum. Moreover, the tedious process of reformulating a matrix optimization problem is not a very practical approach.

The cumulative effect of these factors imply that the direct application of LMIs to large and complex power system problems is a distant reality, may be even impossible; the biggest obstacle to such an application being the inherent computational complexity of LMIs. This thesis addresses this issue by integrating LMIs with a technique called Selective Modal Analysis (SMA) which can be used (as will be shown in the next chapter) to reduce the size of the system to the relevant modes of oscillations. The next section describes

the basics of SMA and explains how it can be combined with LMIs for developing a robust control for such large and complex systems.

2.2 Selective Modal Analysis (SMA)

From (2.6) it is observed that many of the sub-matrices in S_k do not depend on k for any given application. Most of the applications only involve changes in the system matrix A. Even for a modest system the matrix A and hence S can become large when detailed machine models, exciters, PSSs, and the states involved in controls are considered. In such a scenario, the optimization problem can become unwieldy even for a small example. A reduced order model is therefore necessary to minimize the size of the problem. Selective Modal Analysis (SMA) developed by I. J. Perez-Arriaga, G. C. Verghese, and F. C. Schweppe in 1982 is a novel method for creating such reduced-order systems [43-44], [50-51]. While there exist a number of other techniques for forming reduced order models to study inter-area modes [45-46], SMA was chosen in this thesis since it fit the LMI Matlab environment.

SMA is a comprehensive framework for the analysis of selected parts of linear dynamic systems. It can accurately and efficiently focus on selected portions of the structure and behavior of a system. In SMA, the part of the model that is relevant to the dynamics of interest is singled out in a direct manner and the remainder of the model is collapsed in a way that leaves the selected structure and behavior intact [49]. It has been frequently used for performing –

a) Eigen-analysis
b) Determination and decoupling of dynamic patterns
c) Model interpretation and reduction
d) Input-output characterization of models
e) Modal control etc.

Its potential for significantly reducing the computational costs makes it particularly well-suited to the study of complex real-life systems. In this thesis, SMA is used for performing eigen-analysis of reduced order systems. SMA algorithms for reduced order eigen-analysis assume a separation of the state variables into relevant and less relevant categories in accordance with the modes of interest. The modes of interest for the analysis done here are the inter-area modes of oscillations; therefore the relevant variables are the state variables that describe the rotor dynamics namely the rotor angle and speed of the relevant generators. A particular organization of the dynamic equations for the reduced order model can be described as:

$$A = \begin{bmatrix} 0 & \omega_0 I & 0 & 0 \\ A_{21} & A_{22} & A_{23} & A_{24} \\ A_{31} & A_{32} & A_{33} & A_{34} \\ A_{41} & A_{42} & A_{43} & A_{44} \end{bmatrix}, B = \begin{bmatrix} 0 \\ 0 \\ 0 \\ B_2 \end{bmatrix}, x = \begin{bmatrix} \delta \\ \omega \\ x_3 \\ x_4 \end{bmatrix} \tag{2.8}$$

Where δ and ω are differences from values at the reference machine-a large external equivalent. x_3 denotes all the remaining machine states (fluxes, exciters and PSSs) and x_4 denotes the states associated with the controls. The matrices are formed by numerically perturbing the load flow equilibrium using the Matlab suite PST. The matrix B_2 corresponds to the control signals for the DC lines, the ESDs and the SVCs. Both angles and frequencies are used as feedback signals for these controls. Equation (2.8) can be partitioned in the SMA form as follows:

$$A = \begin{bmatrix} A_1 & A_2 \\ A_3 & A_4 \end{bmatrix};\ A_1 = \begin{bmatrix} 0 & \omega_0 I \\ A_{21} & A_{22} \end{bmatrix};\ A_2 = \begin{bmatrix} 0 & 0 \\ A_{23} & A_{24} \end{bmatrix};\ A_3 = \begin{bmatrix} A_{31} & A_{32} \\ A_{41} + B_{21} & A_{42} + B_{22} \end{bmatrix};\ A_4 = \begin{bmatrix} A_{33} & A_{34} \\ A_{43} & A_{44} \end{bmatrix} \quad (2.9)$$

The block diagram in Fig. 2.6 is the key to SMA. The block X denotes the "relevant" portion of the system whose dynamics is of interest. The block Y denotes the "less relevant" part of the system which has been collapsed in such a manner that it does not interfere with the dynamics of the portion of interest. Therefore in accordance with this logic, block X contains the matrix A_1 which has the angles and speeds of the generators as its elements; while block Y contains the matrices A_2, A_3 and A_4 which have information of all the remaining machine states and the states associated with the controls.

Fig. 2.6: Block Diagram of SMA

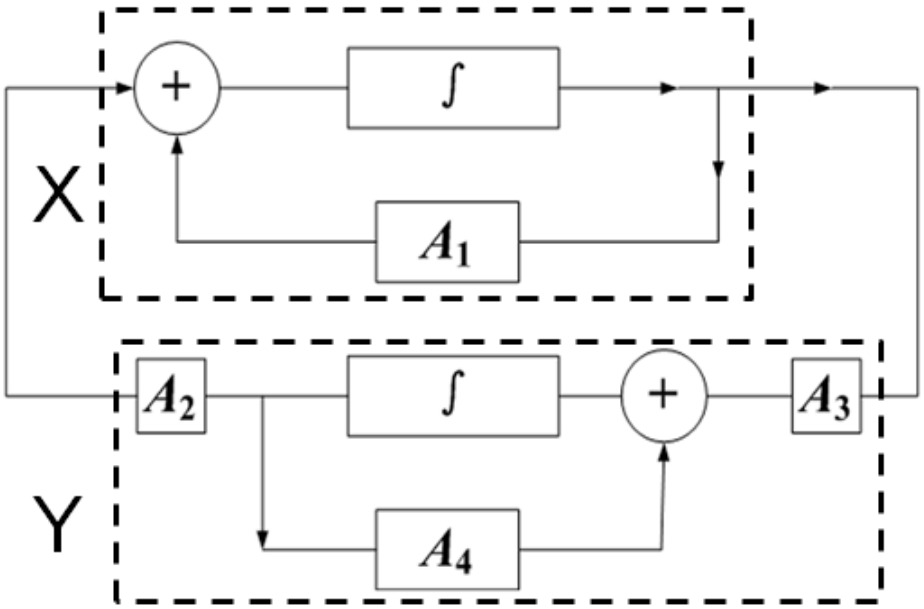

The transfer function of the system in the feedback path denoted by the block Y is,

$$H(s) = A_2(sI - A_4)^{-1}A_3 \quad (2.10)$$

The above equation can be thought of as a combination of two equations as shown below:

$$
\begin{aligned}
&H(s) = H_1(s) + H_2(s) \\
&H_1(s) = A_2(sI - A_4)^{-1}\begin{bmatrix} A_{31} & A_{32} \\ A_{41} & A_{42} \end{bmatrix} \\
&H_2(s) = A_2(sI - A_4)^{-1}\begin{bmatrix} 0 & 0 \\ B_{21} & B_{22} \end{bmatrix}
\end{aligned} \tag{2.11}
$$

The SMA process is an iterative method beginning with the eigenvalues and eigenvectors of A_1. Using $H_1(s)$ to illustrate, if the left eigenvalues and eigenvectors of A_1 are d_i and v_i then w_i, the i^{th} column of the matrix W is formed by

$$
w_i = A_2(d_i I - A_4)^{-1}\begin{bmatrix} A_{31} & A_{32} \\ A_{41} & A_{42} \end{bmatrix} v_i \tag{2.12}
$$

A first correction to A_1 is then formed by,

$$
A_{1next} = A_{1last} + M_1 \; where \; M_1 = WV^{-1} \tag{2.13}
$$

In (2.13), V^{-1} is the inverse of the matrix of left eigenvectors. The process is repeated with the eigenvalues and eigenvectors of $A_1 + M_1$. A few iterations give a good estimate to the eigenvalues of the A matrix. Given the presence of B in (2.11), the right eigenvectors of A_1 are more appropriate for H_2. The result is a reduced order system of the form in (2.14) where M is an approximation to H_1, N is an approximation to H_2 and K is the gain matrix obtained as the output of the LMI control.

$$
\dot{x}_1 = (A_1 + M + NK)x_1 \tag{2.14}
$$

Thus, (2.14) is an approximation to the closed loop eigenvalues using the fixed matrices M, N and K. The application of this technique to the result of the LMI Control on the 4 machine – 2 area system described previously is illustrated below.

2.2.1 Application of SMA+LMI Control on 4 Machine – 2 Area System

The A matrix for the test system has a dimension of 19×19 as discussed earlier. On solving the relevant partial differential equations, the elements of the A-matrix for the base case were found to be the ones seen in Fig. 2.7 below. The eigen-values of A are summarized in Table 2.2.

Fig. 2.7: The A-matrix for the base case of the 4 machine – 2 area Test System with the bold lines indicating its sub-divisions namely A_1, A_2, A_3 and A_4

$A =$

0.0000	0.0000	0.0000	376.9911	0.0000	0.0000	0.0000	0.0000	0.0000	0.0000	0.0000	0.0000	0.0000	0.0000	0.0000	0.0000	0.0000	0.0000	0.0000
0.0000	0.0000	0.0000	0.0000	376.9911	0.0000	0.0000	0.0000	0.0000	0.0000	0.0000	0.0000	0.0000	0.0000	0.0000	0.0000	0.0000	0.0000	0.0000
0.0000	0.0000	0.0000	0.0000	0.0000	376.9911	0.0000	0.0000	0.0000	0.0000	0.0000	0.0000	0.0000	0.0000	0.0000	0.0000	0.0000	0.0000	0.0000
-0.1029	0.0750	-0.0277	-0.2689	-0.0189	-0.0189	-0.0018	-0.0019	-0.0019	-0.0019	-0.0019	-0.0019	-0.0019	-0.0019	-0.0018	-0.0019	-0.0019	-0.0019	-0.0122
0.1200	-0.1242	-0.0411	-0.0173	-0.2737	-0.0173	-0.0017	-0.0017	-0.0017	-0.0017	-0.0017	-0.0017	-0.0017	-0.0017	-0.0017	-0.0017	-0.0017	-0.0017	-0.0126
0.0114	0.0137	-0.1814	-0.0019	-0.0019	-0.2876	-0.0002	-0.0002	-0.0002	-0.0002	-0.0002	-0.0002	-0.0002	-0.0002	-0.0002	-0.0002	-0.0002	-0.0002	0.0050
-0.2688	15.0787	-6.5030	0.4818	0.4818	0.4818	-99.9532	0.0482	0.0482	0.0482	0.0477	0.0482	0.0482	0.0482	0.0468	0.0482	0.0482	0.0482	-0.2796
0.0000	0.0000	0.0000	0.0500	0.0000	0.0000	0.0000	-0.0500	0.0000	0.0000	0.0000	0.0000	0.0000	0.0000	0.0000	0.0000	0.0000	0.0000	0.0000
0.0000	0.0000	0.0000	-187.5000	0.0000	0.0000	0.0000	187.5000	-25.0000	0.0000	0.0000	0.0000	0.0000	0.0000	0.0000	0.0000	0.0000	0.0000	0.0000
0.0000	0.0000	0.0000	-562.5000	0.0000	0.0000	0.0000	562.5000	-25.0000	-25.0000	0.0000	0.0000	0.0000	0.0000	0.0000	0.0000	0.0000	0.0000	0.0000
-14.2480	-5.5473	-36.8006	-23.5570	-23.5570	-23.5570	-2.2871	-2.3557	-2.3557	-2.3557	-102.3324	-2.3557	-2.3557	-2.3557	-2.2871	-2.3557	-2.3557	-2.3557	-15.2059
0.0000	0.0000	0.0000	0.0000	0.0500	0.0000	0.0000	0.0000	0.0000	0.0000	0.0000	-0.0500	0.0000	0.0000	0.0000	0.0000	0.0000	0.0000	0.0000
0.0000	0.0000	0.0000	0.0000	-187.5000	0.0000	0.0000	0.0000	0.0000	0.0000	0.0000	187.5000	-25.0000	0.0000	0.0000	0.0000	0.0000	0.0000	0.0000
0.0000	0.0000	0.0000	0.0000	-562.5000	0.0000	0.0000	0.0000	0.0000	0.0000	0.0000	562.5000	-25.0000	-25.0000	0.0000	0.0000	0.0000	0.0000	0.0000
3.0311	18.4615	-52.9585	-16.6397	-16.6397	-16.6397	-1.6155	-1.6640	-1.6640	-1.6640	-1.6475	-1.6640	-1.6640	-1.6640	-101.6155	-1.6640	-1.6640	-1.6640	-8.9087
0.0000	0.0000	0.0000	0.0000	0.0000	0.0500	0.0000	0.0000	0.0000	0.0000	0.0000	0.0000	0.0000	0.0000	0.0000	-0.0500	0.0000	0.0000	0.0000
0.0000	0.0000	0.0000	0.0000	0.0000	-187.5000	0.0000	0.0000	0.0000	0.0000	0.0000	0.0000	0.0000	0.0000	0.0000	187.5000	-25.0000	0.0000	0.0000
0.0000	0.0000	0.0000	0.0000	0.0000	-562.5000	0.0000	0.0000	0.0000	0.0000	0.0000	0.0000	0.0000	0.0000	0.0000	562.5000	-25.0000	-25.0000	0.0000
0.0000	0.0000	0.0000	0.0000	0.0000	0.0000	0.0000	0.0000	0.0000	0.0000	0.0000	0.0000	0.0000	0.0000	0.0000	0.0000	0.0000	0.0000	-43.6000

Table 2.2: Eigenvalues for the A-matrix for the base case of the 4 machine – 2 area system

Serial Number	Eigenvalues
1, 2	-0.10146 ± i2.9729
3, 4	-0.12644 ± i8.8531
5, 6	-0.14495 ± i8.1709
7	-0.049974
8	-0.05
9	-0.05
10	-24.215
11	-25
12	-25
13	-25
14	-25
15	-25.866
16	-43.6
17	-100
18	-100
19	-103.9

The A-matrix can be partitioned in the SMA form as –

$A_1 =$

0.0000	0.0000	0.0000	376.9911	0.0000	0.0000
0.0000	0.0000	0.0000	0.0000	376.9911	0.0000
0.0000	0.0000	0.0000	0.0000	0.0000	376.9911
-0.1029	0.0750	-0.0277	-0.2689	-0.0189	-0.0189
0.1200	-0.1242	-0.0411	-0.0173	-0.2737	-0.0173
0.0114	0.0137	-0.1814	-0.0019	-0.0019	-0.2876

$A_2 =$

0.0000	0.0000	0.0000	0.0000	0.0000	0.0000	0.0000	0.0000	0.0000	0.0000	0.0000	0.0000	0.0000
0.0000	0.0000	0.0000	0.0000	0.0000	0.0000	0.0000	0.0000	0.0000	0.0000	0.0000	0.0000	0.0000
0.0000	0.0000	0.0000	0.0000	0.0000	0.0000	0.0000	0.0000	0.0000	0.0000	0.0000	0.0000	0.0000
-0.0018	-0.0019	-0.0019	-0.0019	-0.0019	-0.0019	-0.0019	-0.0019	-0.0018	-0.0019	-0.0019	-0.0019	-0.0122
-0.0017	-0.0017	-0.0017	-0.0017	-0.0017	-0.0017	-0.0017	-0.0017	-0.0017	-0.0017	-0.0017	-0.0017	-0.0126
-0.0002	-0.0002	-0.0002	-0.0002	-0.0002	-0.0002	-0.0002	-0.0002	-0.0002	-0.0002	-0.0002	-0.0002	0.0050

$A_3 =$

-0.2688	15.0787	-6.5030	0.4818	0.4818	0.4818
0.0000	0.0000	0.0000	0.0500	0.0000	0.0000
0.0000	0.0000	0.0000	-187.5000	0.0000	0.0000
0.0000	0.0000	0.0000	-562.5000	0.0000	0.0000
-14.2480	-5.5473	-36.8006	-23.5570	-23.5570	-23.5570
0.0000	0.0000	0.0000	0.0000	0.0500	0.0000
0.0000	0.0000	0.0000	0.0000	-187.5000	0.0000
0.0000	0.0000	0.0000	0.0000	-562.5000	0.0000
3.0311	18.4615	-52.9585	-16.6397	-16.6397	-16.6397
0.0000	0.0000	0.0000	0.0000	0.0000	0.0500
0.0000	0.0000	0.0000	0.0000	0.0000	-187.5000
0.0000	0.0000	0.0000	0.0000	0.0000	-562.5000
0.0000	0.0000	0.0000	0.0000	0.0000	0.0000

$A_4 =$

-99.9532	0.0482	0.0482	0.0482	0.0477	0.0482	0.0482	0.0482	0.0468	0.0482	0.0482	0.0482	-0.2796
0.0000	-0.0500	0.0000	0.0000	0.0000	0.0000	0.0000	0.0000	0.0000	0.0000	0.0000	0.0000	0.0000
0.0000	187.5000	-25.0000	0.0000	0.0000	0.0000	0.0000	0.0000	0.0000	0.0000	0.0000	0.0000	0.0000
0.0000	562.5000	-25.0000	-25.0000	0.0000	0.0000	0.0000	0.0000	0.0000	0.0000	0.0000	0.0000	0.0000
-2.2871	-2.3557	-2.3557	-2.3557	-102.3324	-2.3557	-2.3557	-2.3557	-2.2871	-2.3557	-2.3557	-2.3557	-15.2059
0.0000	0.0000	0.0000	0.0000	0.0000	-0.0500	0.0000	0.0000	0.0000	0.0000	0.0000	0.0000	0.0000
0.0000	0.0000	0.0000	0.0000	0.0000	187.5000	-25.0000	0.0000	0.0000	0.0000	0.0000	0.0000	0.0000
0.0000	0.0000	0.0000	0.0000	0.0000	562.5000	-25.0000	-25.0000	0.0000	0.0000	0.0000	0.0000	0.0000
-1.6155	-1.6640	-1.6640	-1.6640	-1.6475	-1.6640	-1.6640	-1.6640	-101.6155	-1.6640	-1.6640	-1.6640	-8.9087
0.0000	0.0000	0.0000	0.0000	0.0000	0.0000	0.0000	0.0000	0.0000	-0.0500	0.0000	0.0000	0.0000
0.0000	0.0000	0.0000	0.0000	0.0000	0.0000	0.0000	0.0000	0.0000	187.5000	-25.0000	0.0000	0.0000
0.0000	0.0000	0.0000	0.0000	0.0000	0.0000	0.0000	0.0000	0.0000	562.5000	-25.0000	-25.0000	0.0000
0.0000	0.0000	0.0000	0.0000	0.0000	0.0000	0.0000	0.0000	0.0000	0.0000	0.0000	0.0000	-43.6000

Using 2.12 and 2.13 and performing a few iterations of SMA, we get the eigenvalues of $\mathrm{A}_1 + \mathrm{M}_3$ as,

$$\mathrm{Eigenvalues}(\mathrm{A}_1 + \mathrm{M}_3) = \begin{matrix} -0.10146 \pm \mathrm{i}2.9729 \\ -0.12644 \pm \mathrm{i}8.8531 \\ -0.14495 \pm \mathrm{i}8.1709 \end{matrix} \tag{2.15}$$

On comparing 2.15 with the first three elements of Table 2.2, we observe that the complex eigenvalues of the smaller matrix $\mathrm{A}_1 + \mathrm{M}_3$ perfectly match those of the larger A matrix. This is further confirmed by plotting the eigenvalues of the two matrices in the complex plane as shown in Fig. 2.8 below. In that figure, the black dots represent the eigenvalues of the A matrix, whereas the red circles denote the eigenvalues of $\mathrm{A}_1 + \mathrm{M}_3$

Fig. 2.8: SMA identifying the complex eigenvalues of the 4 machine – 2 area system

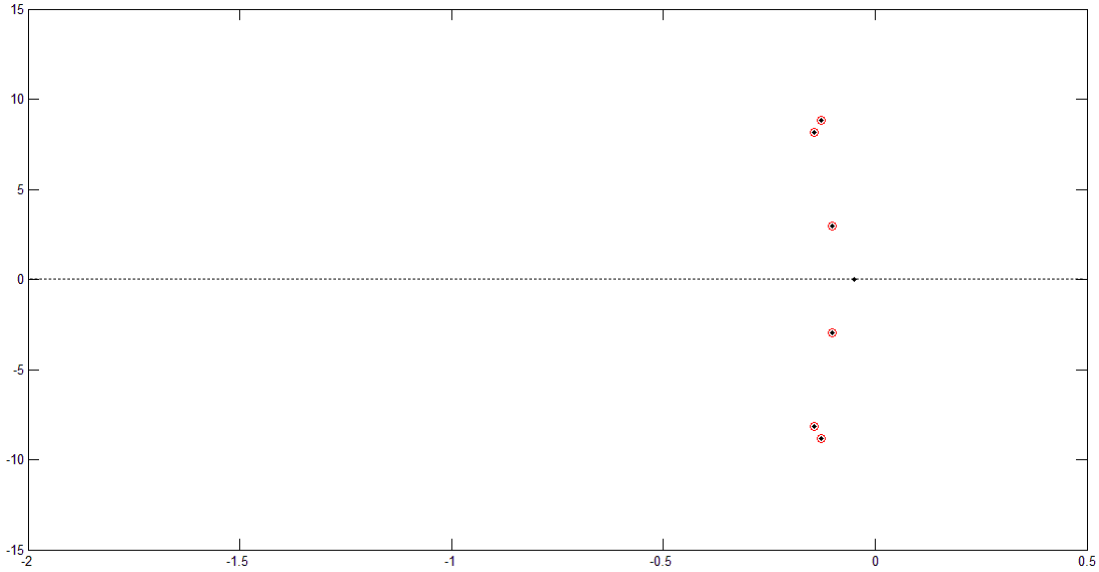

Figure 2.9 denotes the application of a rudimentary LQR control on the system denoted by $A_1 + M_3$. It can be seen that at the maximum feedback gain used in the plot the eigenvalues have shifted towards the left implying that they are now more negative than what they were previously. The example also demonstrates that the control for the reduced order system can be transferred back to the full system. In the figure below, the red dots represent the eigenvalue movement for the reduced system, whereas the green circles denote that for the full system

Fig. 2.9: Transition of Eigenvalues on the application of an LQR Control

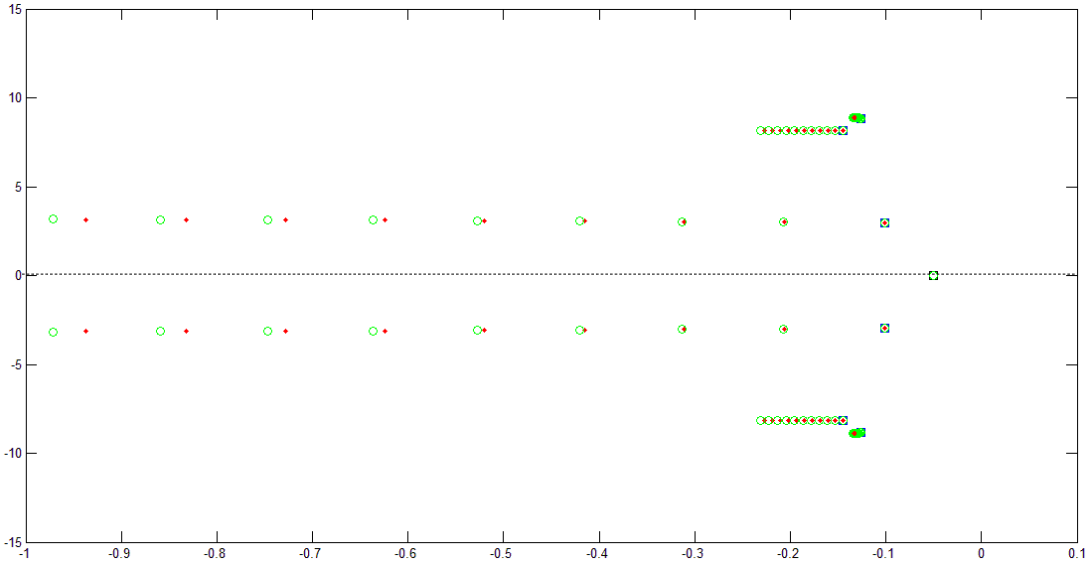

Thus, by using SMA, the dynamics of the 19×19 A matrix was performed by the 6×6 $A_1 + M_3$ matrix. SMA was then applied on the other four contingency cases resulting in a 11×9 LTI system. The collection of the five cases resulted in a 11×51 polytopic system while the closed loop system had a size of 11×46. On performing the LMI optimization as described previously a single feedback gain matrix was obtained for all the five cases defined in Table 2.1. The computational time for the LMI optimization of this reduced system was found to be 1.209831 seconds. Fig. 2.10 shows the eigenvalues of the closed loop matrices for the five cases. Fewer eigenvalues appear in Fig. 2.10 in comparison to Fig. 2.5 because of the traditional SMA approach. Table 2.3 gives a comparison of the LMI control without and with the combination of SMA.

Fig. 2.10: Output of the LMI Control for the 4 machine system using the traditional SMA approach

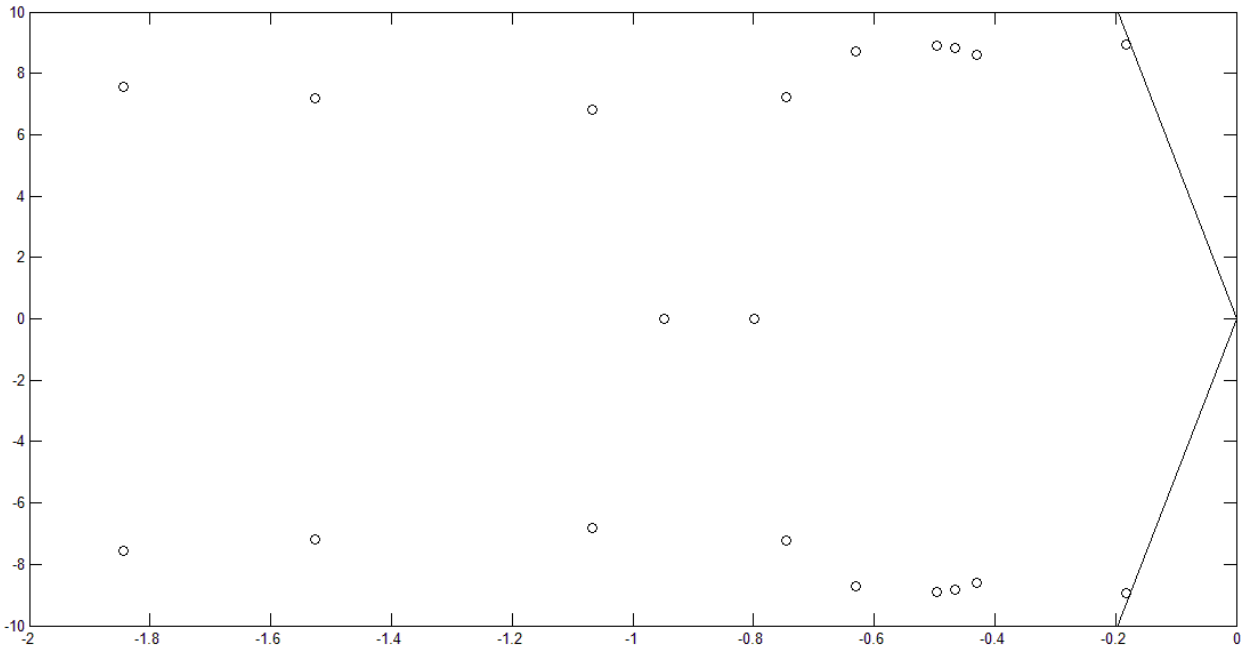

Table 2.3: Comparison of LMI optimization without and with the traditional SMA approach

	LMI Control	**LMI Control + Traditional SMA**
System Size (A/A_1)	19×19	6×6
Size of individual LTI system	24×22	11×9
Size of Polytopic System	24×116	11×51
Size of Closed Loop System	24×111	11×46
CPU Time* (seconds)**	29.286383	1.209831

*** The computations were performed on an Intel (R) Core ™ i5 Processor having a speed of 2.40 GHz and an installed memory (RAM) of 5.86 GB

2.3 Conclusion

This chapter describes the mathematical concepts of the two techniques that have been used in this thesis, namely Linear Matrix Inequalities (LMIs) and Selective Modal Analysis (SMA). Wide Area Measurements in combination with LMIs appears to provide a robust damping control for all kinds of oscillations. A small 4 machine – 2 area system is used to illustrate how this technique can be applied in power system problems. The size of the polytopic system appears to be an issue for large systems, but the use of SMA appears to alleviate this problem. In this chapter, SMA has been used to reduce the system size to twice the number of machines present in the system with respect to the swing machine. Although the reduction was found to be substantial, it was still not enough for applying this combinatorial technique to real-life power system problems having hundreds of buses. The next chapter introduces an algorithm which uses SMA to systematically reduce the system size to the relevant modes of oscillations, thereby making it more suitable for larger systems.

Chapter 3 – Proposed Control

In the previous chapter, the concepts of LMI and SMA were explained. The biggest obstacle to the global use of LMIs for solving complex problems was found to be its inherent computational complexity. Since there is no method of knowing whether or not it is possible to reduce a system problem to an LMI without actually doing it, it becomes impractical to apply LMI techniques directly to large systems. Even for a moderately sized power system problem having detailed machine states, exciters and PSSs, the optimization was found to become unwieldy when eight cases were considered.

The use of SMA appears to offer a solution to this problem. A polytopic system using SMA to reduce the system size to twice the number of machines present in the system with respect to the swing machine was developed in [42]. The procedure for doing so was described in details in the previous chapter. The system model denoted by (2.14) had been used for the polytopic design. However, it was observed that if the generator angles (δ) and the generator speeds (ω) of all the machines with respect to the swing machine are kept in A_1, the size of A_1 would still be an issue for large systems. An algorithm is developed in this thesis which uses SMA to systematically reduce A_1 to its smallest possible size. This chapter describes the proposed approach.

The proposed technique requires the following conditions/assumptions to hold true for its successful application:

a) The modes of interest lie in a pre-defined frequency range (≈0.1 – 0.7 Hz)
b) An A_1 matrix has been obtained containing the δ and ω modes of all the machines
c) Certain generators have greater "participation" towards certain modes

The first assumption is self-explanatory as our primary focus is on damping the low frequency inter-area modes of oscillations. The second condition implies that prior to application of this technique, the traditional SMA approach has to be used to collapse all the remaining machine states and the states associated with the controls so that they do not interfere with the relevant portion of the dynamics. The way to do this has been described in details in the previous chapter. The third hypothesis has its basis in the concept of "participation factors" which is illustrated in some details below.

Originally proposed in [50], a matrix called the "Participation Matrix", denoted by P, provides a measure of association between the state variables and the oscillatory modes. If U and V denote the left and the right eigen-vectors respectively, then the matrix P can be defined as,

$$P = [p_1 \quad p_2 \quad \cdots \quad p_n] \tag{3.1}$$

Where,

$$p_i = \begin{bmatrix} p_{1i} \\ p_{2i} \\ \vdots \\ p_{ni} \end{bmatrix} = \begin{bmatrix} U_{1i}V_{i1} \\ U_{2i}V_{i2} \\ \vdots \\ U_{ni}V_{in} \end{bmatrix} \tag{3.2}$$

The element $p_{ki} = U_{ki}V_{ik}$ is defined as the Participation Factor. It gives a measure of the participation of the k^{th} state variable to the i^{th} mode, and vice-versa. Since U_{ki} measures the activity of the state k in the i^{th} mode and V_{ik} weighs the contribution of this activity to that mode, the product p_{ki} becomes a measure of the net participation. Therefore, it becomes a very good indicator of the importance of a state to the mode. Based on this study, the following inferences have been drawn [53]. For any mode,

a) If the corresponding participation factor of the generator is real and positive, it implies that adding damping at that generator will increase the damping of the mode
b) If the corresponding participation factor of the generator is real and negative, it implies that adding damping at that generator will decrease the damping of the mode
c) If the corresponding participation factor of the generator is zero, it implies that adding damping at that generator will have no effect on the mode

On the basis of this analysis, it can be understood that the third assumption implies that the generators present in the system can be classified on the basis of their participation factors for different modes. When these three necessary conditions are satisfied for a system, the proposed control technique can be applied to it, as described below.

3.1 Proposed Control Technique

A flowchart describing the proposed control technique is illustrated in Fig. 3.1. This procedure is to be followed after the traditional SMA approach described in Chapter 2 has been used to obtain an A_1 matrix containing the δ and ω modes of all the machines. The steps to be followed are:

Step 1: Compute for the oscillatory modes of the system and identify machines primarily responsible for those modes on the basis of their Participation Factors. Arrange them in descending order of frequency (top-to-down) and participation percentage (left-to-right).

Step 2: Drop the machine which (a) is largely responsible for the highest frequency of oscillation amongst all the oscillatory modes and (b) has significantly low participation for the low frequency inter-area modes.

Step 3: Perform iterations in SMA for this reduced order model of the system and check for its convergence. The convergence of SMA ensures that the reduced model has the same dynamic response as the full model.

Fig. 3.1: Flowchart of Proposed Algorithm

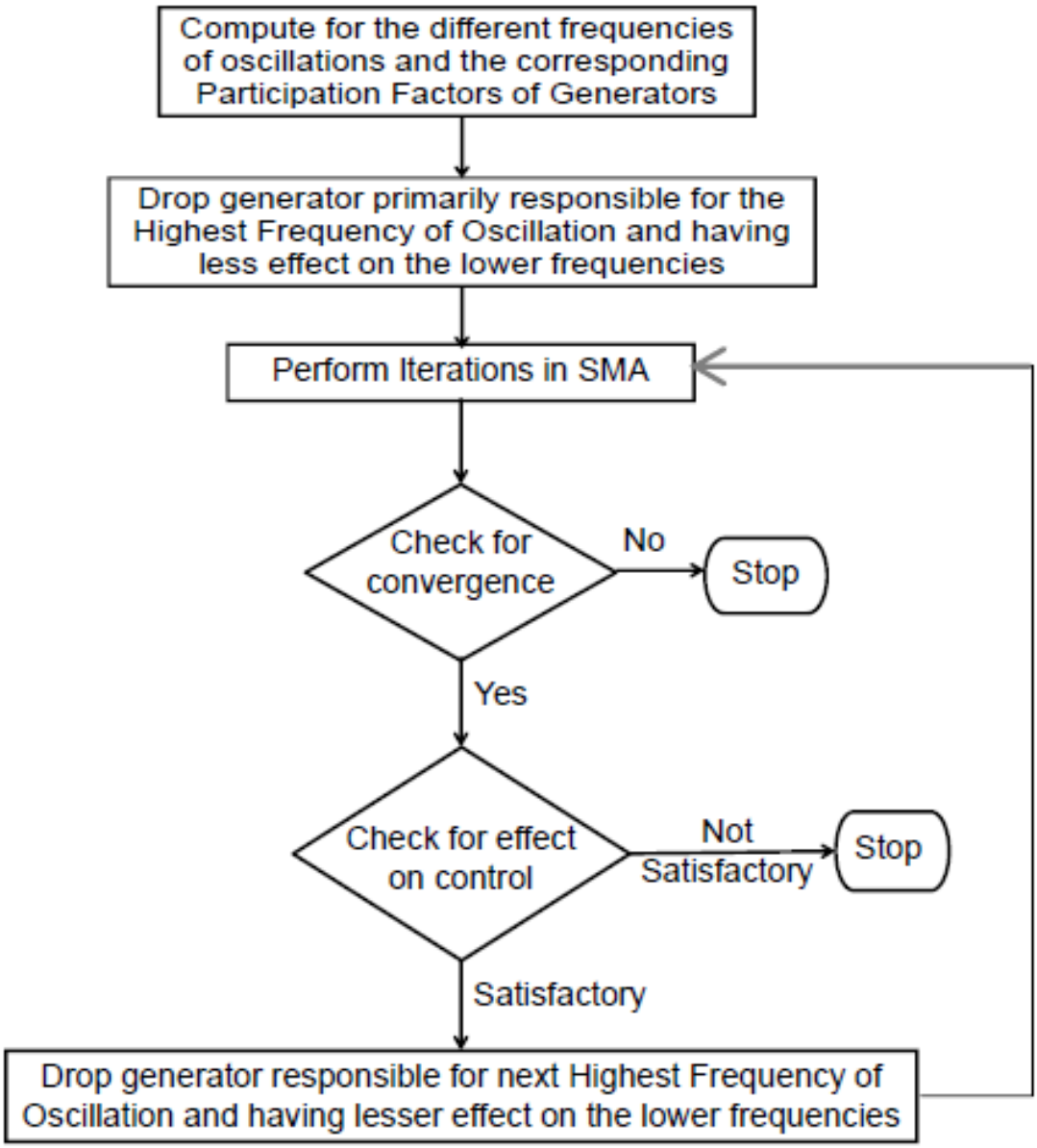

Step 4: If SMA converges, then do an elementary check of the control. This check detects any possible negative damping of the local modes thereby preventing excessive reduction in the size of the system.

Step 5: If the control is also found to be satisfactory, then drop the next machine in the sequence and repeat Steps 3 and 4. If SMA is not found to converge or the control is not found to be satisfactory, then the stable and converged system obtained one level before is the smallest possible size of A_1.

The primary objective of this algorithm is to reduce the system size further than what was achieved using the traditional SMA approach, without affecting the control of the inter-area modes of oscillations.

Although, control of some of the local modes can be slightly affected, Step 4 of the algorithm ensures that the system as a whole remains stable throughout this process.

3.1.1 Example Test System: 16 Machine System

A benchmark model consisting of 16-machines, 68-buses and five-areas, shown in Fig. 3.2, is used as the study system for the damping control design. The first nine machines (G1–G9) are a simple representation of the New England Test System (NETS) generation. Machines G10–G13 denote the New York Power System (NYPS) generation. The last three machines (G14–G16) are the dynamic equivalents of the three neighboring groups connected to the NYPS.

The tie-lines connecting NETS and NYPS carry 700 MW. Area #5 exports 1550 MW to NYPS and imports 24 MW from Area #4 while 610 MW flows from Area #3 to NYPS and 175 MW from Area #3 to Area #4. The detailed description of the test system including network data and dynamic data for the machines, buses, and branches can be found in the appendix. In order to damp the inter area modes and study the effectiveness of the polytopic control, the test system is modified by adding parallel DC lines and SVCs.

Fig. 3.2: The 16 machine – 68 Bus System

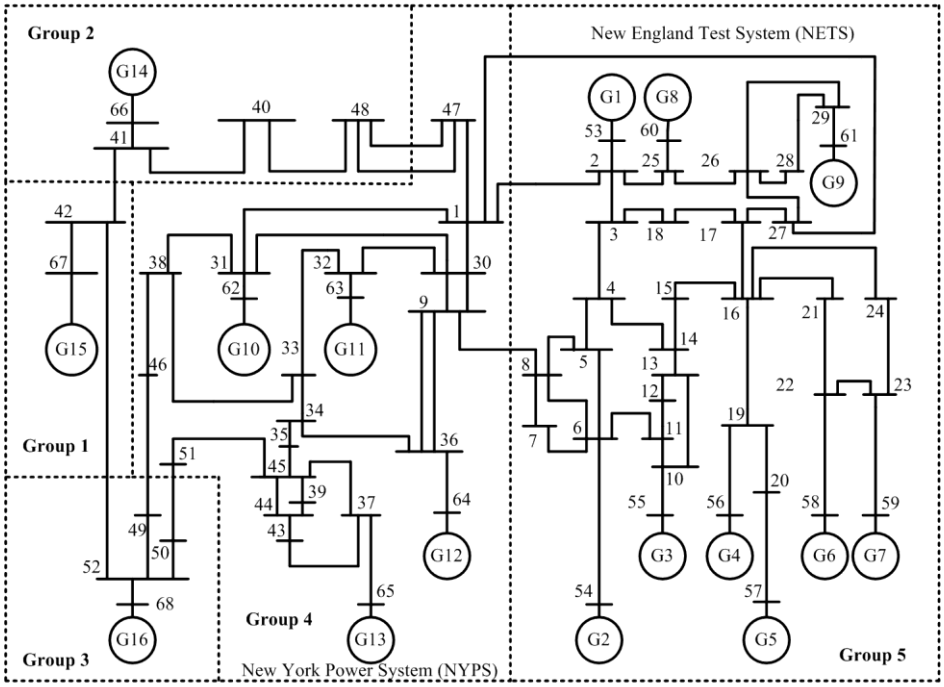

The three DC lines are added in parallel with the tie-lines (Bus 41 to Bus 42, Bus 42 to Bus 52, and Bus 46 to Bus 49). SVCs were installed at Buses 26, 46, and 51. All machines have simple exciters and turbine models. Machine 16 is the reference, and all machines except machines 1, 2, 7, 14, have PSSs

as described in [53]. The WECC load model is assumed at all the load buses. The real power is 80% constant current, the reactive power is 80% constant admittance and all loads have the remaining 20% as an induction motor load. The eight cases selected for this test are described in Table 3.1. In all the cases apart from the base case (no-contingency case), tie-line 1-27 is assumed to be out of commission in addition to the particular contingency under test. This is done to increase the severity of the contingency and to further test the robustness of the control.

Table 3.1: Case Bank for the 16 machine NE-NY system

Case Number	**Case Details**
1	No-Contingency Case
2	Flow in Line 50-52 increased from 700 MW to 900 MW
3	Flow in Line 50-52 decreased from 700 MW to 100 MW
4	Outage of Tie-line 1-2
5	10% decrease in inertial equivalent of Machine 14 (Bus Number 66)
6	10% increase in inertial equivalent of Machine 14 (Bus Number 66)
7	All Loads reduced to 90% of their original value, keeping generation constant
8	All Loads raised to 110% of their original value, keeping generation constant

The A matrix for each of the eight cases is 129×129. Fig. 3.3 shows a portion of the eigenvalues corresponding to the no-contingency case highlighting all the oscillatory modes along with some of the non-oscillatory ones. The black dots represent the eigenvalues of the A matrix whereas the red circles denote the eigenvalues of the A_1 matrix obtained after applying SMA to this system. Of special interest are the low frequency inter-area modes of oscillations which have been identified in the figure. The figure also shows the local modes of oscillations present in the system and the real eigenvalues (non-oscillatory modes) which correspond to the other states and controls. From the figure, it also becomes clear that the traditional form of SMA described in the previous chapter is able to correctly identify all the oscillatory modes within three iterations.

Fig. 3.3: Eigenvalues of the 16 machine system corresponding to the base case

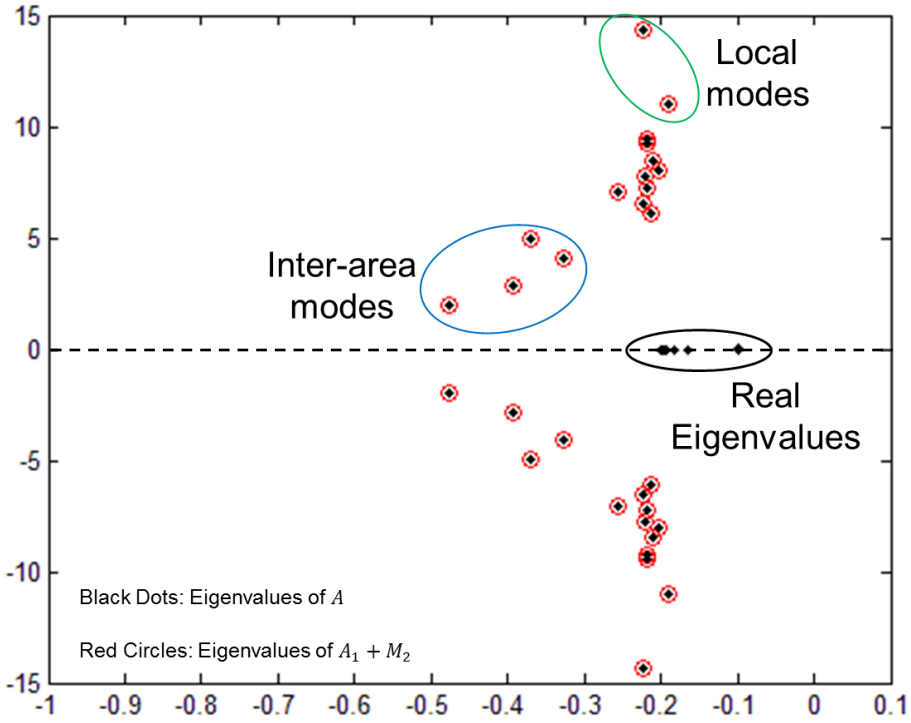

In order to apply the proposed algorithm, Table 3.2 was constructed to denote the participation percentage of the generators for the different frequencies. This table was constructed using the SSAT module of DSA Tools [54]. The logic which is to be used for selecting the sequence of machines to be dropped (Step 2 of the proposed algorithm) is illustrated in more details below –

a) Select the machine which has the maximum participation percentage to the highest frequency of oscillation
b) Check for its participation in the pre-defined frequency range, i.e. if dropping that machine from control results in the low frequency modes moving to the right then it implies that *that* machine has high participation for the low frequency modes and should not be dropped from control
c) If its participation percentage appears to be low, then drop that machine; if not, select the machine that has the next highest participation percentage to the highest frequency of oscillation and perform the check
d) Once a selected machine is dropped, go back to the machines corresponding to the higher frequencies of oscillation and check for the convergence of SMA after dropping them, one at a time
e) If it so happens that dropping a machine results in the corresponding frequency losing control from all the other machines, then that machine should not be dropped

Table 3.2: Frequency-Participation Percentage Table for the Base Case of the 16-machine system

Serial Number	Frequency (in Hz)	Bus Number based on Participation Factor Percentage															
1	1.8309	63	62	53	64												
2	1.6314	53	60	62	56	63											
3	1.5371	56	59	57	58	60											
4	1.5214	59	58	56	57	60											
5	1.3491	62	60	53	64	61	63	58	54	57	55	59					
6	1.2958	62	60	53	64	55	61	54	63	58	57	59					
7	1.2897	54	55	60	62	53	64										
8	1.2003	57	58	59	56	54											
9	1.1727	64	65	62	55	54	63	60	53	61							
10	1.0794	55	54	57	58	56	59	64	65	62	53	60	63	61			
11	0.9793	61	57	58	56	59	55	54	60								
12	0.7876	67	66	68													
13	0.5999	65	61	58	59	56	57	55	54	53	60	64	67	62	68	63	66
14	0.5213	68	66	67	65												
15	0.3351	65	67	66	68	64	58	61	55	53	56	57	54	59	60	63	62
16	0.0038	65	68	66	67	64	53	55	58	61	62	54	63	56	59	57	60

On the basis of this reasoning, the sequence which is to be followed for dropping control of the machines for the 16 machine system is shown in Table 3.3. It is important to note here that although this sequence was generated corresponding to the no-contingency case, it works perfectly well for the rest of the cases. The reason for this was that the contingencies being tested were sufficient to test the robustness of the control but not severe enough to make the system collapse.

Table 3.3: Sequence to be followed for dropping machines for the 16-machine system

Serial Number	Machine Number
1	63
2	53
3	62
4	57
5	61
6	60

The transition in the selection of the eigenvalues in accordance with the proposed algorithm is depicted in Figs. 3.4-3.9. Fig. 3.10 shows the effect of applying a rudimentary control (LQR optimization) to the system obtained in Fig. 3.8. The red dots denote the feedback to the reduced-order system whereas the green circles denote the feedback to the complete system. The blue squares denote the starting positions. It becomes clear from the figure that the proposed control obtained from the reduced-order system successfully moves all the low–frequency modes of oscillations to the left thereby increasing the

damping of the inter-area modes. Although some of the high frequency local modes of oscillations move towards the right, none of them cross the imaginary axis. Figure 3.11 illustrates the effect of dropping one more machine, on the control for the system described by Fig. 3.9. It is clear from these figures that the smallest number of machines that is to be controlled for a stable operation of this system is 10. That is, using the technique developed in this thesis, the first five machines mentioned in Table 3.3 could be safely dropped from the LMI control.

Fig 3.4: Applying proposed algorithm to reduce system size for base case – 14 machine system

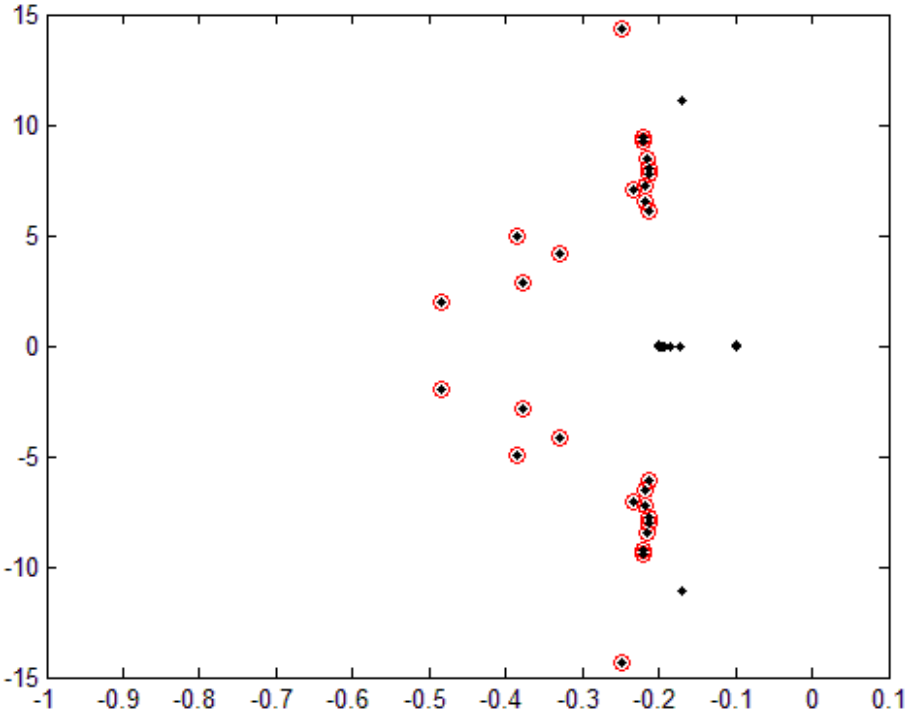

Fig 3.5: Applying proposed algorithm to reduce system size for base case – 13 machine system

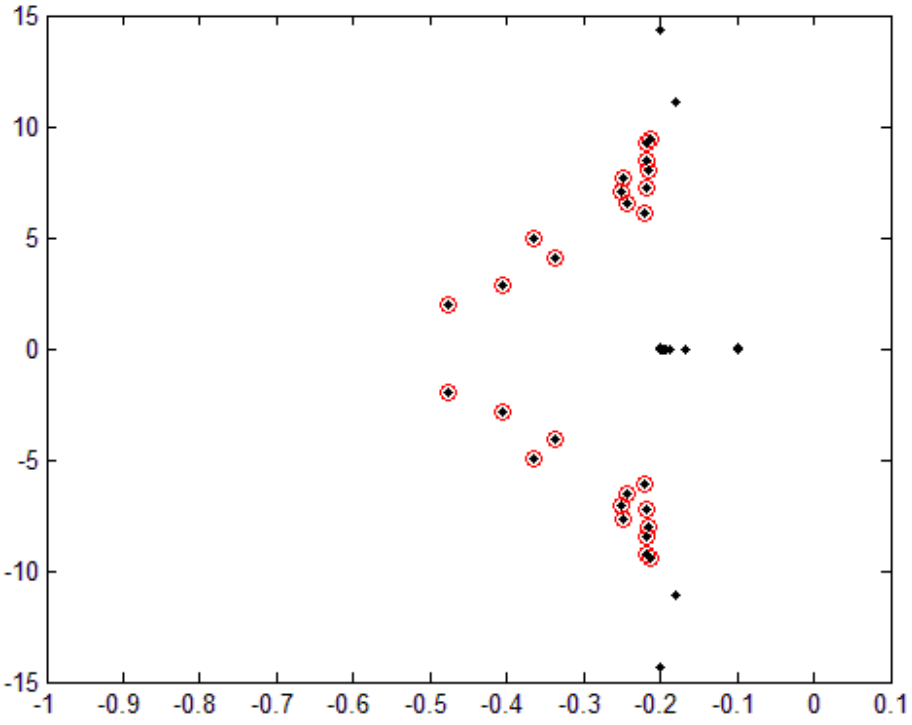

Fig 3.6: Applying proposed algorithm to reduce system size for base case – 12 machine system

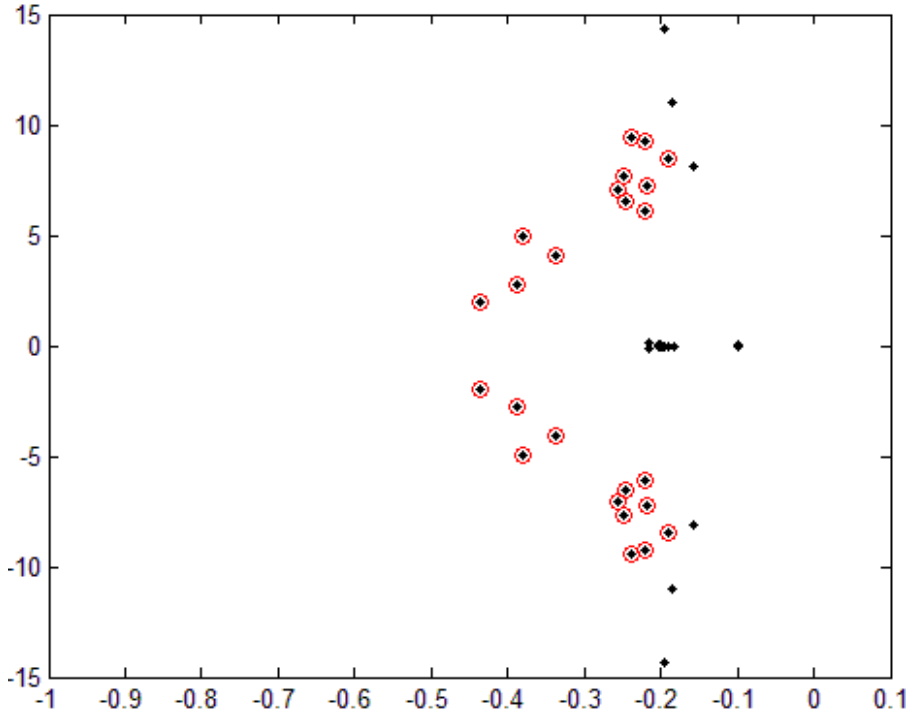

Fig 3.7: Applying proposed algorithm to reduce system size for base case – 11 machine system

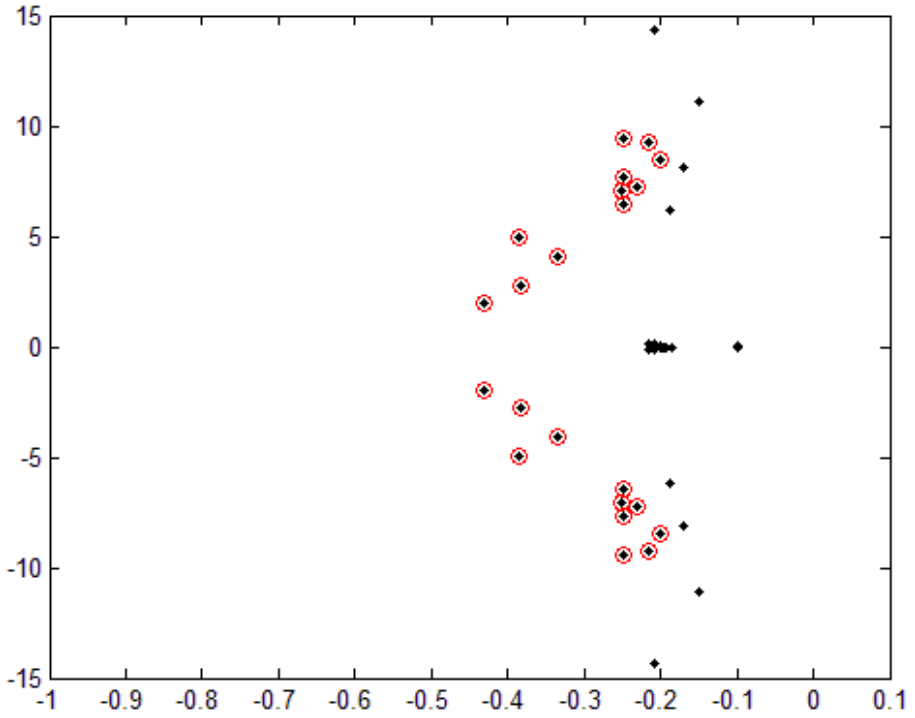

Fig 3.8: Applying proposed algorithm to reduce system size for base case – 10 machine system

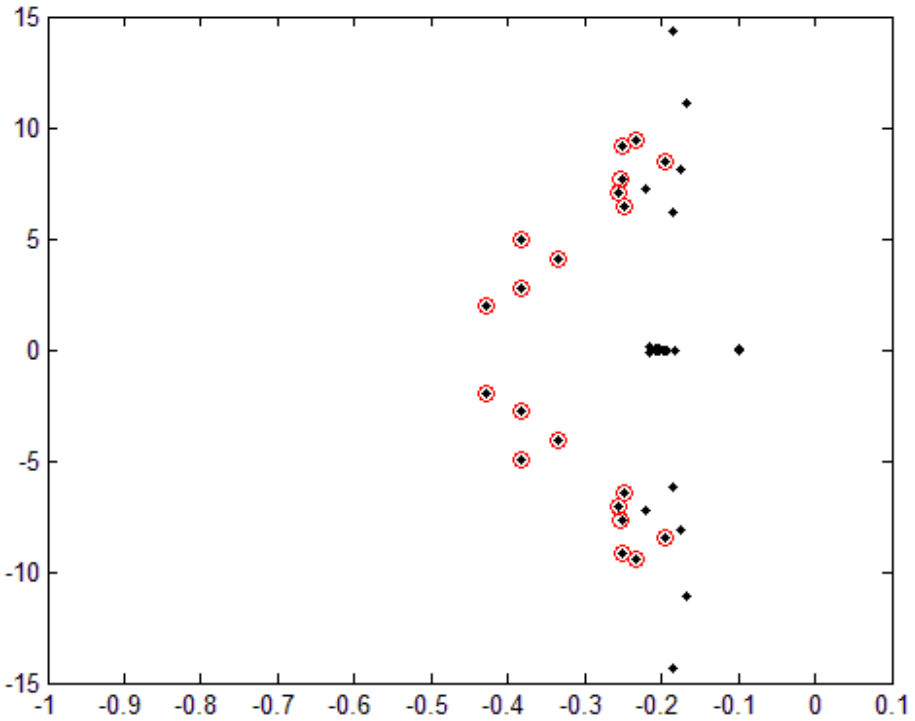

Fig 3.9: Applying proposed algorithm to reduce system size for base case – 9 machine system

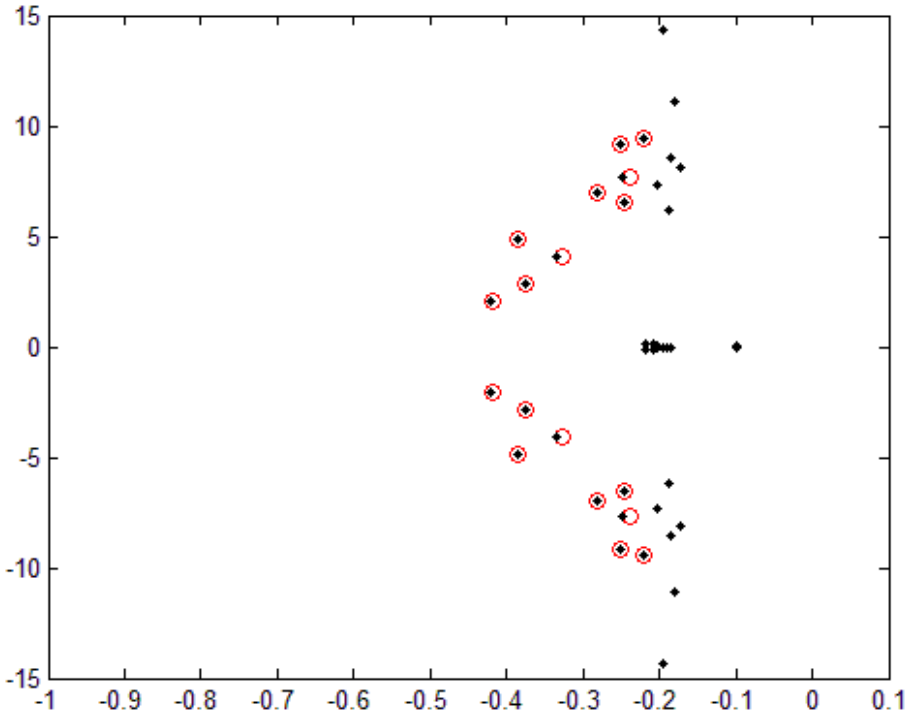

Fig. 3.10: Applying the control check described in Step 4 of the algorithm to the 10 machine system

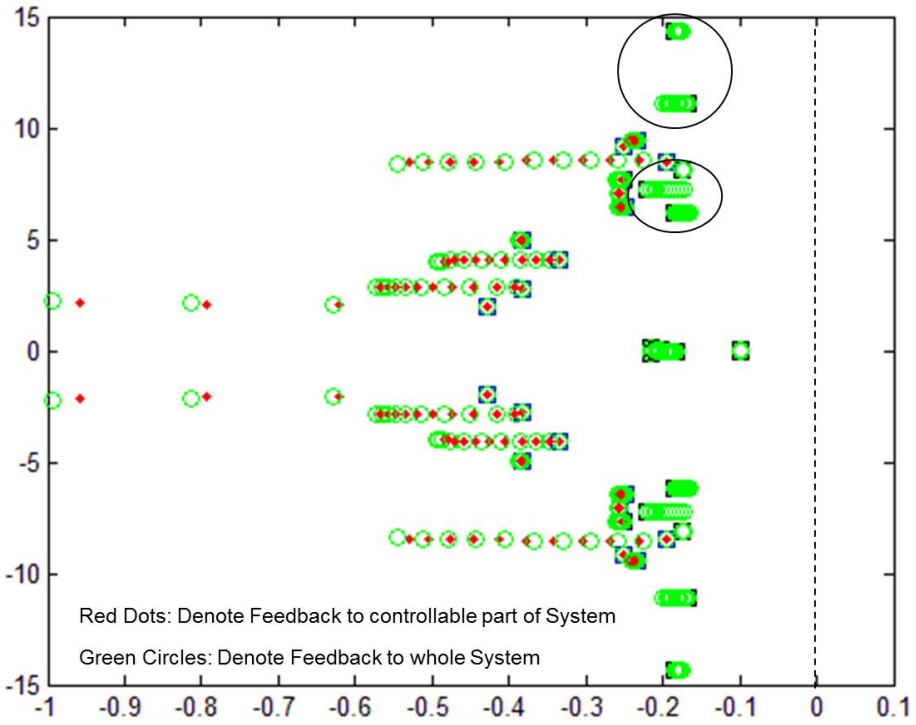

Fig. 3.11: Applying the control check described in Step 4 of the algorithm to the 9 machine system

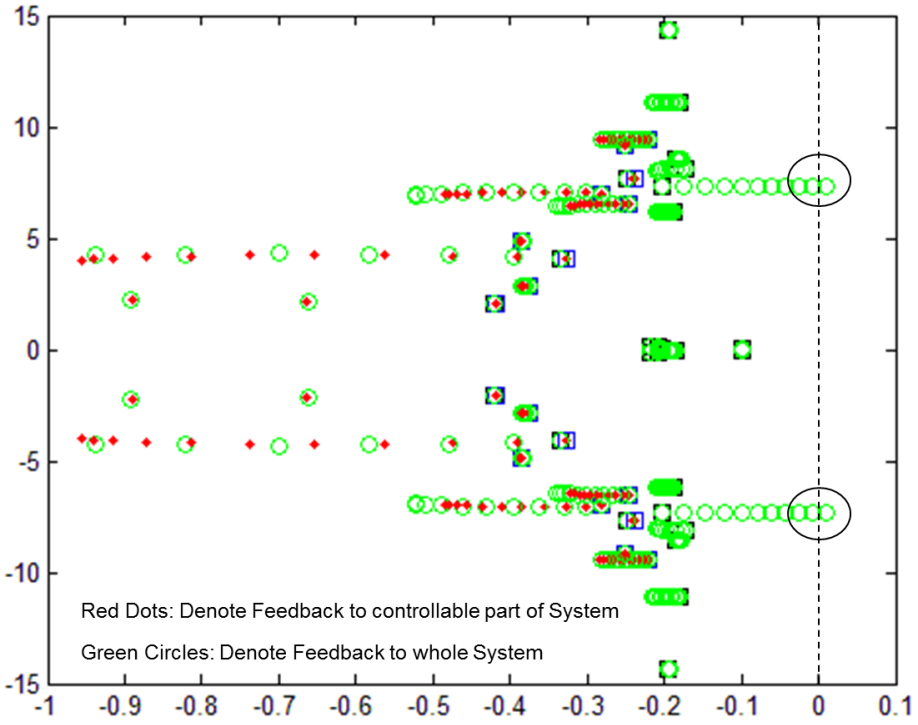

The system size reduction performed above for the no-contingency case was then applied to the remaining seven cases. By doing so, all the eight cases were reduced to have a 20×20 A_1 matrix. In essence, this implied that the system had been reduced from a 15 machine system to a 10 machine one (with one machine being the reference). Every A_1 matrix now contained the angles and frequencies of only those machines which corresponded to the significant modes of oscillations. Therefore, we are now in a position to apply the LMI control to this reduced-order system.

Each of the LMI problems with 20 retained states is described by a 32×33 LTI system. The collection of the eight cases results in a 32×273 polytopic system while the closed loop system has a size of 32×225. The LMI optimization yields a single feedback gain matrix for all the eight cases defined above. Table 3.4 gives a comparison of the LMI control to this system when the traditional SMA approach is applied with that which is obtained when the proposed algorithm is applied to it. From the results it becomes clear that by reducing the system to two-thirds of its initial size the computational time has been reduced by a factor of eight.

Table 3.4: Comparison of proposed algorithm with traditional SMA approach for 16-machine system

	Traditional SMA + LMI Control	**Proposed Algorithm + LMI Control**
System Size (A_1)	30×30	20×20
Size of individual LTI system	47×51	32×33
Size of Polytopic System	47×417	32×273
Size of Closed Loop System	47×337	32×225
CPU Time* (seconds)**	606.328895	75.493861

*** The computations were performed on an Intel (R) Core ™ i5 Processor having a speed of 2.40 GHz and an installed memory (RAM) of 5.86 GB

Reduction factor: It is used to determine the relationship between the dimensions of the full-order and the reduced-order systems and the computational time required for the LMI control to work on both the systems. This is a quantitative measure of the efficiency of the proposed technique. If S_1 denotes the dimension of the full-order system and S_2, the dimension of the reduced-order system, then mathematically, the reduction factor n can be defined as,

$$n = \frac{\ln(T_1) - \ln(T_2)}{\ln(S_1) - \ln(S_2)} \tag{3.3}$$

Where T_1 and T_2 denote the computation time for the full-order and reduced order systems

The reduction factor n for the 16-machine system is found to be –

$$n = \frac{\ln(606.328895) - \ln(75.493861)}{\ln(15) - \ln(10)}$$

$$=> n \approx 5.14$$

Typically, the reduction factor was found to be in the range of 4-5. It was found to decrease slightly as the size of the optimization problem was increased.

Figures 3.12 and 3.13 show the eigenvalues of the closed loop matrices for the eight cases denoted in Table 3.1 for the full-order and the reduced-order systems respectively. Fewer eigenvalues appear in Fig. 3.13 because of the proposed algorithm. The conic region is used as the LMI region for pole placement. It is obvious from Fig. 3.13 that all the closed-loop poles lay in the LMI region.

Fig. 3.12: Closed-Loop eigenvalues for the 8 cases of the (15+1) machine system

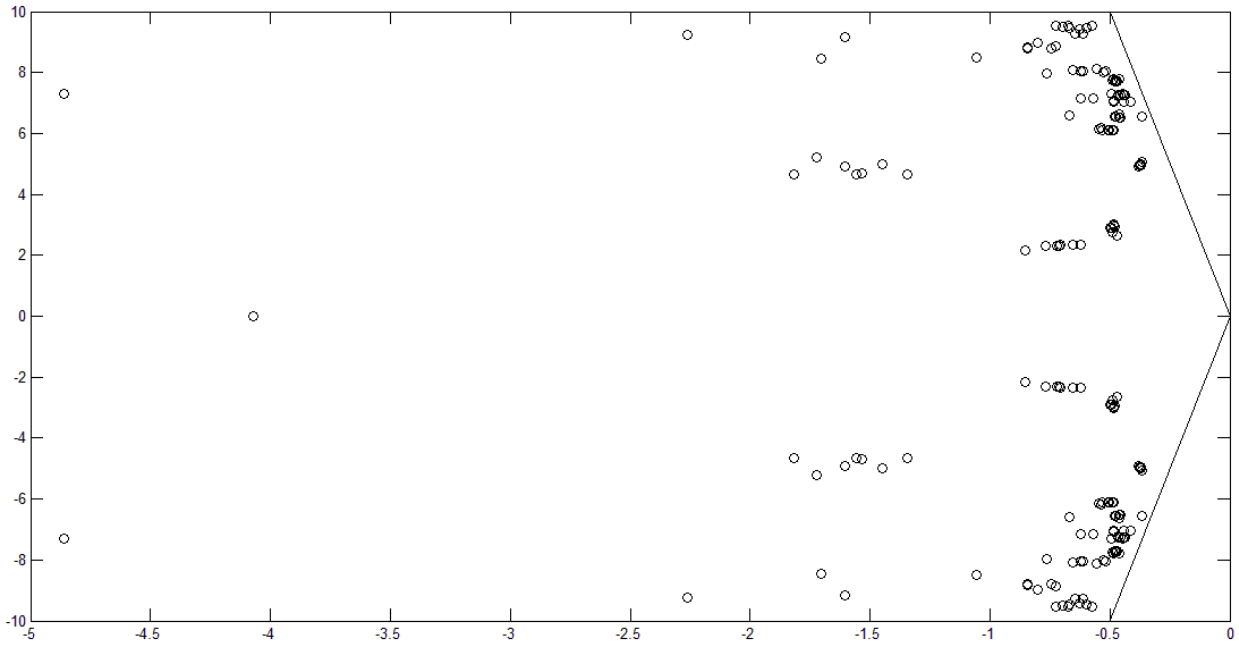

Fig. 3.13: Closed-Loop eigenvalues for the 8 cases of the (10+1) machine system

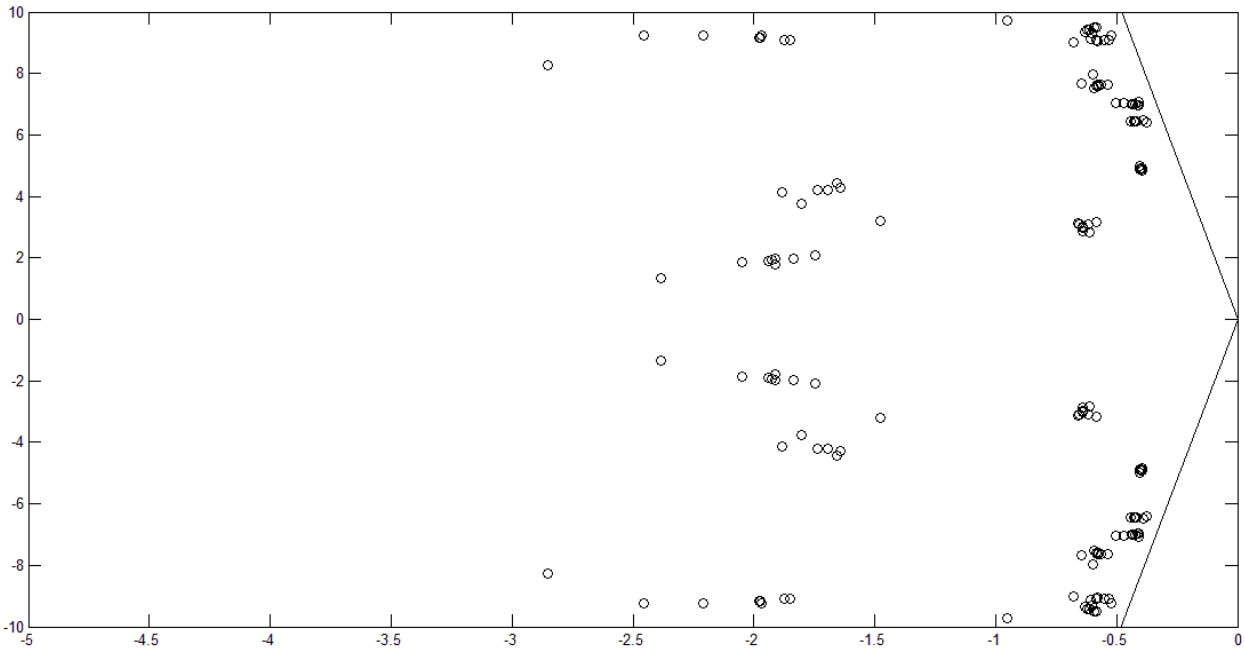

The root loci starting at the eigenvalues of the original system as the feedback gain is increased to its final values for all the eight cases for the reduced order system are shown in Figs. 3.14-3.21. The circles denote the starting positions and the dots represent the trajectory followed as the gain is increased. The

plots confirm the fact that the control described in this thesis successfully damps all the low frequency inter-area modes of oscillations present in the test system. Some of the local modes do move towards the right but none of them become unstable. Thus, it can be inferred that although one-third of the machines originally present in the system have been removed, the proposed control is robust enough to keep the system stable under a wide variety of contingencies. Also, the fact that the computational complexity has been reduced by a large factor implies that this technique can be readily applied to bigger systems.

Fig. 3.14: Root Locus plot for Case 1 using the proposed algorithm

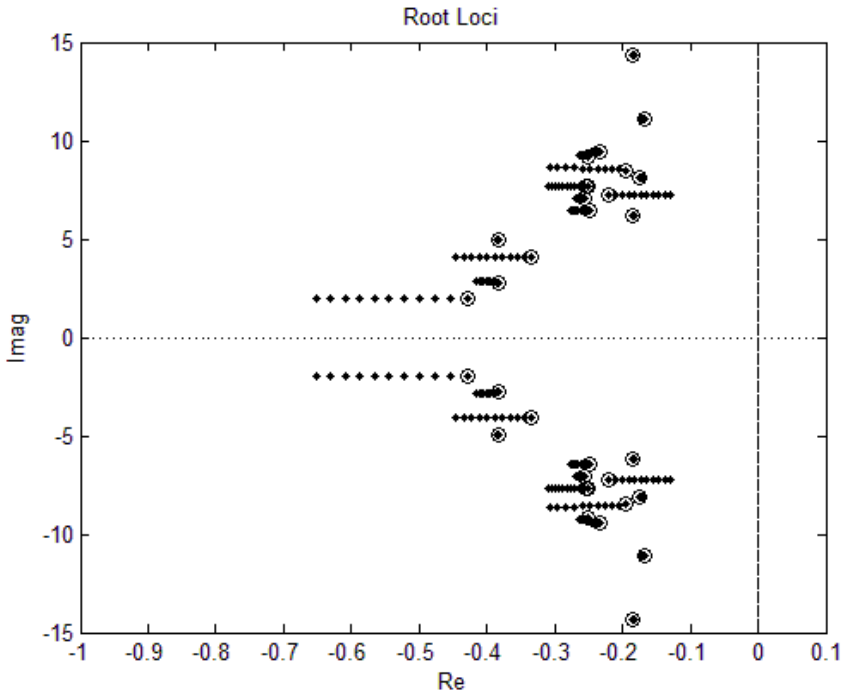

Fig. 3.15: Root Locus plot for Case 2 using the proposed algorithm

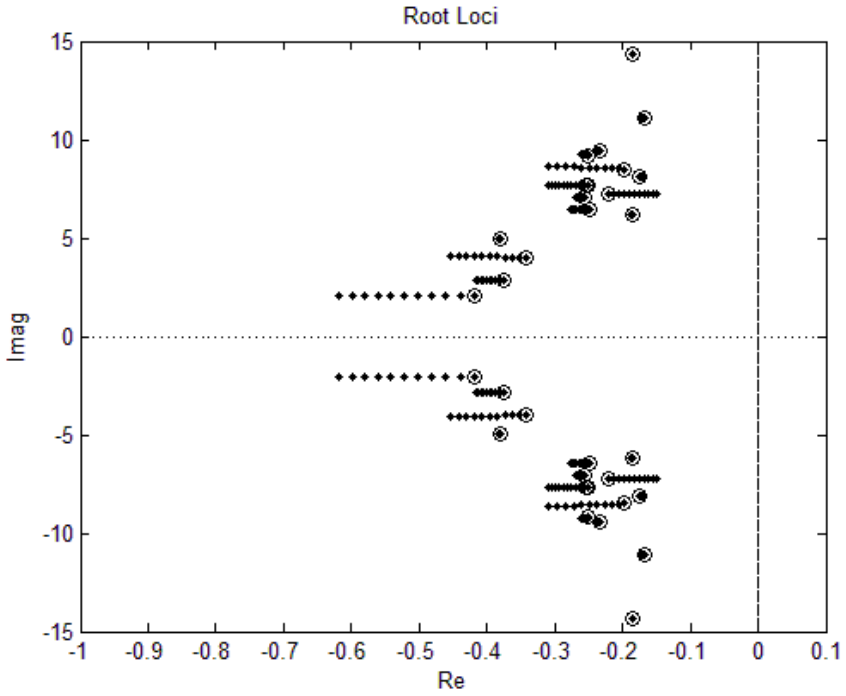

Fig. 3.16: Root Locus plot for Case 3 using the proposed algorithm

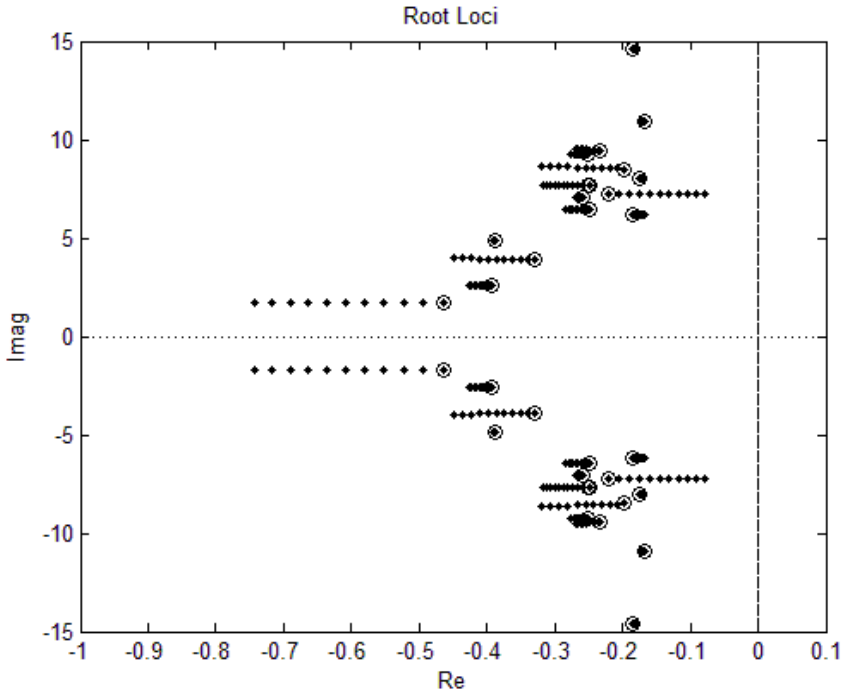

Fig. 3.17: Root Locus plot for Case 4 using the proposed algorithm

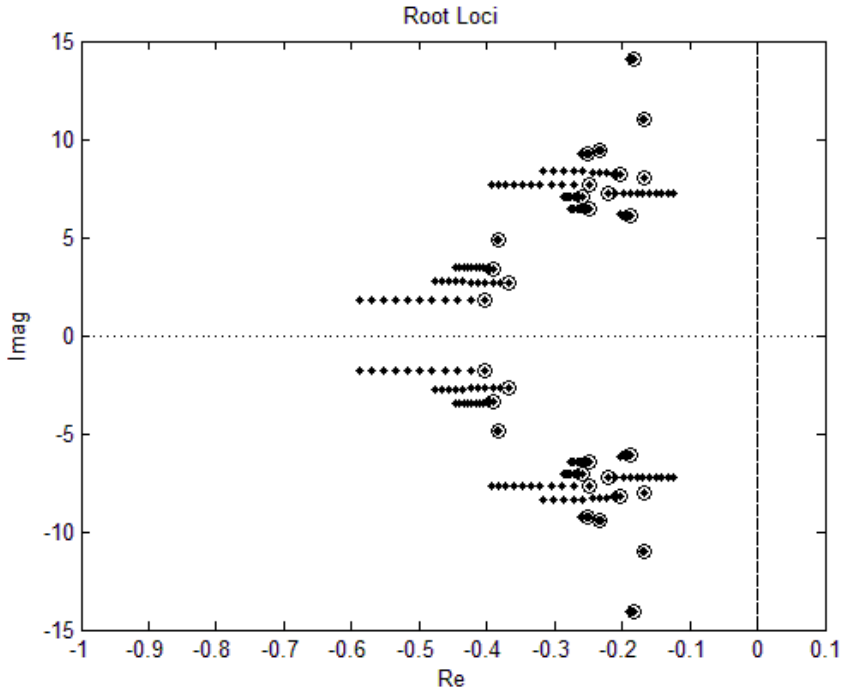

Fig. 3.18: Root Locus plot for Case 5 using the proposed algorithm

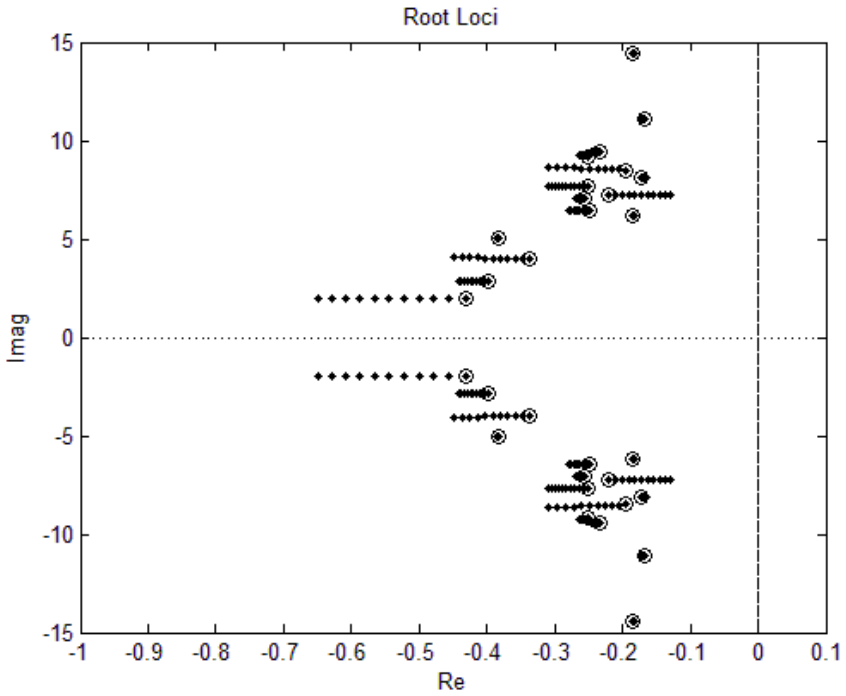

Fig. 3.19: Root Locus plot for Case 6 using the proposed algorithm

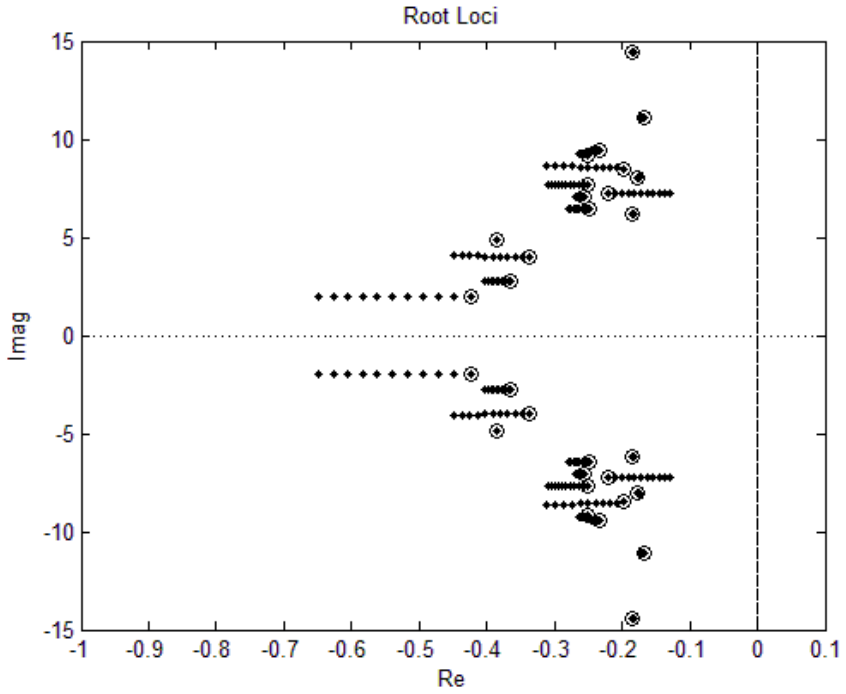

Fig. 3.20: Root Locus plot for Case 7 using the proposed algorithm

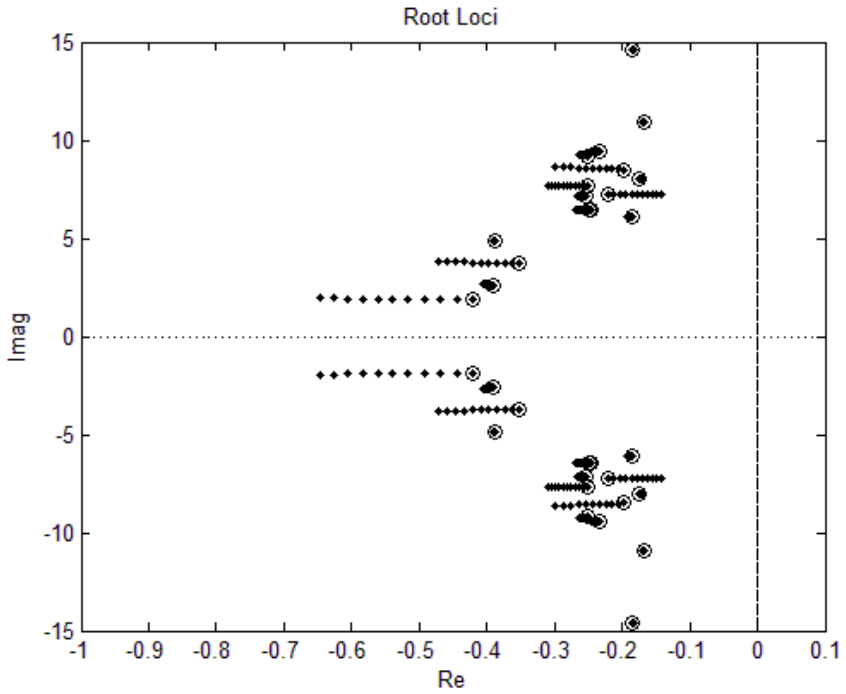

Fig. 3.21: Root Locus plot for Case 8 using the proposed algorithm

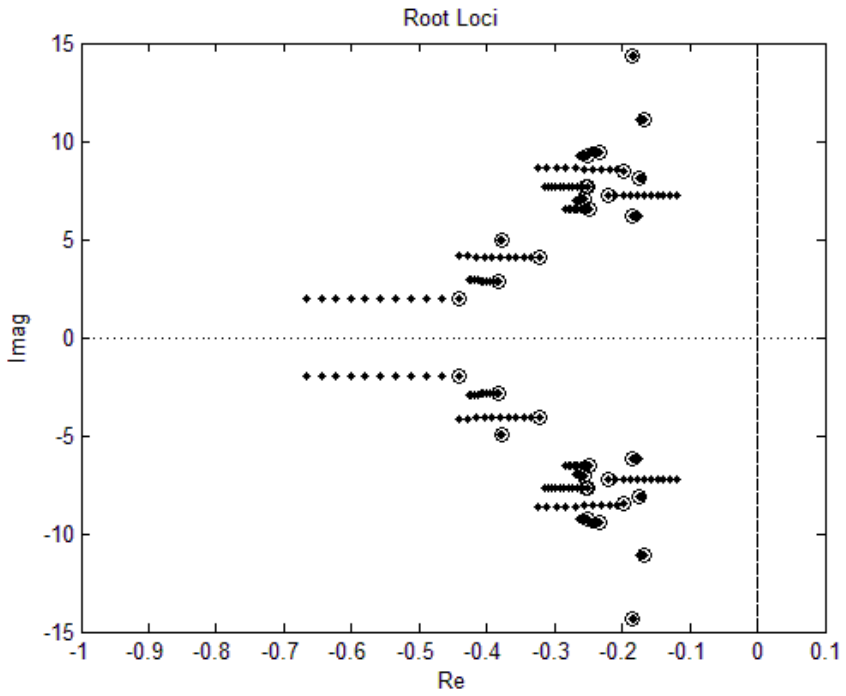

3.2 Conclusion

This chapter describes in details the algorithm that is proposed in this thesis. The devised method reduces the size of the polytopic system to its smallest possible stable state so as to alleviate the issue of computational complexity which prevents application of LMI control to large systems. A moderately sized 16 machine, 68 bus system which is an equivalent model of the New England-New York inter-connected power system is used as the test case with DC lines and SVCs acting as the controls for this system. The system is reduced to two-thirds of its initial size using the proposed technique and subjected to a variety of contingencies. The results show that all the low-frequency inter-area modes of oscillations are adequately damped along with most of the local modes. The fact that such a reduced version of the original system is capable of producing such good control is an indication of the robustness of the method developed herein. Moreover, the enormous reduction in computational time implies that this method can now be readily applied to larger and more complex real-life systems as is done in the next chapter.

Chapter 4 – Simulation Results for 29 Machine WECC System

The previous chapter described the application of the proposed algorithm on a benchmark power system problem. The control designed for the 16 machine, 68 bus system was found to be sufficiently robust to justify attempting to apply this technique to larger systems. In this chapter, the technique is applied to a reduced-order model of the WECC system comprising of 29 machines and 127 buses. The single-line diagram of the system is shown in Fig. 4.1. The detailed data of the system is given in the appendix.

4.1 The 29 Machine Model of the WECC System

The system consists of 29 machines, 127 buses and 215 lines. It has a generating capacity of 61.4 GW with a load of 60.8 GW, the difference between the two being accounted for by the losses of the system. It contains two HVDC lines extending from Celilo in the North to Sylmar in the South and from Inter-mountain in the East to Adelanto in the South-West. An SVC is also located at Adelanto. It is a relatively older network that was developed in [55] for analyzing the low frequency interaction phenomena between DC links and the electro-mechanical stability cases. Typical line and machine parameters were adopted and the controllers tuned to guarantee a stable base-case. Moreover, the machines depicted in this system are equivalents of the actual machines present in the real world. The California model is represented by a 12 machine, 60-bus network whereas the “rest of WECC” is depicted by a 17 machine, 67-bus network. The inter-ties connecting California with the “rest of WECC” were identified as the critical tie-lines of the system. The HVDC lines of the network were modeled as constant PQ loads at Celilo and Sylmar (representing the Pacific DC Intertie) and at Inter-Mountain & Adelanto (representing the Inter Mountain-Adelanto HVDC line).

The control developed for this system had two main objectives –

a) Ensure a specified percentage of damping on all the low frequency modes of oscillations. For e.g., if the minimum damping of all the modes was at-least (say) 5% then the minimum damping percentage of all the modes after the application of the control should be at-least (say) 7.5%
b) Provide more damping to the inter-area modes of oscillation. For e.g., if the minimum damping of the inter-area modes was (say) 5%, then after the application of the control, it should be around (say) 15%

In order to test the proposed control along these objectives, a variety of contingency cases were identified. These included outage of critical tie-lines, changes in line flows of important lines, increase/decrease of loads in key areas etc. A polytope comprising of these cases was then used for the development of the control. The eight cases that were selected to test the robustness of the control are summarized in Table 4.1.

Fig. 4.1: Single-Line Diagram of the 127-Bus WECC System [56]

(Courtesy of Dr. David Elizondo)

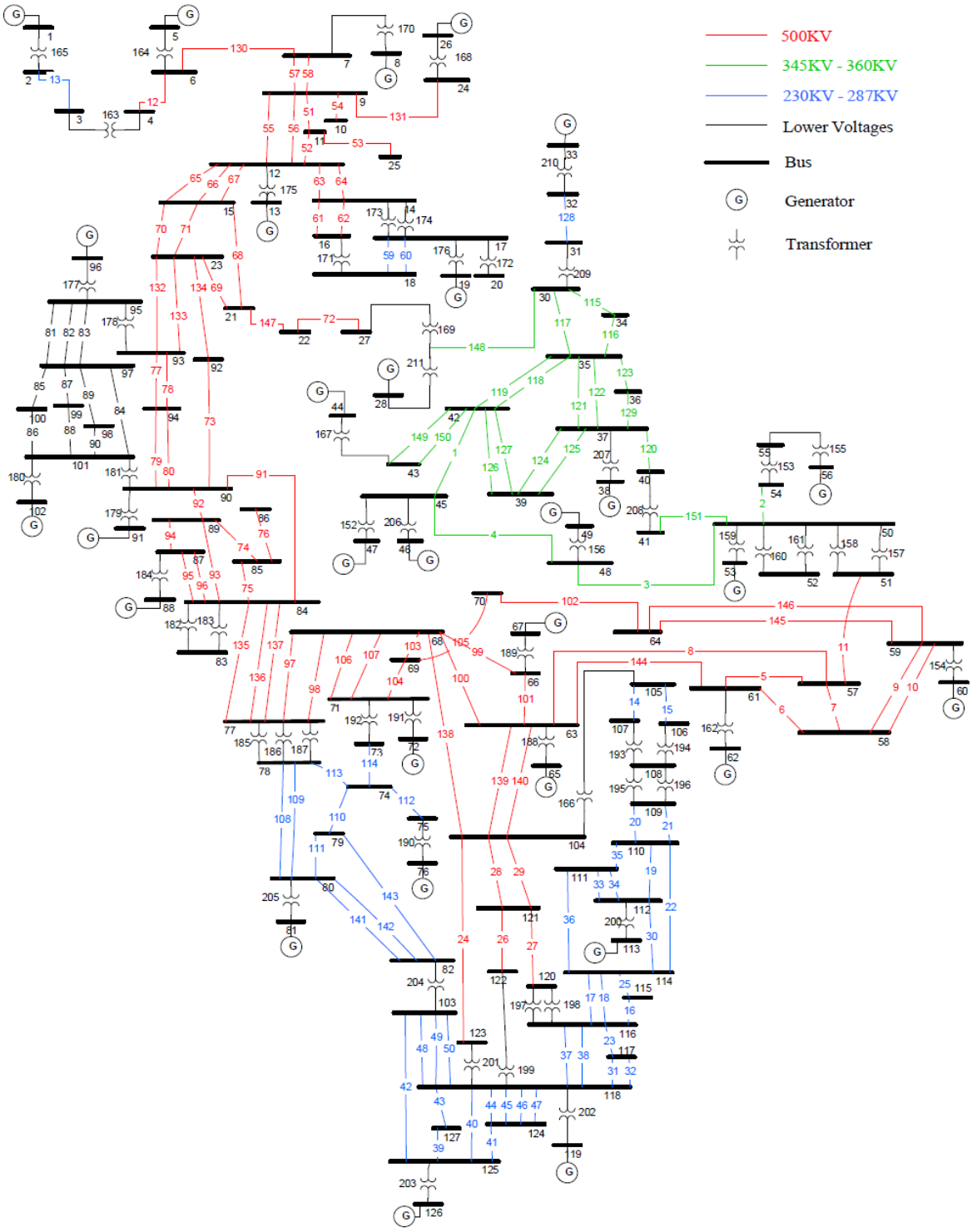

Table 4.1: Case Bank for the 29 machine WECC system

Case Number	Case Details
1	No-Contingency Case
2	Outage of Tie-line 59-64
3	Outage of Tie-line 77-84
4	Outage of Line 12-15
5	Flow in Line 12-14 decreased by 250 MW
6	Flow in Line 12-14 increased by 250 MW
7	Loads at Buses 6 and 7 decreased by 10%
8	Loads at Buses 6 and 7 increased by 10%

4.2 Three-Element Control

Since two HVDC lines and one SVC were already present in the system, they were chosen as the preferred forms of control. The $A, B, C,$ and D matrices for this system had dimensions of 171×171, 171×6, 29×171, and 29×6 respectively. Using the traditional SMA approach described in Chapter 2, the A matrix was partitioned into A_1, A_2, A_3 and A_4, each having dimensions of 56×56, 56×115, 115×56, and 115×115 respectively.

Fig. 4.2 shows a portion of the eigenvalues of the A matrix corresponding to the no-contingency case highlighting the oscillatory modes for this system. The black dots represent the eigenvalues of the A matrix whereas the red circles denote the eigenvalues of the A_1 matrix. It becomes clear from the figure that the traditional SMA approach has been successful in identifying the oscillatory modes present in the system. In order to apply the proposed algorithm, Table 4.2 was constructed to denote the participation percentage of the generators for the different frequencies similar to what was done for the 16 machine example system described in the previous chapter. The machines to be dropped from the LMI control logic are summarized in Table 4.3.

Fig. 4.2: Eigenvalues of the 29 machine system corresponding to the base case

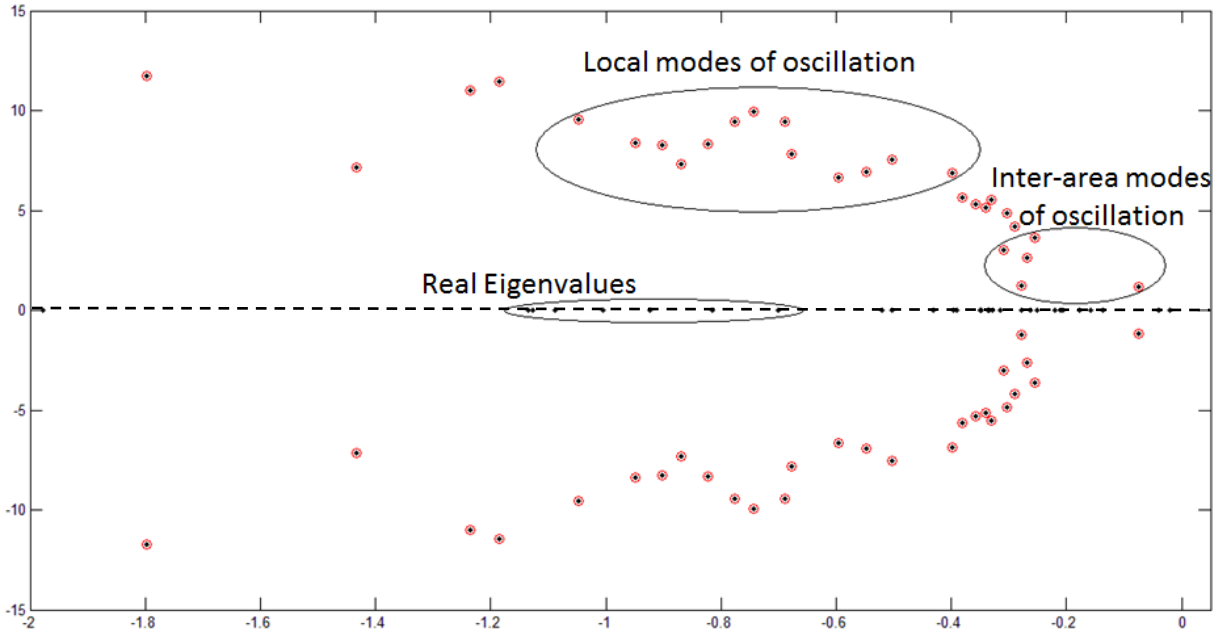

Table 4.2: Frequency-Participation Percentage Table for the Base Case of the 29-machine system

Serial Number	Frequency (in Hz)	Bus Number based on Participation Factor %																											
1	1.9415	119	81																										
2	1.7999	46	47	49																									
3	1.7443	49	53	46	47																								
4	1.7267	19	33																										
5	1.5622	38	44																										
6	1.4531	113	72	81	126	62																							
7	1.3933	81	126	72	62	67	113																						
8	1.3446	72	126	81	113	62	88	28	76	67	53	13	56	49															
9	1.3384	102	91																										
10	1.3112	62	53	126	67	49	56	60	72	65	88																		
11	1.2584	28	13	44	91	38	88	72	8	126	96	33	67	81	62														
12	1.2352	56	53	49	62	67	126	60	44	65	47	72	88	81	91														
13	1.1910	88	126	81	72	113	91	67	96	76	56	102	62	119	65	13	53												
14	1.1552	91	13	96	102	8	28	88	126	67	19	26	113	72	5	44	81	38	76	56									
15	1.1001	33	44	38	96	13	56	47																					
16	1.0996	96	13	33	19	44	102	38	28	126	8	67	91	81															
17	1.0765	88	67	126	81	72	76	113	96	65	8	91	56	28	13	62	119	26	5	44	33								
18	1.0434	65	67	81	88	126	72	76	60	113	13	96	62	91	56														
19	0.9595	8	13	5	96	91	65	28	76	19	33	44	38	102	72	113	88	126											
20	0.8761	56	65	53	49	67	47	8	60	33	46	76	5	44	38	81	72	126	28	88	113	91							
21	0.8676	76	60	65	67	47	62	46	91	56	53	26	72	81	96	113	49	44	13	38									
22	0.8340	60	65	67	56	53	76	47	49	46	8	5	62	81	72	88	113	126											
23	0.8220	33	47	44	38	46	5	8	91	28	60	76	13	65	102	96	67	88	81	19									
24	0.7966	5	13	91	28	47	96	60	19	46	102	76	33	53	56	8	44	38	49	26	1	88							
25	0.6648	26	76	47	91	60	46	38	53	44	28	56	49																
26	0.5318	47	46	44	38	76	60	33	26	53	65	49	67	56	28	5	81	62	72	8	126	88	113	91					
27	0.4435	5	8	60	13	76	1	26	91	65	62	67	53	56	28	47	19	96	49	72	81	46	102	126	113				
28	0.2138	1	60	76	65	62	67	91	26	53	72	47	81	5	49	56	13	38	88	44									
29	0.0000	1	8	60	5	91	76	13	65	67	62	26	72	81	53	28	88	47	38	44	49	56	96	102	19	126	46	113	33	119

Table 4.3: Sequence to be followed for dropping machines for the 29-machine system

Serial Number	Machine Number
1	119
2	19
3	33
4	113
5	126
6	102
7	65
8	81

Figure 4.3 denotes the application of the traditional SMA algorithm to the 29-machine WECC system. The transition in the selection of the eigenvalues in accordance with the proposed algorithm is depicted in Figs. 4.4-4.11. Fig. 4.12 shows the effect of applying a rudimentary control (LQR optimization) to the system obtained in Fig. 4.10. The red dots denote the feedback to the reduced-order system whereas the green circles denote the feedback to the complete system. The blue squares denote the starting positions. It becomes clear from the figure that the proposed control obtained from the reduced-order system successfully moves all the low frequency modes of oscillations to the left thereby increasing the damping of the inter-area modes. Although some of the high frequency local modes of oscillations move towards the right, none of them cross the imaginary axis. Figure 4.13 illustrates the effect of dropping one more machine, on the control for the system described by Fig. 4.11. It is clear from these figures that the smallest number of machines that is to be controlled for a stable operation of this system is 21. That is, using the technique developed in this thesis, the first seven machines mentioned in Table 4.3 could be safely dropped from the LMI control.

The system size reduction performed above for the no-contingency case was then applied to the remaining seven cases. By doing so, all the eight cases were reduced to have a 42×42 A_1 matrix. In essence, this implied that the system had been reduced from a 28 machine system to a 21 machine system (with one machine being the reference). Every A_1 matrix now contained the angles and frequencies of only those machines which corresponded to the significant modes of oscillations. Therefore, we were now in a position to apply the LMI control to this reduced-order system.

Fig 4.3: Applying proposed algorithm to reduce system size for base case – 28 machine system

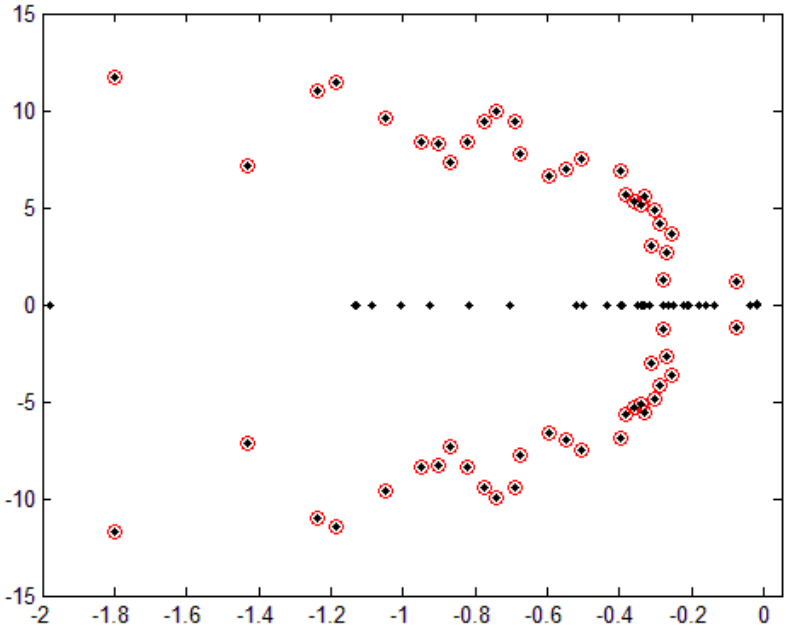

Fig 4.4: Applying proposed algorithm to reduce system size for base case – 27 machine system

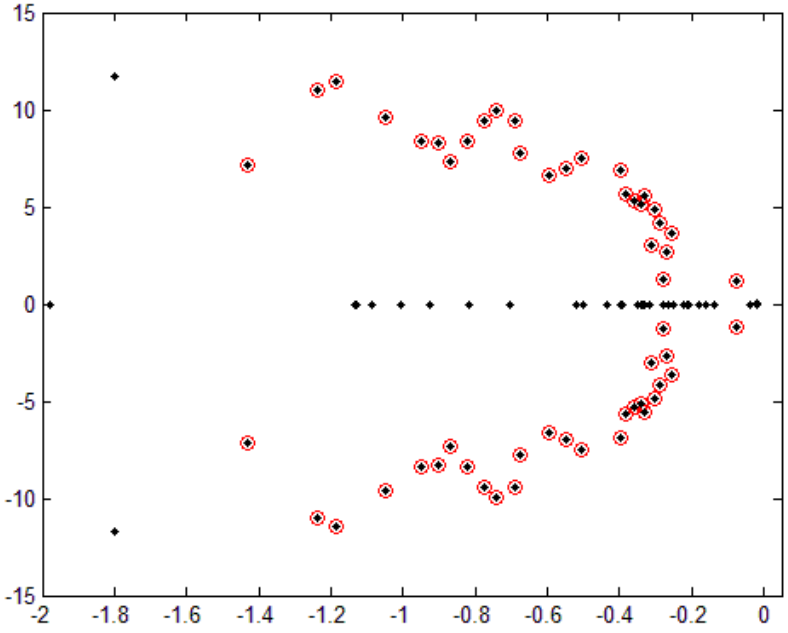

Fig 4.5: Applying proposed algorithm to reduce system size for base case – 26 machine system

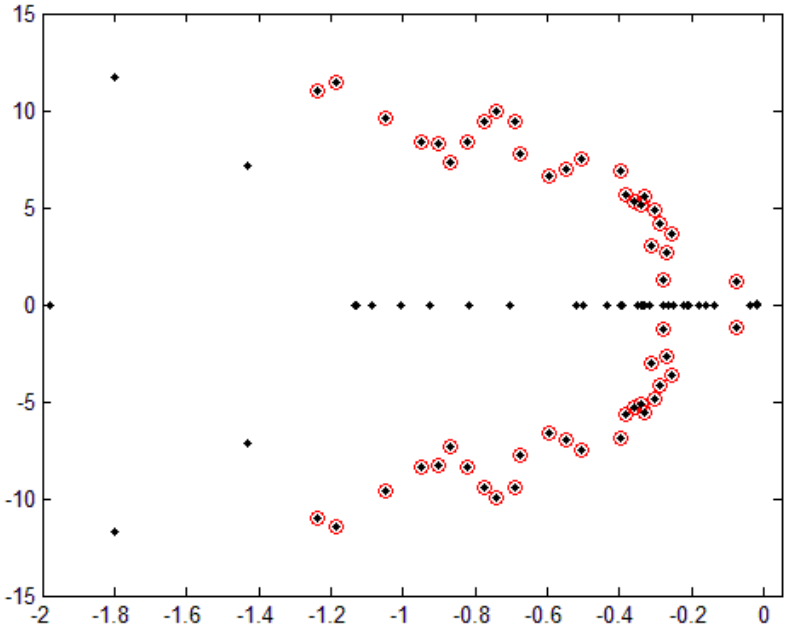

Fig 4.6: Applying proposed algorithm to reduce system size for base case – 25 machine system

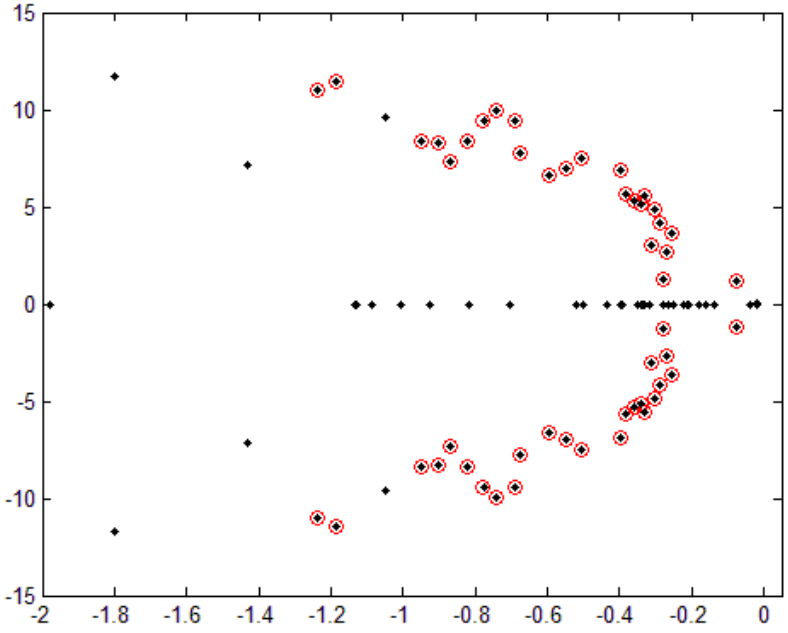

Fig 4.7: Applying proposed algorithm to reduce system size for base case – 24 machine system

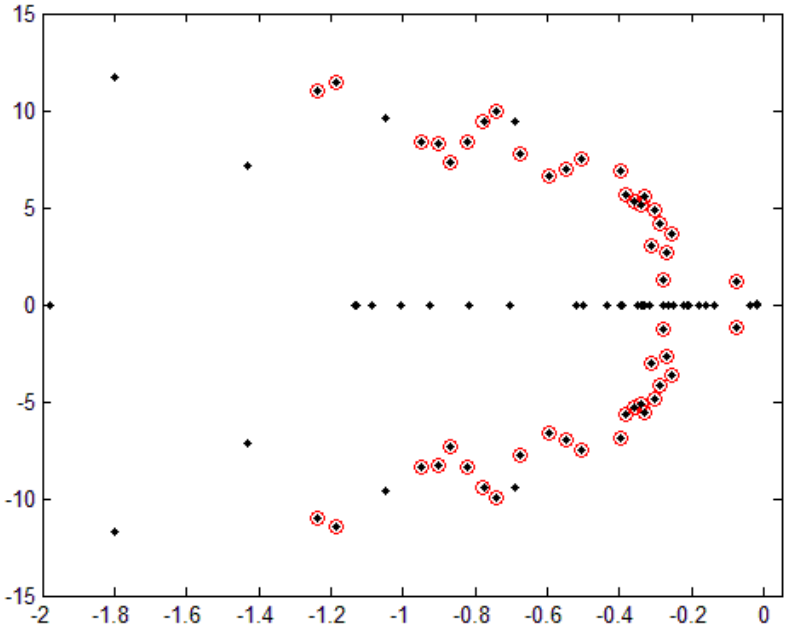

Fig 4.8: Applying proposed algorithm to reduce system size for base case – 23 machine system

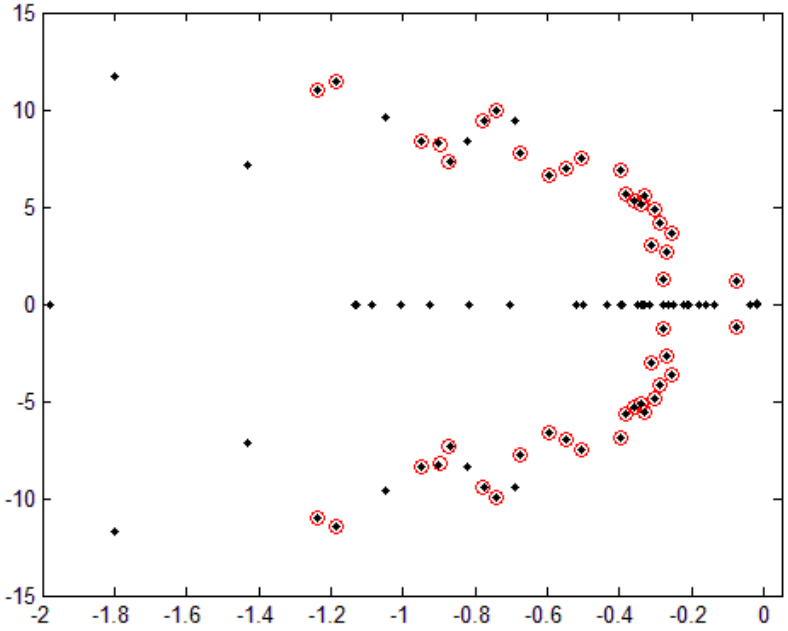

Fig 4.9: Applying proposed algorithm to reduce system size for base case – 22 machine system

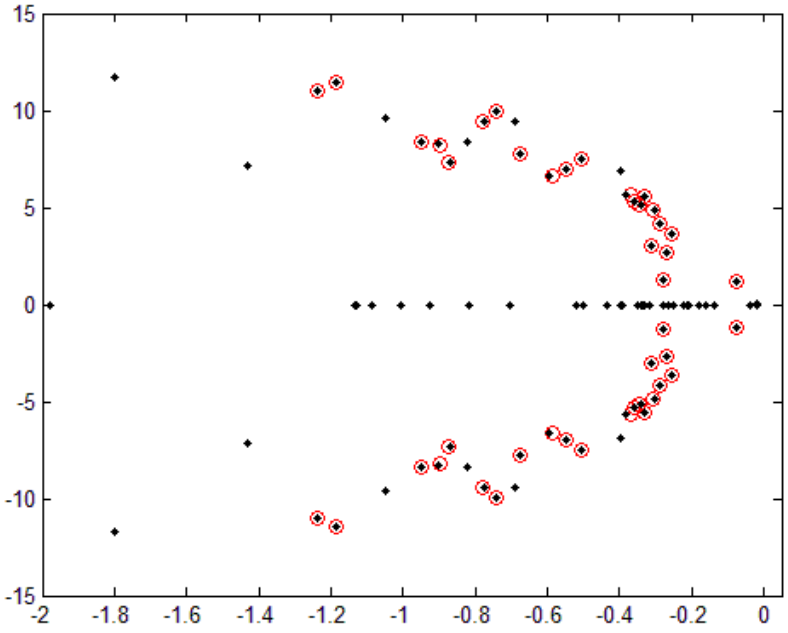

Fig 4.10: Applying proposed algorithm to reduce system size for base case – 21 machine system

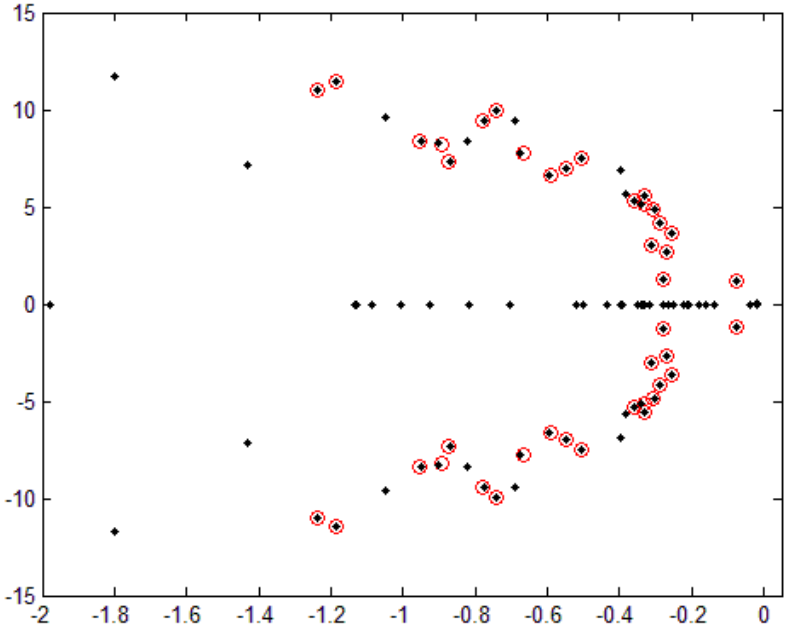

Fig 4.11: Applying proposed algorithm to reduce system size for base case – 20 machine system

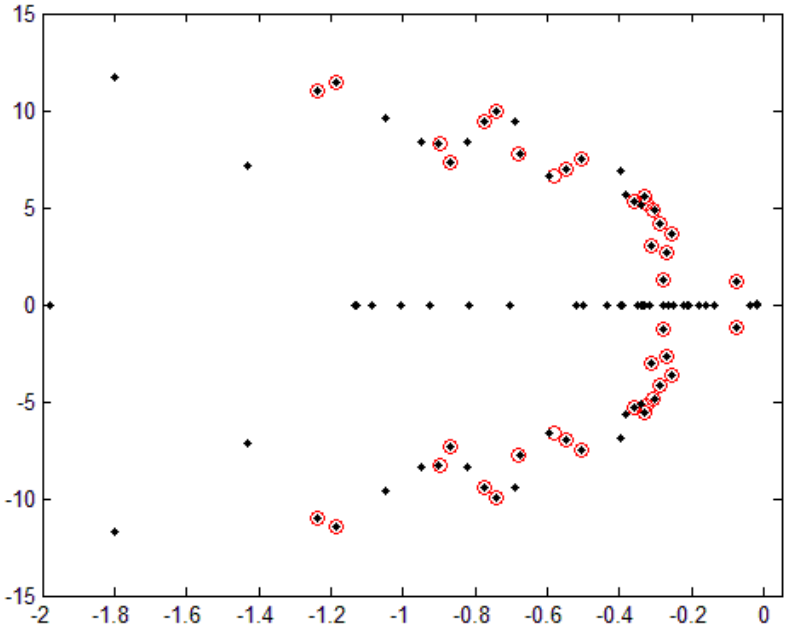

Fig. 4.12: Applying control check described in Step 4 of proposed algorithm to 21 machine system

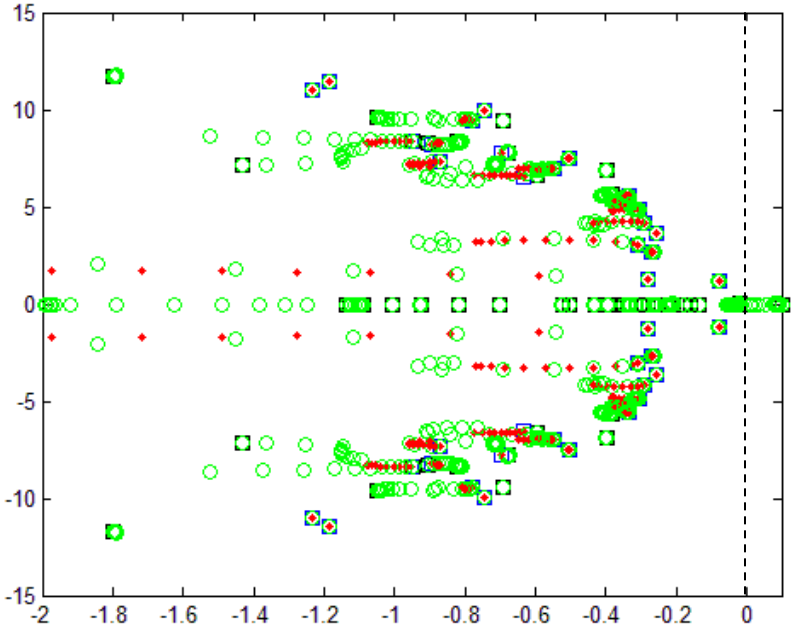

Fig. 4.13: Applying control check described in Step 4 of proposed algorithm to 20 machine system

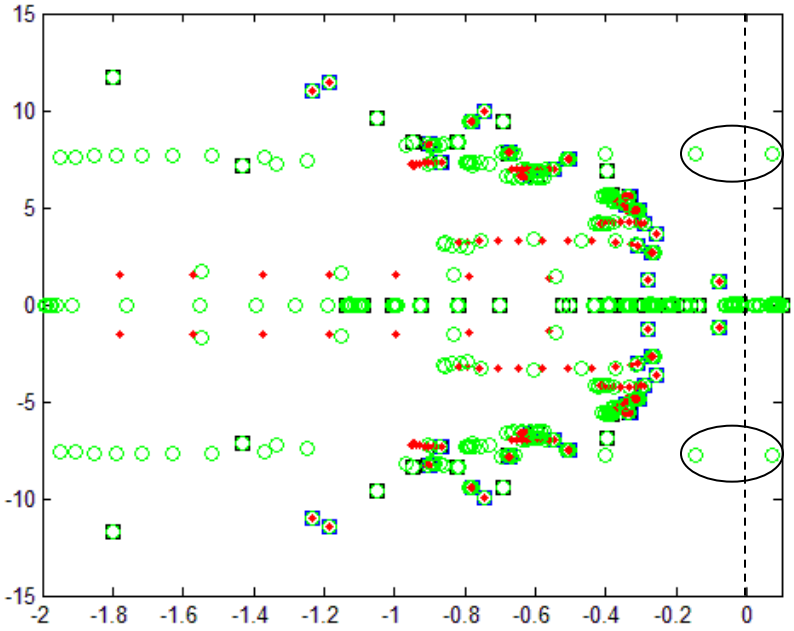

Each of the LMI problems with 42 retained states is described by a 65×49 LTI system. The collection of the eight cases results in a 65×401 polytopic system while the closed loop system has a size of 65×377. The LMI optimization yields a single feedback gain matrix for all the eight cases defined in Table 4.1. Figure 4.14 shows the eigenvalues of the closed loop matrices for the reduced-order system when the control has not been forced. Fig. 4.15 depicts the same reduced-order system when the three-element control has been forced onto it.

On comparing the two figures, it is realized that although all the eigenvalues attain the minimum desired amount of damping (7.5%) on the application of the control, some of the more critical modes remain relatively unaffected. The most acute amongst the latter group being the lowest frequency inter-area mode which had much less damping (≈8%) than what it was expected to have (about 15%) on the application of the control. The inference drawn from these results was that the three elements used for the control were not enough for providing the requisite amount of damping to all the low frequency inter-area oscillations present in the system. It therefore became necessary to add more number of controls into the system.

Fig. 4.14: Closed loop eigenvalues for the reduced-order system when control is not forced on it

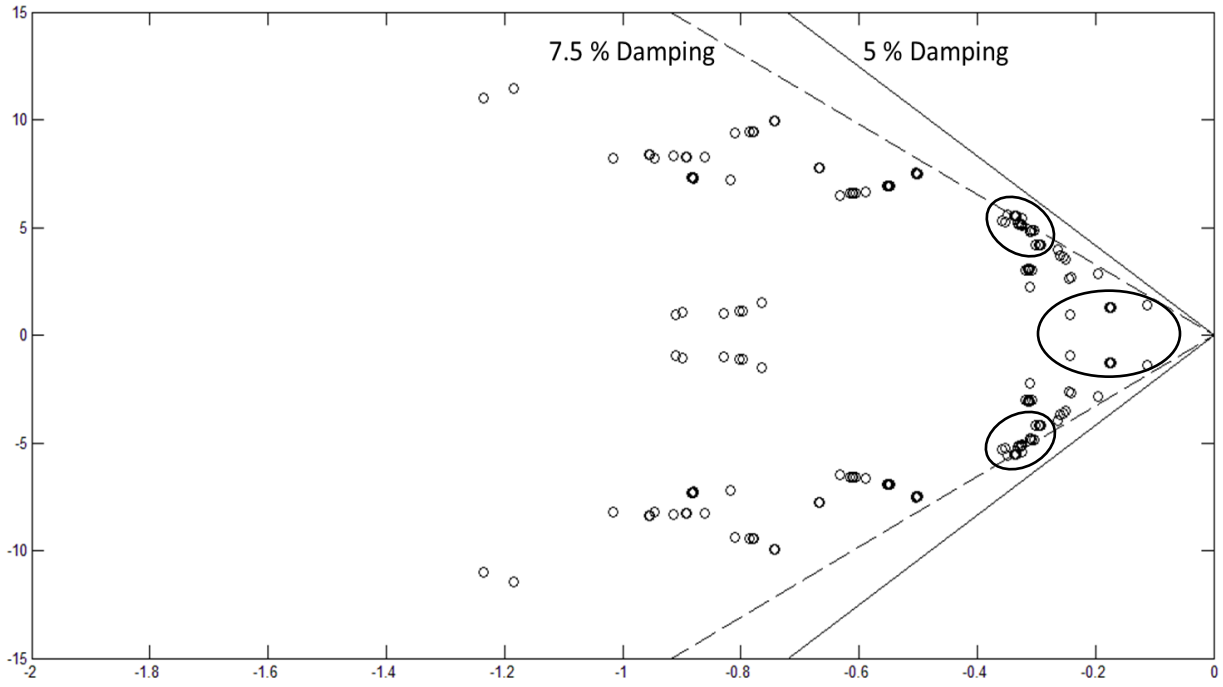

Fig. 4.15: Closed loop eigenvalues for reduced-order system when 3-element control is forced on it

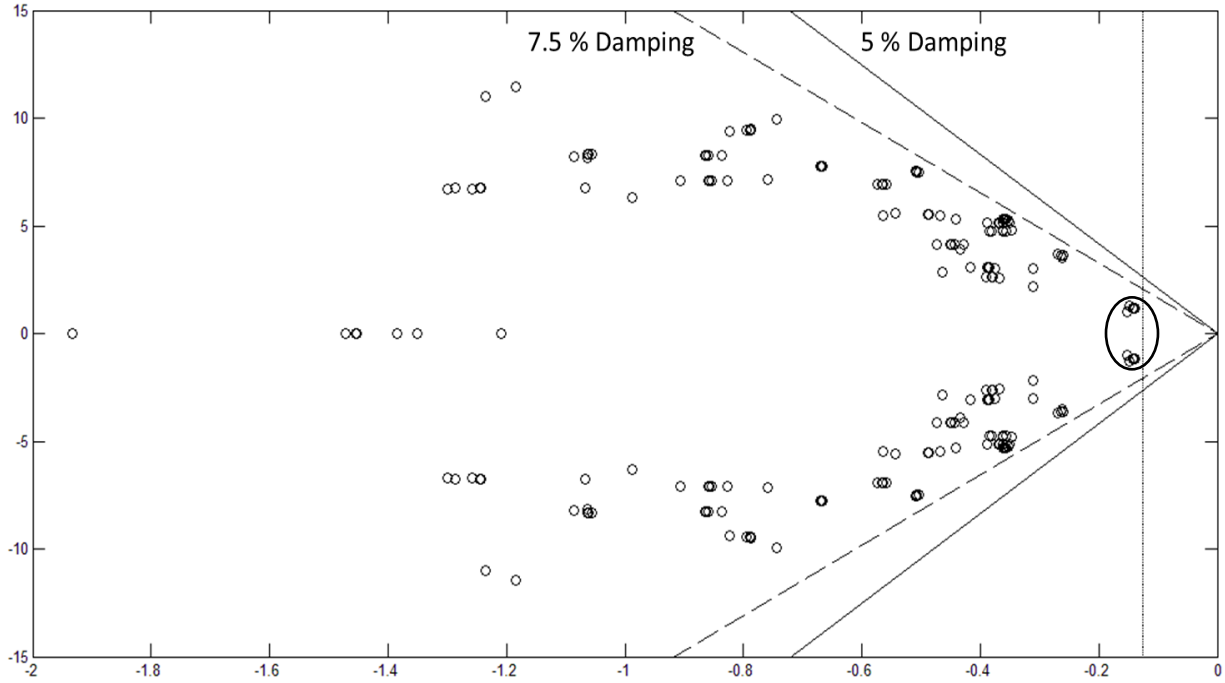

4.3 ESDs as a form of Control

The inference that was drawn from the previous section was that for the 29 machine model of the WECC system, the three elements selected for control purposes were not enough for providing the requisite amount of damping to the various low frequency inter-area modes of oscillations present in the system. Therefore, in order to achieve the desired control objectives, there is a need for introducing more number of controls. The solution to this problem was found in the addition of Energy Storage Devices (ESDs) into the system.

Use of ESDs as a form of control has been proposed for quite some time now. While they do not necessarily represent energy sources, these devices provide valuable added benefits to improve stability, power quality, and reliability of supply. To illustrate, when power system disturbances occur, synchronous generators are not always able to respond rapidly enough to keep the system stable. If a high-speed real or reactive power control is available, load shedding or generator dropping may be avoided during the disturbance. Flexible AC Transmission Systems (FACTS) devices make high speed reactive power control possible, but their role in the control of real power is limited. In such situations, a better solution is to introduce ESDs into the systems which have the ability to rapidly vary real power without impacting the power circulation. Thus, they can play a very important role in maintaining system reliability and power quality [57].

In recent times, with the significant reduction in the capital cost of ESDs, they are becoming a viable solution for modern power applications. Being composed of static elements, they have a much faster dynamic response when compared to other storage devices [58]. The four types of ESDs which have been reckoned to have great potential in the domain of power systems are –

Super-conducting Magnetic Energy Storage (SMES) Systems

Battery Energy Storage Systems (BESS)

Advanced Capacitors (AC)

Fly-wheel Energy Storage (FES) Systems

Although several of these technologies were initially envisioned for large-scale load-leveling applications, they are now been seen more as a tool to enhance system stability, aid power transfer, and improve power quality in power systems [59-62]. In addition to all this, it has now been realized that ESDs can also be used to increase the system damping of undesirable inter-area oscillations as a cost-effective damping controller [59-60].

But just like with the other types of controllers proposed earlier, local or un-coordinated control strategies can cause destabilizing interactions among the ESDs. The damping of oscillations can be adversely

influenced by negative interactions within the ESD controls. In addition to this, the controllers might fail to produce adequate damping due to variations in generation and load patterns and changes in transmission networks [63]. However, the coordinated form of control proposed in this thesis appears to perfectly counter such adverse effects. Therefore, with the aid of PMUs and WAMS, it is proposed in this thesis that ESDs can be used in the integrated control design just like the DC lines and the other FACTS devices described herein.

An important issue that needs to be addressed before using ESDs as a form of control is the criteria for "site selection". The intended system application influences the required number of installations. A judicious choice of locations is necessary to meet the criteria of cost and intended applications. The focus is therefore on damping many inter-area modes with fewer ESDs. Courtesy WAMS, it is now possible for a relatively small number of synchronized stabilizing signals from different locations of power systems to be coordinated to damp a relatively large number of inter-area modes [64]. Moreover, it has also been proved that remote signals are more effective than local signals for damping out inter-area oscillations [65-68]. Keeping this in mind, the concept of Controllability Indices described in [22] is used in this thesis to identify the best locations for the ESDs.

The Geometric Measure of Controllability (GMC) associated with the inter-area mode k is given by [22],

$$GMC_i(k) = \cos\big(\alpha(\psi_k, b_i)\big) = \frac{|b_i^T \psi_k|}{\|b_i\|\|\psi_k\|} \tag{4.1}$$

Where b_i is the i^{th} column of the input matrix B, ψ_k is the left-eigenvector associated with the mode k, and $\alpha(\psi_k, b_i)$ is the geometric angle between the i^{th} input vector and the k^{th} left eigenvector. $\|\psi_k\|$ and $\|b_i\|$ are the Euclidean Norms of ψ_k and b_i respectively whereas $|b_i^T \psi_k|$ denotes the modulus of $b_i^T \psi_k$. Then, in accordance with the concept of controllability indices, the most suitable locations of ESDs with respect to the critical inter-area modes were found to be the generators with the highest GMC [22].

4.4 Six-Element Control

The results obtained on applying this concept to the 29 machine WECC System is shown in Table 4.4. From the table, it is realized that buses 1, 5 and 76 (highlighted in bold) are the best locations for adding the ESDs into the system. Since the system matrix had to be modified to incorporate the presence of the three ESDs, the dimensions of all of its derivative matrices had to be recomputed. The new dimensions of A, B, C, and D matrices were found to be 174×174, 174×12, 29×174, and 29×12 respectively. Similarly, the new dimensions of A_1, A_2, A_3 and A_4, were found to be 56×56, 56×118, 118×56, and 118×118 respectively. However, since the addition of ESDs into the system did not change the participation factors of the machines or the frequencies of the oscillations, Table 4.2 and 4.3 remained the same.

Table 4.4: Normalized GMCs corresponding to the three lowest inter-area modes

Mode 1		Mode 2		Mode 3	
Bus Number	**GMC**	**Bus Number**	**GMC**	**Bus Number**	**GMC**
1	**1.0000**	**5**	**1.0000**	**76**	**1.0000**
91	0.0169	8	0.1353	60	0.4967
5	0.0161	1	0.0501	67	0.3292
60	0.0154	91	0.0293	126	0.3106
19	0.0136	60	0.0239	88	0.2315
44	0.0135	126	0.0173	62	0.2255
126	0.0118	76	0.0162	72	0.1820
76	0.0115	81	0.0145	91	0.1277
8	0.0114	88	0.0120	102	0.1114
81	0.0099	72	0.0116	113	0.0943
72	0.0088	44	0.0112	81	0.0827
38	0.0064	65	0.0093	44	0.0815
113	0.0063	113	0.0091	53	0.0645
102	0.0055	26	0.0083	28	0.0489
65	0.0051	62	0.0083	65	0.0394
62	0.0046	67	0.0080	38	0.0365
28	0.0045	28	0.0060	119	0.0333
96	0.0045	38	0.0027	19	0.0333
88	0.0044	96	0.0017	49	0.0299
67	0.0043	119	0.0017	8	0.0183
26	0.0026	102	0.0012	26	0.0151
33	0.0012	56	0.0010	96	0.0073
119	0.0012	19	0.0008	46	0.0072
46	0.0008	47	0.0008	47	0.0050
49	0.0006	33	0.0004	33	0.0044
53	0.0006	53	0.0004	56	0.0022
56	0.0004	46	0.0002	1	0.0021
47	0.0000	49	0.0001	5	0.0017

By applying the proposed algorithm in a manner similar to what was done for the three-element control, the A_1 matrix of all the eight cases was reduced to a dimension of 42×42. Then, each of the LMI problems with these 42 retained states is described by a 65×55 LTI system. The collection of the eight cases results in a 65×449 polytopic system while the closed loop system has a size of 65×401. The LMI optimization yielded a single feedback gain matrix for all the eight cases defined in Table 4.1. Table 4.5 gives a comparison of the LMI control to this system when the traditional SMA approach is applied with that which is obtained when the proposed algorithm is applied to it. From the results it becomes clear

that by reducing the system to three-fourths of its initial size the computational time has been reduced by a factor of about four.

Table 4.5: Comparison of proposed algorithm with traditional SMA approach for 29-machine system (with 6 controls)

	Traditional SMA + LMI Control	**Proposed Algorithm + LMI Control**
System Size (A_1)	56×56	42×42
Size of individual LTI system	86×69	65×55
Size of Polytopic System	86×561	65×449
Size of Closed Loop System	86×513	65×401
CPU Time* (seconds)**	5435.701939	1543.530256

*** The computations were performed on an Intel (R) Core ™ i5 Processor having a speed of 2.40 GHz and an installed memory (RAM) of 5.86 GB

The reduction factor n for the 29-machine system was found to be –

$$n = \frac{\ln(5435.701939) - \ln(1543.530256)}{\ln(28) - \ln(21)}$$

$$=> n \approx 4.3761$$

Figures 4.16 and 4.17 show the eigenvalues of the closed loop matrices for the eight cases denoted in Table 4.1 for the full-order and the reduced-order systems respectively. Fewer eigenvalues appear in Fig. 4.17 because of the proposed algorithm. The conic region is used as the LMI region for pole placement. It is obvious from Fig. 4.17 that all the closed-loop poles lay in the LMI region.

The root loci starting at the eigenvalues of the original system as the feedback gain is increased to its final values for all the eight cases for the reduced order system are shown in Figs. 4.18-4.25. The circles denote the starting positions and the dots represent the trajectory followed as the gain is increased. The plots confirm the fact that the control described in this thesis successfully damps all the low frequency inter-area modes of oscillations present in this system. Some of the local modes do move towards the right but none of them become unstable. Thus, it can be inferred that although one-fourth of the machines originally present in the system have been removed, the proposed control is robust enough to keep the system stable under a wide variety of contingencies.

Fig. 4.16: Closed loop eigenvalues for full-order system when 6-element control is forced on it

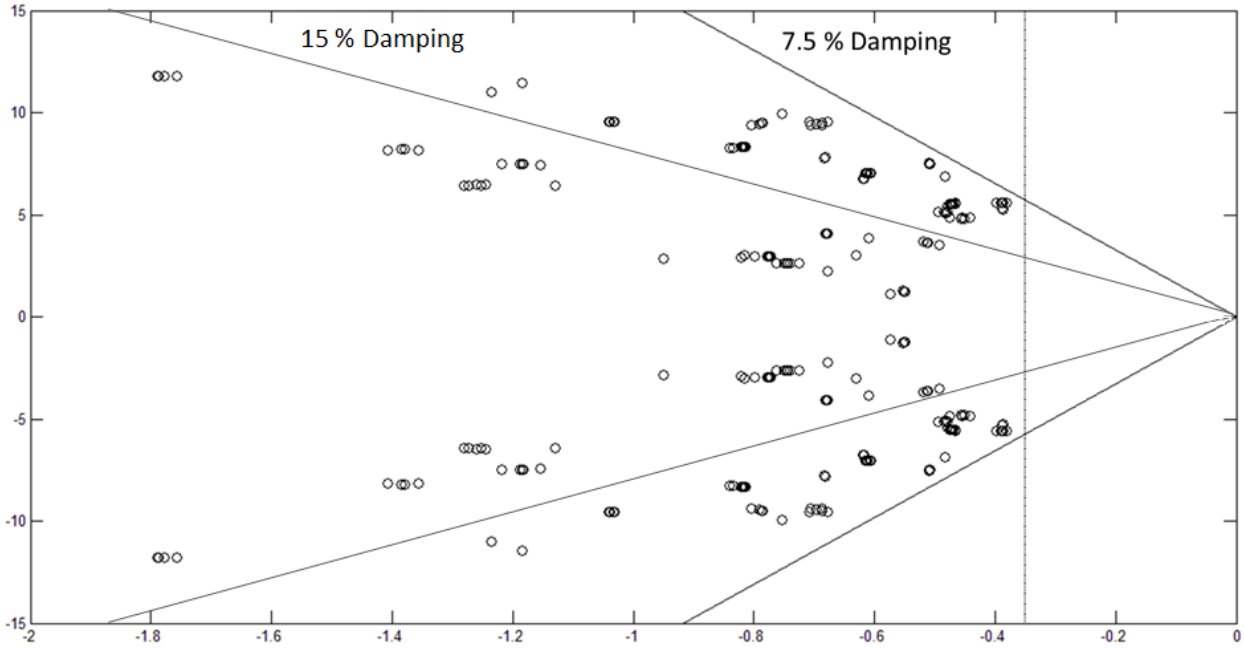

Fig. 4.17: Closed loop eigenvalues for reduced-order system when 6- element control is forced on it

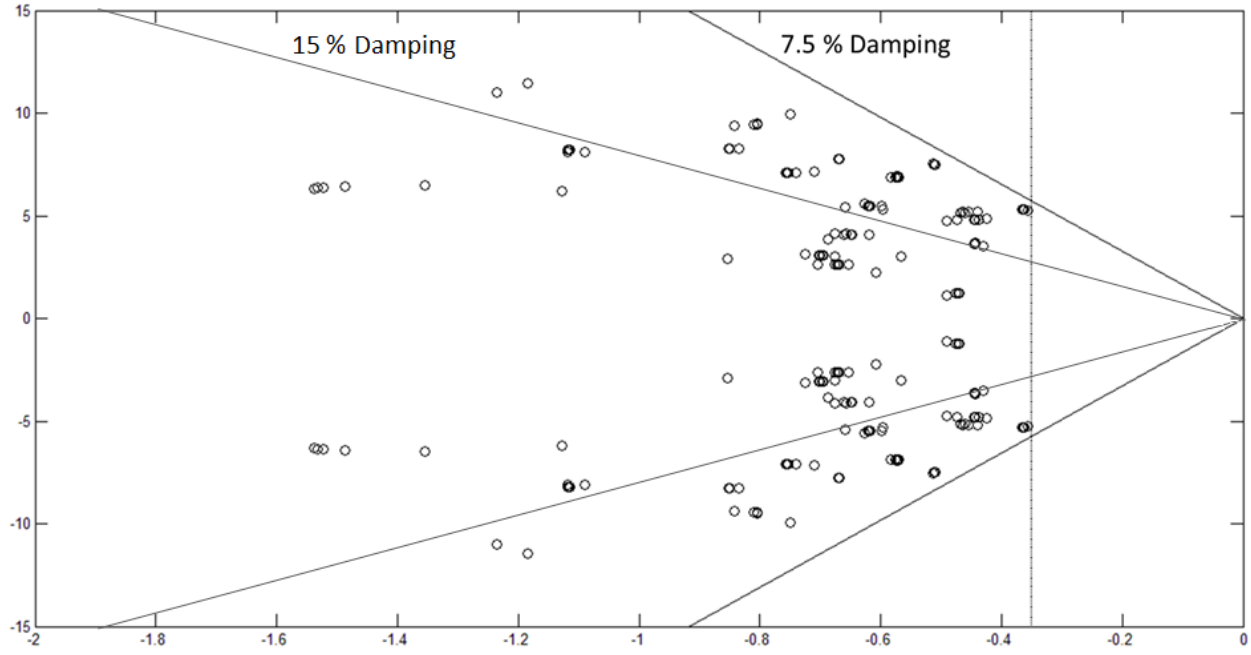

Fig. 4.18: Root Locus plot for Case 1 using the proposed algorithm

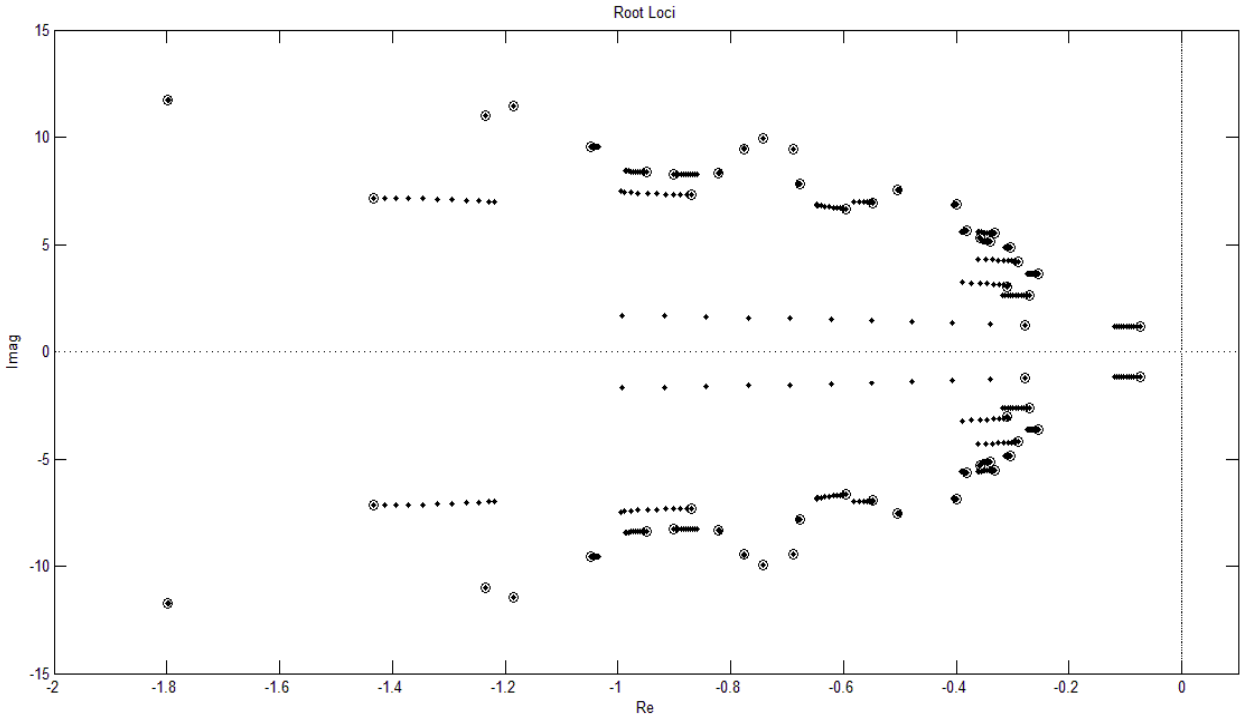

Fig. 4.19: Root Locus plot for Case 2 using the proposed algorithm

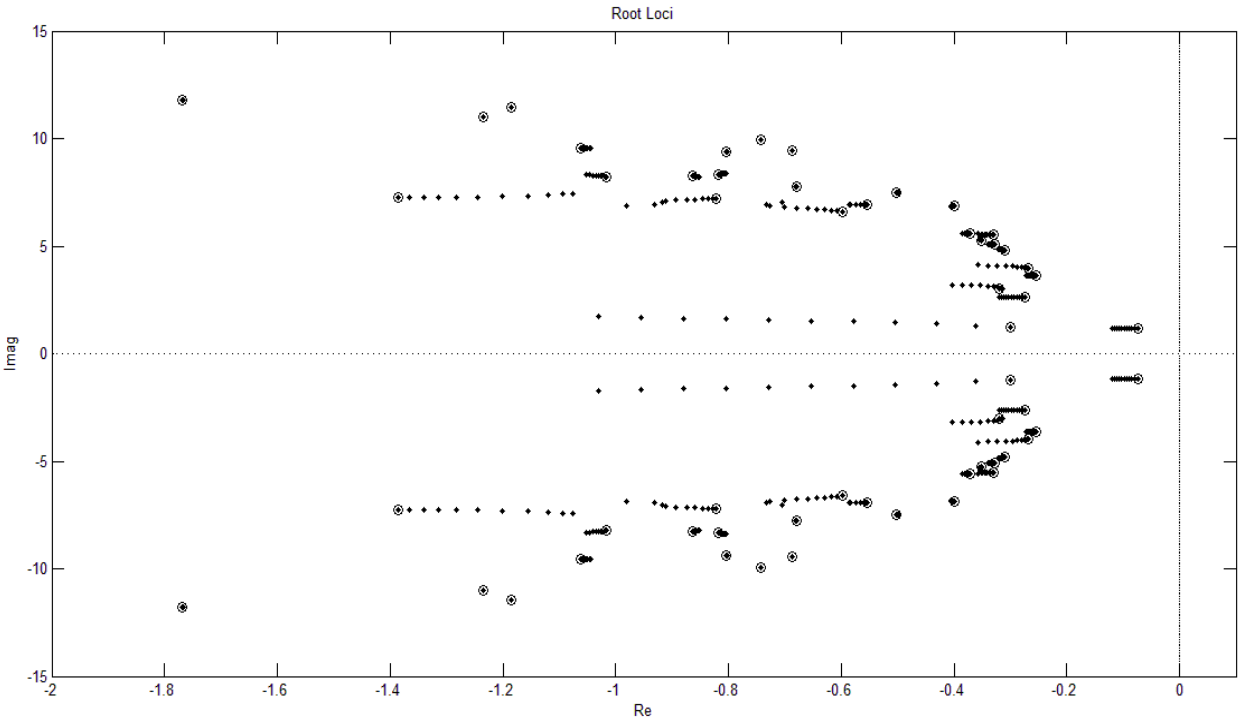

Fig. 4.20: Root Locus plot for Case 3 using the proposed algorithm

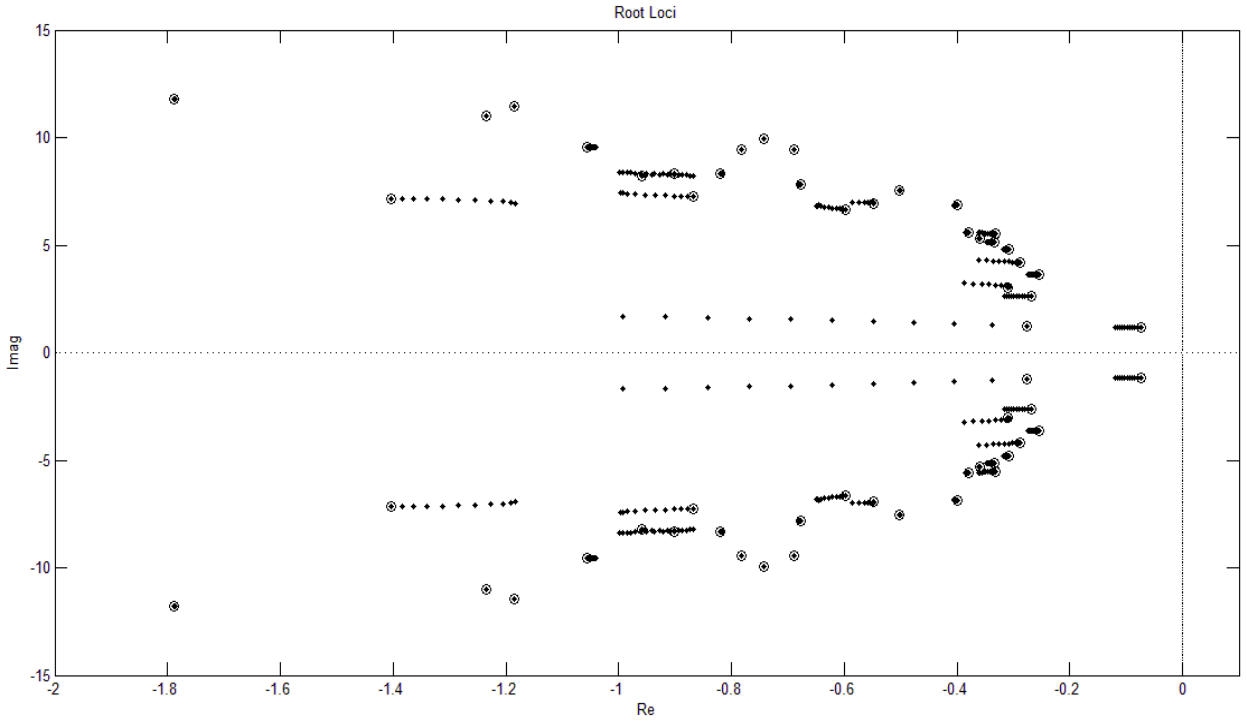

Fig. 4.21: Root Locus plot for Case 4 using the proposed algorithm

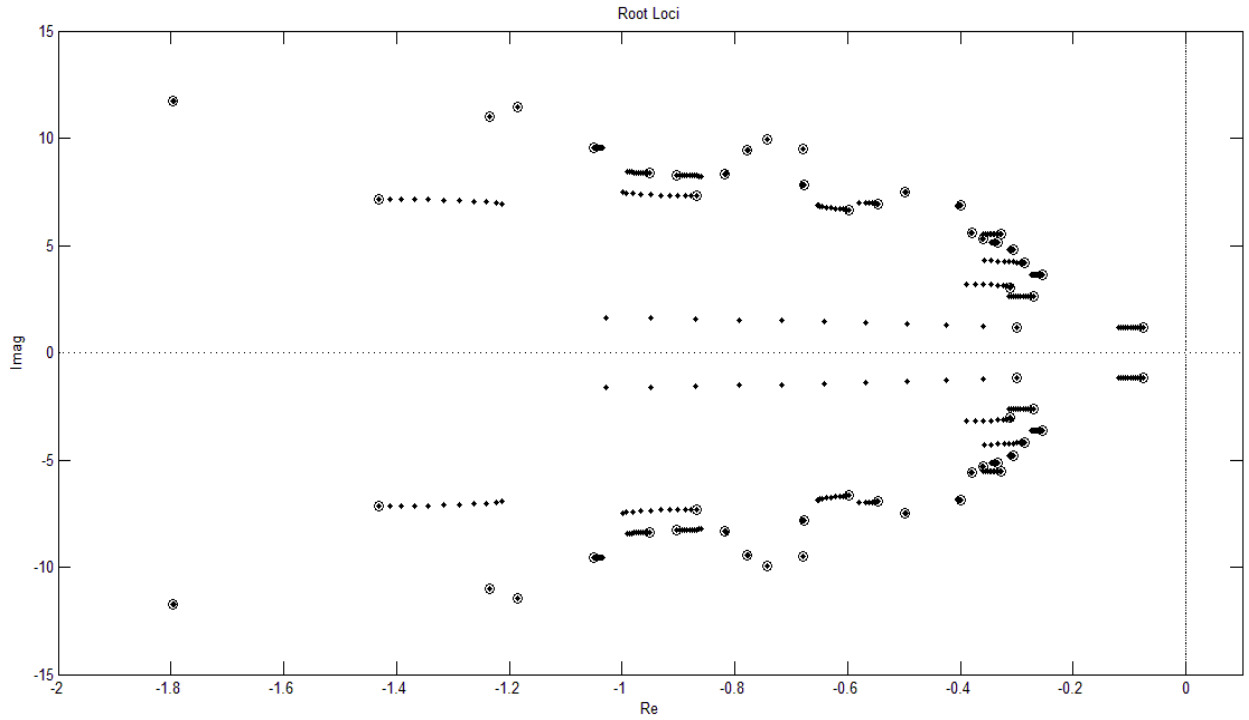

Fig. 4.22: Root Locus plot for Case 5 using the proposed algorithm

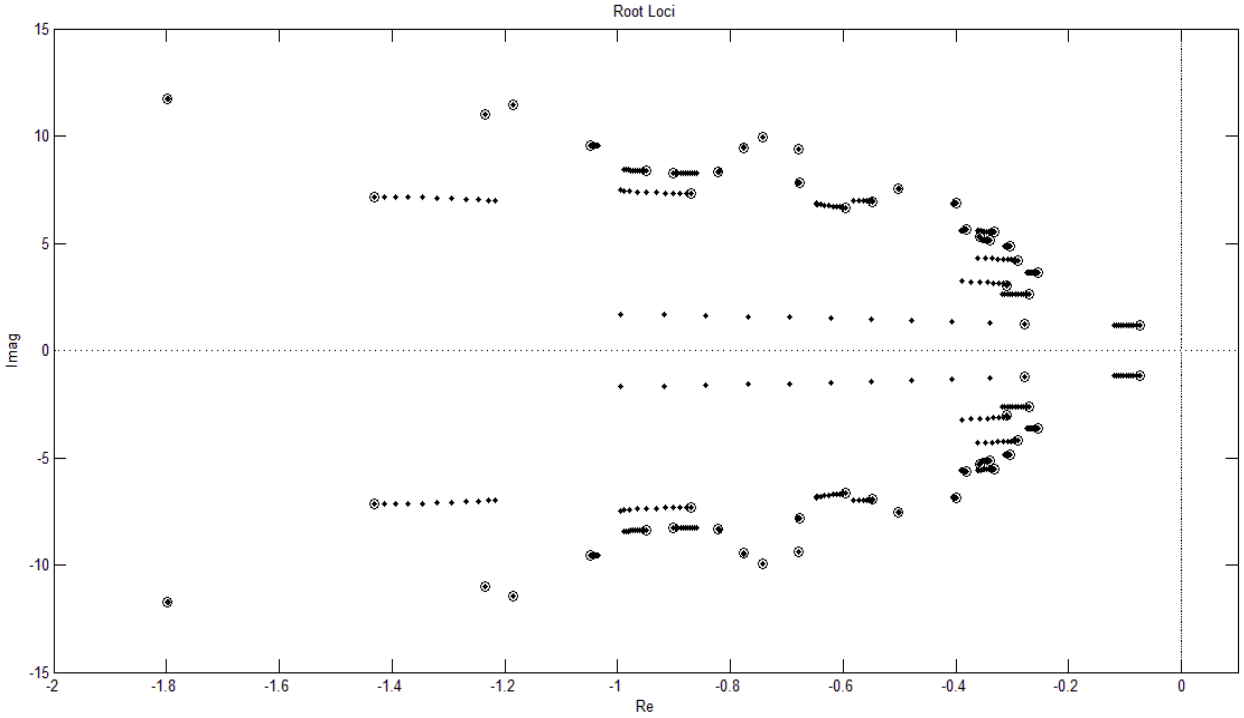

Fig. 4.23: Root Locus plot for Case 6 using the proposed algorithm

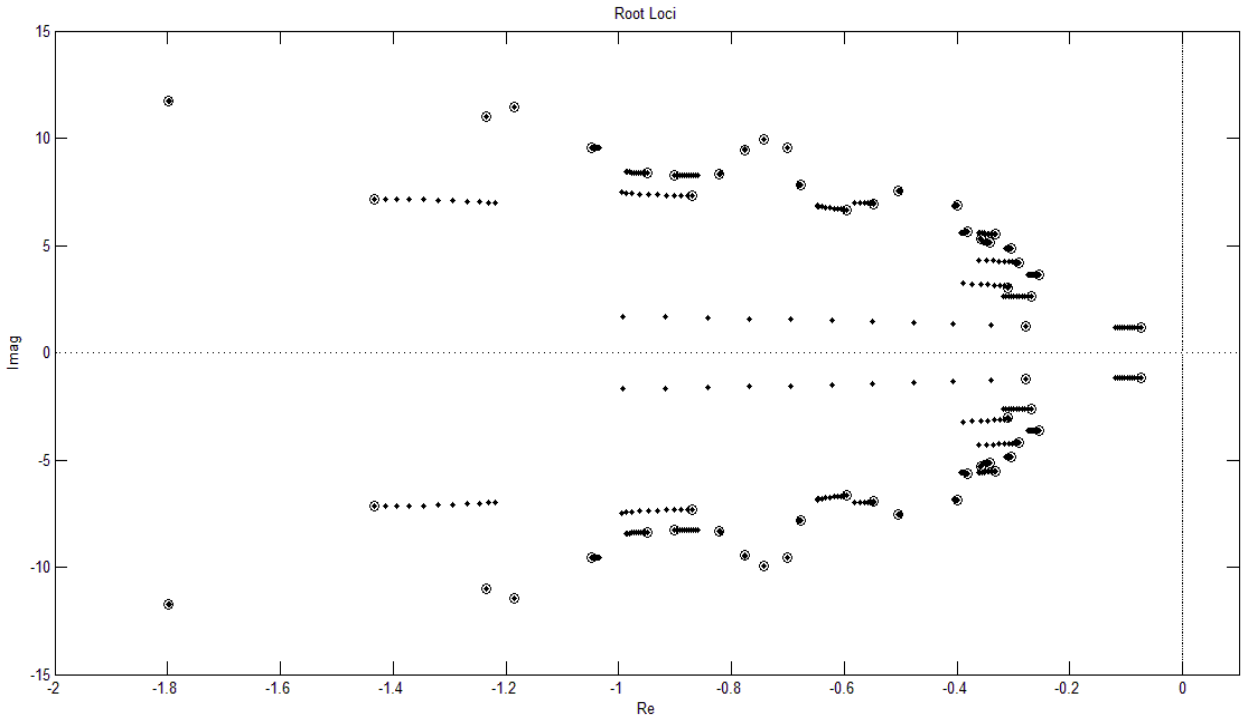

Fig. 4.24: Root Locus plot for Case 7 using the proposed algorithm

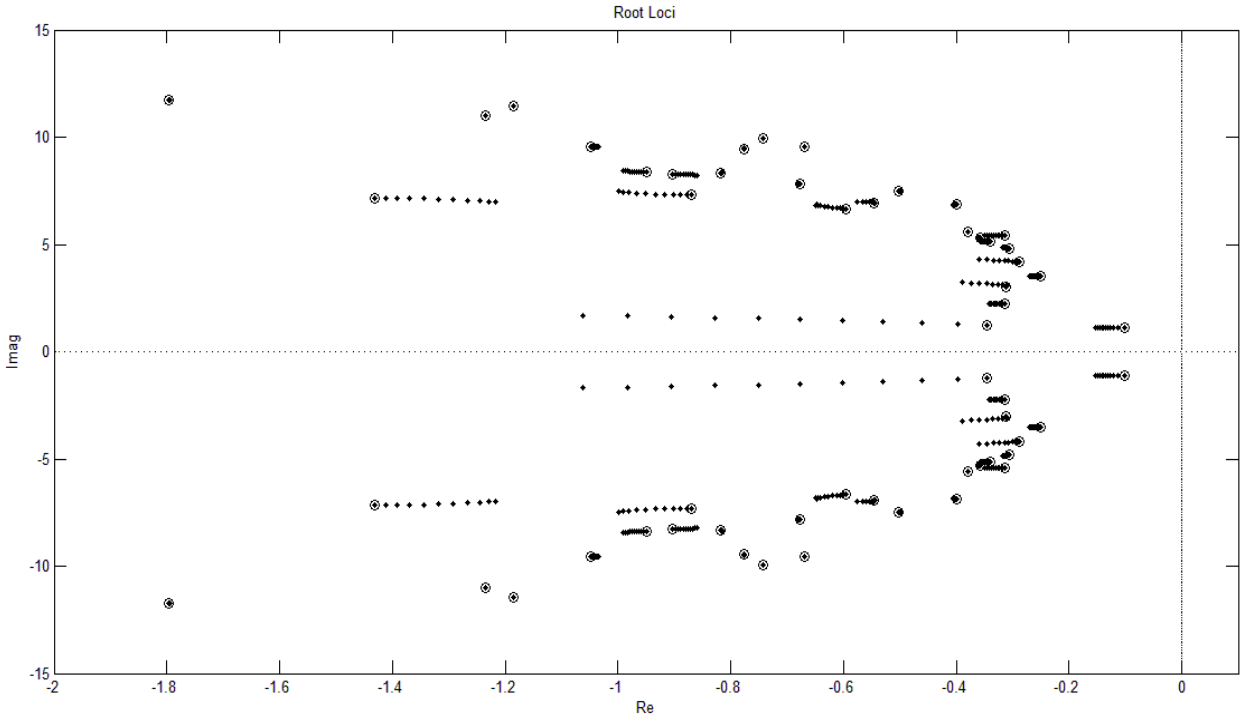

Fig. 4.25: Root Locus plot for Case 8 using the proposed algorithm

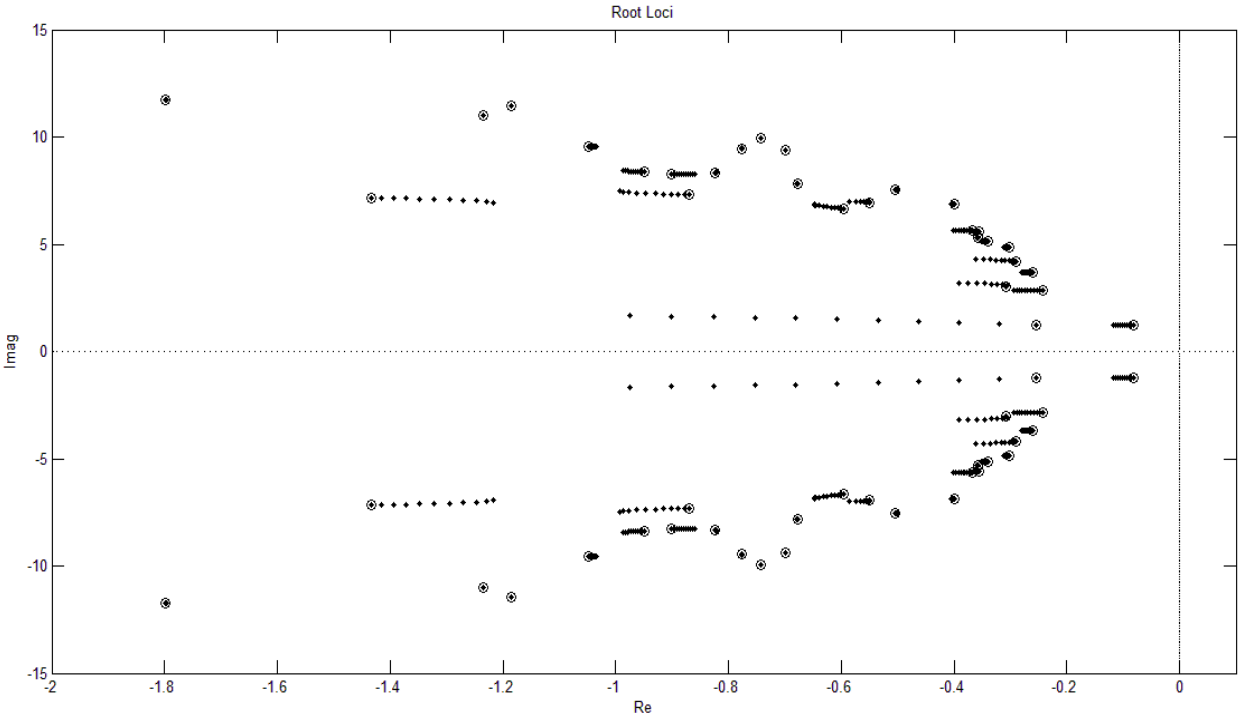

4.5 Conclusion

This chapter gives a detailed description of application of the proposed control technique to a larger and more complex power system, namely the 29 machine model of the WECC system. The system size is reduced to the relevant modes of oscillations following which the polytopic model is created to develop the control. The initial control designed using the HVDC lines and SVCs already present in the model was not found to be robust enough for damping all the low frequency inter-area modes of oscillations present in the system. Three more controllers in the form of Energy Storage Devices (ESDs) are introduced into the system to get the desired effect. The theory of Controllability Indices is used to come up with the optimum locations for the ESDs. The results indicate that by having six controllers in the system, all the low-frequency inter-area modes of oscillations can be adequately damped along with most of the local modes. The fact that different types of controllers can be integrated together to develop the control is also a compliment to the method developed herein.

Chapter 5 – Modeling in PSLF

In the previous chapter, a control law was formulated in the Matlab suite Power System Toolbox (PST) for the 29 machine, 127 bus model of the WECC system. The simulation results showed that the proposed control was able to move the eigenvalues to the left for all the inter-area modes and most of the local modes over a wide range of contingencies. This control, however, was developed in the environment of Matlab; whereas most power system controls are simulated on more standard benchmark software like PSLF, PSS/E or DSA. Therefore, to test the versatility of the control developed herein, it was applied to an equivalent model of the same system created in PSLF. Once the control was fine-tuned to work on the reduced-order system (127 bus model), it was next applied to the full-order model of the WECC system comprising of 4000+ buses. This chapter elaborates on the procedure to be followed for transferring the control and summarizes the results that were subsequently obtained.

5.1 Transfer Control Process

The output of the LMI control developed in PST is a gain matrix K. Its rows correspond to the number of controls present in the system whereas its columns correspond to twice the number of machines that are to be controlled. The reason for it being two times the number of controlled machines is that the first half is associated with the generator angles (δ) whereas the second half is associated with the generator speeds (ω). Therefore, the K matrix for the 29 machine model has a dimension of 6×42 as it has 6 controls and 21 machines that are controlled, as illustrated in the previous chapter.

Now, the control vector (u) corresponding to the gain matrix (K) and the state vector (x) is given by,

$$u = -Kx \tag{5.1}$$

For the i^{th} control, the increment in the control can be denoted as,

$$\Delta u_i = -[k_{i,1} \quad k_{i,2} \quad \dots \quad k_{i,42}] \begin{bmatrix} \Delta\delta \\ \Delta\omega \end{bmatrix} \tag{5.2}$$

Also, let the initial load at the bus corresponding to the i^{th} control be $P_i + jQ_i$. Then, based on the type of controller, the following changes can occur.

Case 1: When the i^{th} control is a SVC

Since an SVC controls the voltage magnitude, it primarily affects the reactive power of the bus on which it is placed. Now, if the reactive power output of that bus at time step t be Q_i^t, then the new output at time step $t + 1$ can be found to be,

$$Q_i^{t+1} = Q_i^t + \Delta Q_i^t \tag{5.3}$$

Where,

$$\Delta Q_i^t = -[k_{i,1} \quad k_{i,2} \quad \dots \quad k_{i,42}] \begin{bmatrix} \Delta\delta_i^t \\ \Delta\omega_i^t \end{bmatrix} \tag{5.4}$$

In (5.4), $\Delta\delta_i^t$ and $\Delta\omega_i^t$ represent the change in the generator angles and the generator speeds of the machines being controlled. Mathematically, they are expressed as,

$$\Delta\delta_i^t = \delta_i^t - \delta_i^{t-1} \tag{5.5a}$$

And,

$$\Delta\omega_i^t = \omega_i^t - \omega_i^{t-1} \tag{5.5b}$$

As the control is fed back after one time-step, it is necessary that the time step be small for the control to remain effective. This condition is satisfied during the modeling in PSLF by setting the time-step to be approximately 4 milliseconds.

Case 2: When the i^{th} control is an ESD

As ESDs were modeled to control the real power outputs, they primarily affect the real power of the bus on which they are placed. Then, proceeding in a manner similar to what was done in the previous case, if the real power output of that bus at time step t be P_i^t, then the new output at time step $t+1$ is found to be,

$$P_i^{t+1} = P_i^t + \Delta P_i^t \tag{5.6}$$

Where,

$$\Delta P_i^t = -[k_{i,1} \quad k_{i,2} \quad \dots \quad k_{i,42}] \begin{bmatrix} \Delta\delta_i^t \\ \Delta\omega_i^t \end{bmatrix} \tag{5.7}$$

Case 3: When the i^{th} control is a HVDC Line connecting buses (say) A and B

As the HVDC lines were modeled as active and reactive power injections, they affect both the real as well as the reactive powers of the buses which they connect. The modeling is done in a manner such that the real power enters through one end of the line and exits from the other end, whereas the reactive power enters the line at both ends. The reactive power input is set at approximately 30% of the real powers at either ends. Then, proceeding in a manner similar to what was done in the previous cases, if the real and reactive power outputs of the connecting buses A and B at time step t be $P_{i\,A}^t$, $Q_{i\,A}^t$, $P_{i\,B}^t$, and $Q_{i\,B}^t$ respectively, then the new outputs at time step $t+1$ are found to be,

$$P_{i\ A}^{t+1} = P_{i\ A}^{t} + \Delta P_i^t \tag{5.8}$$

$$Q_{i\ A}^{t+1} = Q_{i\ A}^{t} + 0.3 \times \Delta P_i^t \tag{5.9}$$

$$P_{i\ B}^{t+1} = P_{i\ B}^{t} - \Delta P_i^t \tag{5.10}$$

$$Q_{i\ B}^{t+1} = Q_{i\ B}^{t} + 0.3 \times \Delta P_i^t \tag{5.11}$$

Where,

$$\Delta P_i^t = -[k_{i,1} \quad k_{i,2} \quad \dots \quad k_{i,42}] \begin{bmatrix} \Delta\delta_i^t \\ \Delta\omega_i^t \end{bmatrix} \tag{5.12}$$

This completes the transfer process of the control.

5.2 PSLF Outputs

Positive Sequence Load Flow (PSLF) developed by GE, was the power system simulator that was used to test the transfer of the control. It is a large-scale power system simulation package, which includes the following main modules [69]:

Menu and Command Selector

Main Load Flow Program and Working Case Maintenance Commands (PSLF)

Graphics Sub-system (OLGR)

Short-Circuit Subsystem (SCSC)

Dynamics Subsystem (PSDS)

Dynamic Results Viewer (PLOT)

Control Language Processor (EPCL)

Linearized Network Analysis Subsystem (LINA)

Economic Dispatch Subsystem (ECON)

The programming language that was used in this thesis was the Engineering Process Control Language, commonly called EPCL. It differs from ordinary programming languages in the sense that it was primarily designed to work in conjunction with PSLF and that it has direct access to its data tables and processing functions. The biggest advantage of using EPCL being that it efficiently handles the many themes and variations of data manipulations and generates reports that one needs to successfully execute power

system studies. The combination of EPCL and PSLF was therefore found to be very effective in organizing the database and executing the fundamental processes of power system simulation.

5.2.1 Application of Control to 127-Bus Model

In order to simulate the proposed control on the 127-bus model of the WECC system, an equivalent system was created in PSLF corresponding to the one developed in the Matlab suite PST. The two DC lines were modeled as power injections whereas the ESDs and SVCs were modeled as real and reactive power inputs respectively. The system was made more realistic by adding exciters and turbo-governors to the generators similar to what was present in the real system. The reason for doing so being that the full-order system had all the other elements in place (exciters, power system stabilizers, turbo-governors etc.) and to make the control more effective in that system, it had to be tested on something similar to it, but not as complex.

It is important to note here that the presence/absence of exciters or turbo-governors did not affect the control developed in Matlab as the use of SMA had made the system sensitive to only the generator angles (δ) and the generator speeds (ω). Finally, a program was created in the Control Language Processor of PSLF i.e. EPCL, which performed the control transfer process described in the previous section. The generator angles obtained for the stable base case are shown in Fig. 5.1.

Fig. 5.1: Generator angles for Base Case of 29 machine model of the WECC system

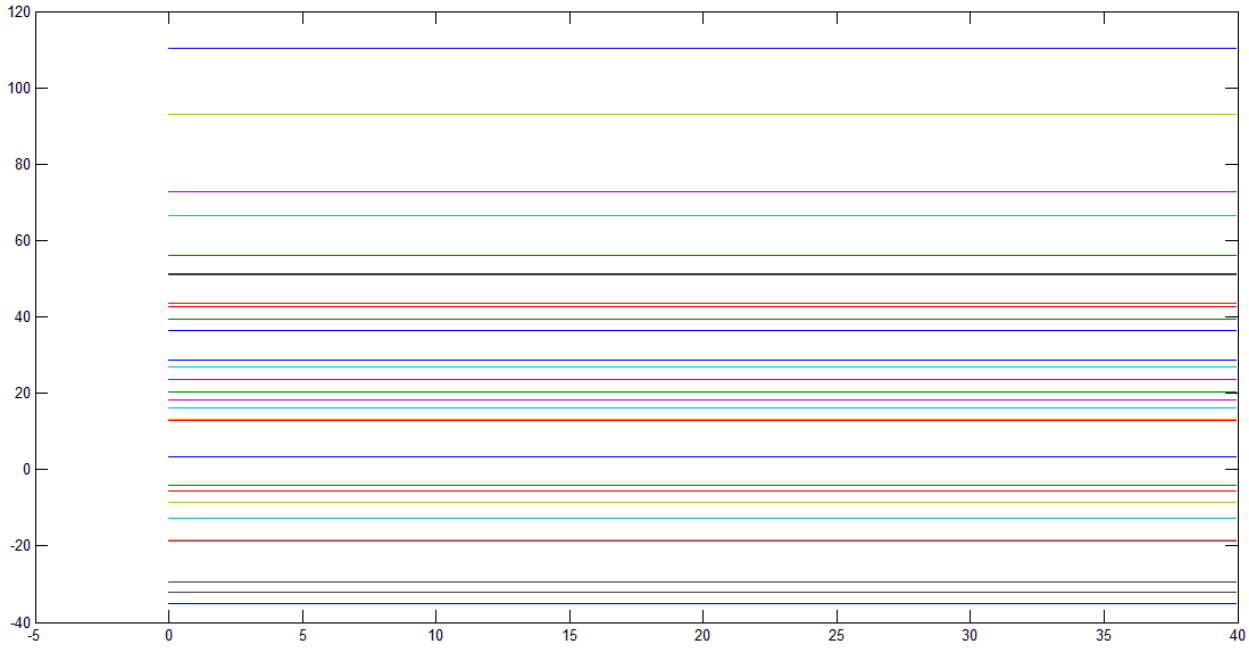

In order to test the effectiveness of the control, a hitherto untested contingency (which was not part of the case bank used to develop the control) was applied to this system. The contingency that was simulated was a step change of 20% in the North-South HVDC Line extending from Celilo to Sylmar (Pacific DC

Intertie), at time $t = 1\,second$ and lasting for 10 cycles. The reason for using this particular case was that previous studies on the 29 machine WECC model had showed that this particular contingency excited all the low frequency inter-area modes of oscillations present in the system. The oscillations produced in the system corresponding to this step input are shown in Fig. 5.2.

For the development of the control, the differences in generator angles $(\Delta\delta)$ and the generator speeds $(\Delta\omega)$ for two consecutive time-steps were used as feedbacks. The loads of the control buses were updated based on whether the control was from a SVC, or an ESD, or a HVDC line. The plot of the generator angles at every time step was used as the response. Since PSLF does not compute the eigenvalues of the system, the success of the control was tested on the basis of the time-domain plots generated by the simulator. Also, PSLF can only plot six variables at a time. Therefore, in order to plot all the modes of oscillations and get a global view of the performance of the control, the output file of PSLF was synchronized with Matlab to generate the figures seen below.

Fig. 5.2: Oscillations produced due to a step input in the 29-machine system in absence of control

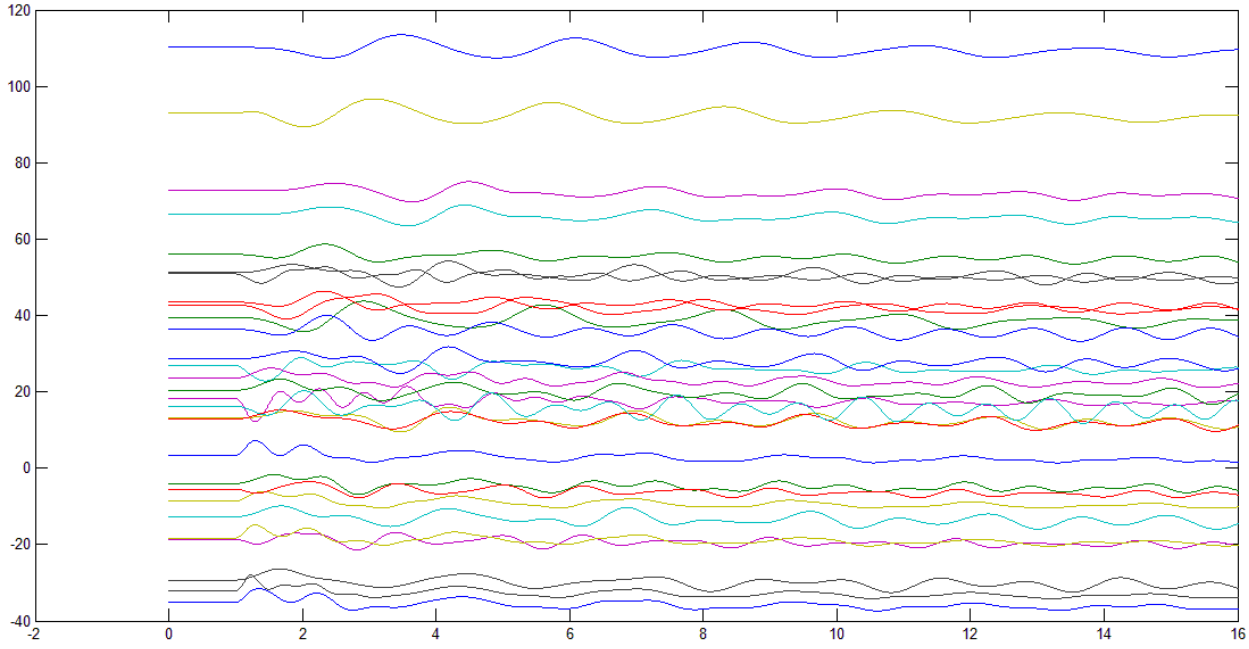

On applying the six-element control developed in Matlab to this system, it was observed that the control did not have much influence on the damping of the oscillations. Therefore, in order to force the control further, the gain of the control was multiplied by a factor of two. The resulting plot obtained shown in Fig. 5.3, shows prominent signs of damping. Thus, the control was acting in the correct direction but it had lost some of its potency due to the difference in the two models. Another fact which becomes clear from this analysis is that even though the gain of the control is doubled, none of the oscillations increase substantially implying that there was no negative interaction amongst the controllers.

Fig. 5.3: Oscillations produced due to a step input in the 29-machine system in presence of control (with twice the gain)

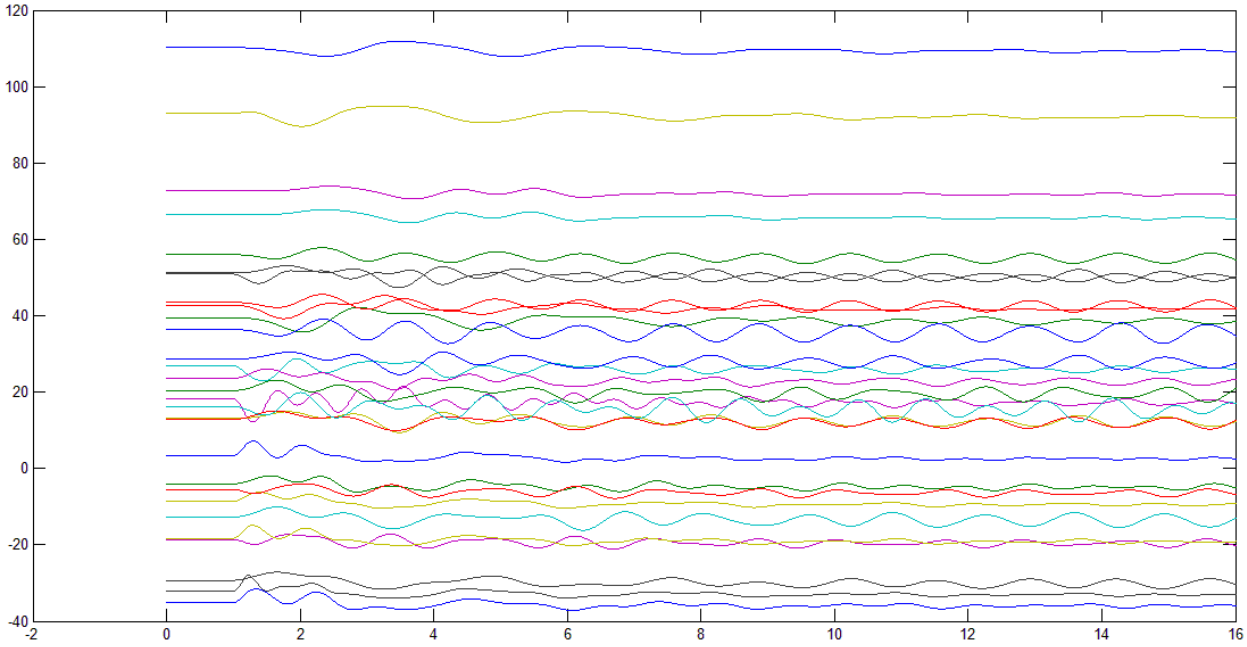

Figure 5.4 depicts the generator angles of five machines which had dominant inter-area modes of oscillations. The plot on the left is obtained when the control is absent whereas the one on the right is obtained when the proposed six-element control with twice the gain is applied to this system. From this figure, it can be inferred that by multiplying the gain by two, the control is able to –

a) Reduce the number of ripples present in a given time frame
b) Decrease the magnitude of the individual ripples

Figure 5.5 shows the generator angles of some of the machines which had dominant local modes of oscillations. As expected, although damping of some of the local modes either remains the same or is slightly decreased (due to the doubling of the gain), none of them become increasingly high so as to make the system become unstable. The fact that the local modes could not be damped as much as they had been in Matlab was attributed to the differences in the two models used. The inference that is drawn from this analysis is that if the two models are made more similar to one another, the results can also be made to look more alike.

Fig. 5.4: Generator angles of five machines with dominant inter-area modes of oscillations (Left: In absence of Control; Right: In presence of twice the control)

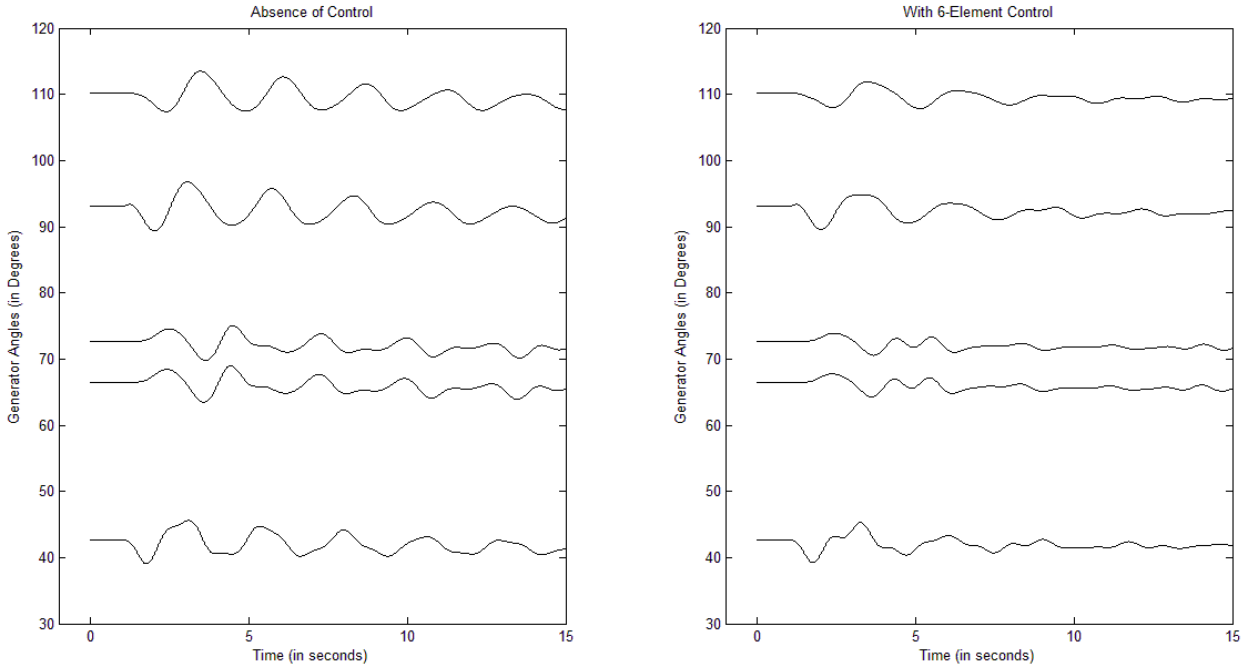

Fig. 5.5: Generator angles of seven machines with dominant local modes of oscillations (Left: In absence of Control; Right: In presence of twice the control)

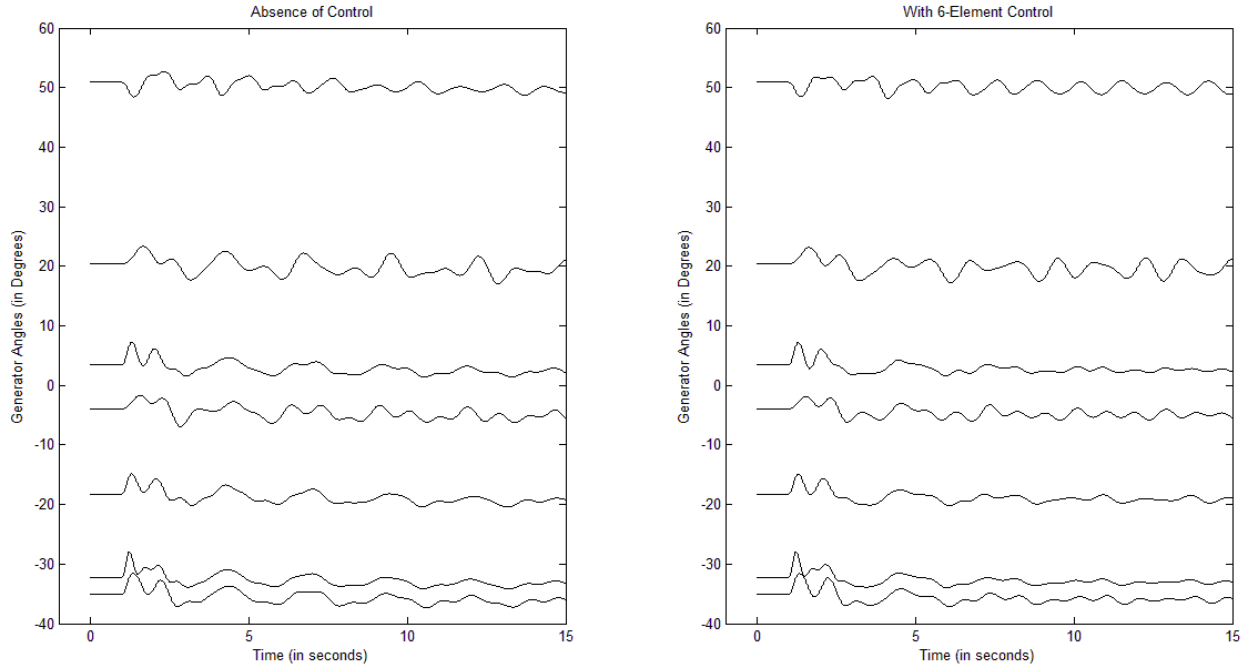

In order to better examine the effect of the control on the inter-area modes, Prony Analysis [70] was done on the uncontrolled and controlled waveforms. Prony extracts valuable information from a uniformly sampled signal and builds a series of damped complex exponentials or sinusoids [71]. As compared to other oscillatory signal analysis techniques (such as Fourier), Prony has the advantage of estimating damping coefficients apart from frequency, phase and amplitude. Moreover, it best fits a reduced-order model to a high-order system both in time and frequency domains [72]. It has been widely used in the areas of power systems, biomedical monitoring, radioactive decay, radar, sonar, geophysical sensing, speech processing etc. Figures 5.6 and 5.7 depict the two most critical inter-area modes of oscillations present in this system as identified by Prony Analysis. Similar results were obtained for the other inter-area modes. From these results, it becomes clear that the proposed control (with twice the gain) has been able to significantly improve the damping of all the inter-area modes of oscillations present in the system.

Fig. 5.6: Lowest inter-area mode of oscillation present in 29 machine system (Left: In absence of Control; Right: In presence of twice the control)

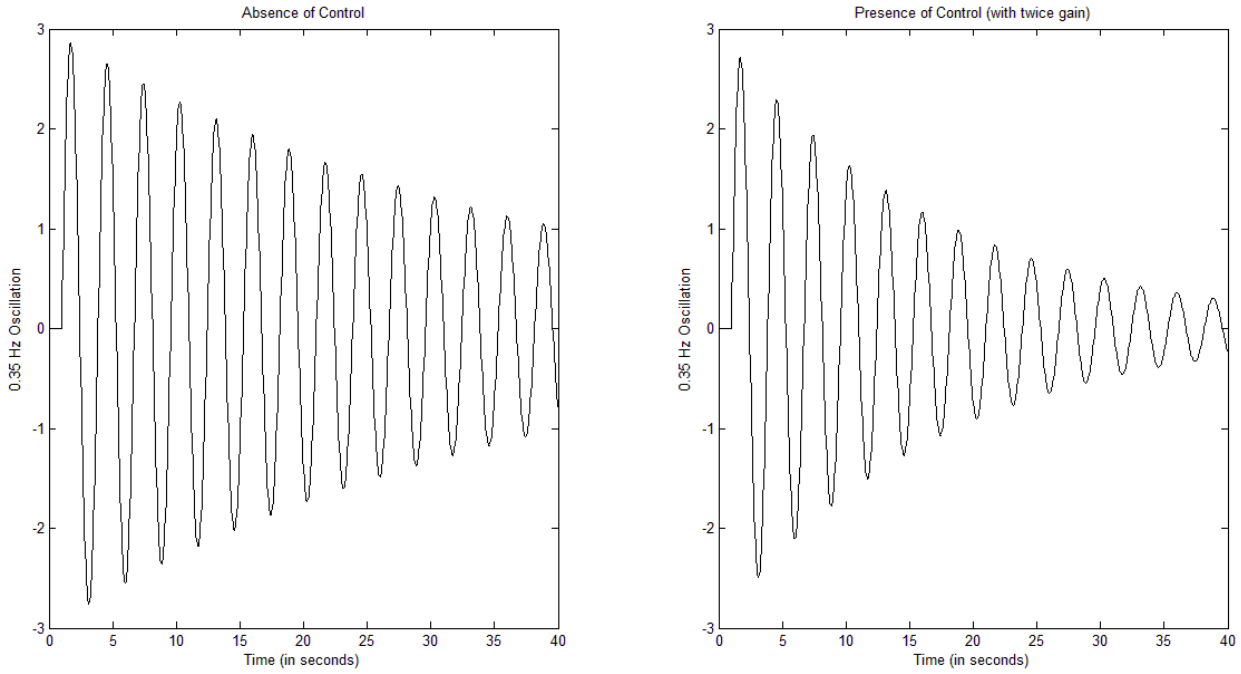

Fig. 5.7: Second lowest inter-area mode of oscillation present in 29 machine system (Left: In absence of Control; Right: In presence of twice the control)

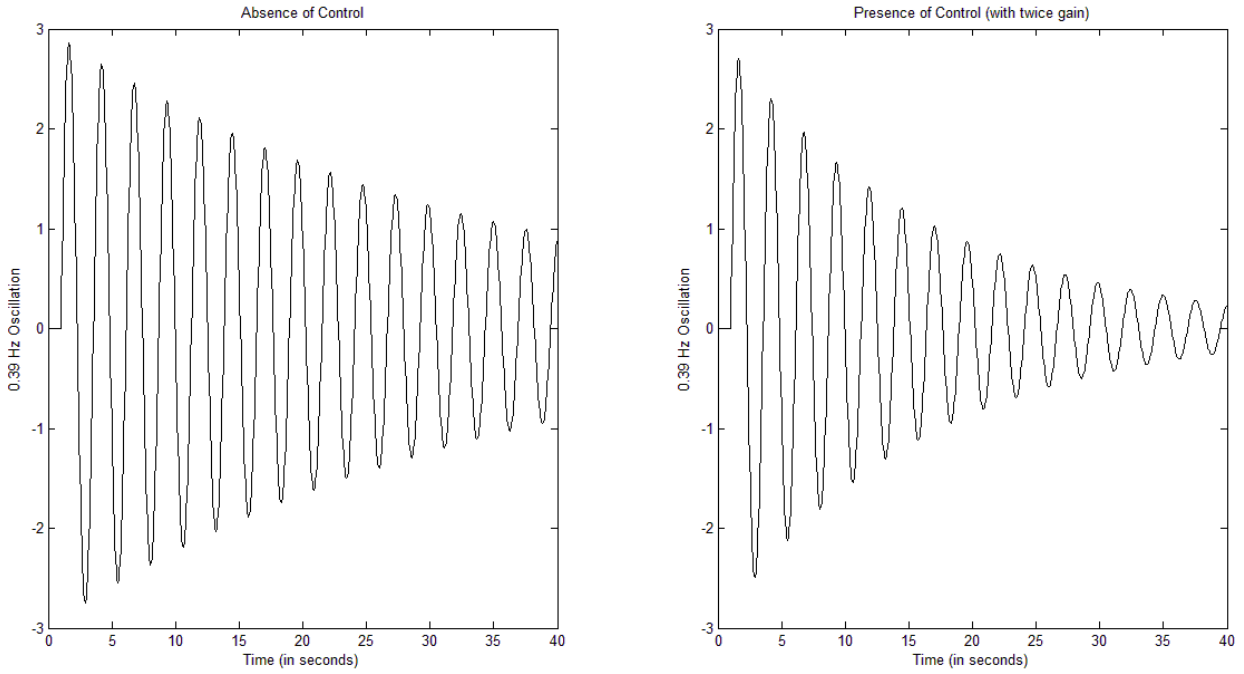

5.2.2 Application of Control to 4000-Bus Model

As the proposed technique was found to give encouraging results on the 127-bus model, it was now applied to the full-order model of the WECC System. In this big system, California is represented in detail by a 4000+ bus system whereas the “rest of WECC” is represented by a 67-bus equivalent network extracted from the 127-bus model. Since the “rest of WECC” was similar to what it was in the 127-bus model, the control for that portion of the big system remained the same. The only change that was needed to be done was to find real measurements for the California region in the big system corresponding to the equivalent measurements obtained in the 127-bus system. This is done as shown in Table 5.1 below.

Table 5.1: Selection of Measurements in the California region for the 4000+ Bus Model

Machines in the 127-Bus Equivalent	**Machines in the 4000+ Bus Model**
Mohav1CC	MNTV-ST
Miraloma	San Onofr
Litehipe	AlamT G
Tevatr2	Dukmoss
Round Mt.	Hyatt

Figures 5.8-5.14 compare the damping obtained in the absence and presence of the proposed control on the new model for the seven contingency cases outlined in the polytope. As the number of generators were too many in this system (more than one thousand), and as inter-area oscillations are system-wide phenomena, the real power flow across the seven tie-lines present in the system was used for comparison purposes. The plots on the left corresponded to those without control whereas the ones on the right represented those with control. The plots were obtained as a result of Prony Analysis done on the original waveforms. But from these figures, it was realized that a single case (out of the list of seven contingency cases) is not able to excite all five of the inter-area modes of oscillations that are present in this system. Therefore, we were in need of a new contingency case which would simultaneously excite all the inter-area modes of oscillations that are present in this system and thereby act as a suitable test to measure the robustness of the proposed control.

Fig. 5.8: Comparison of damping w.r.t. Dominant Modes for Second Case

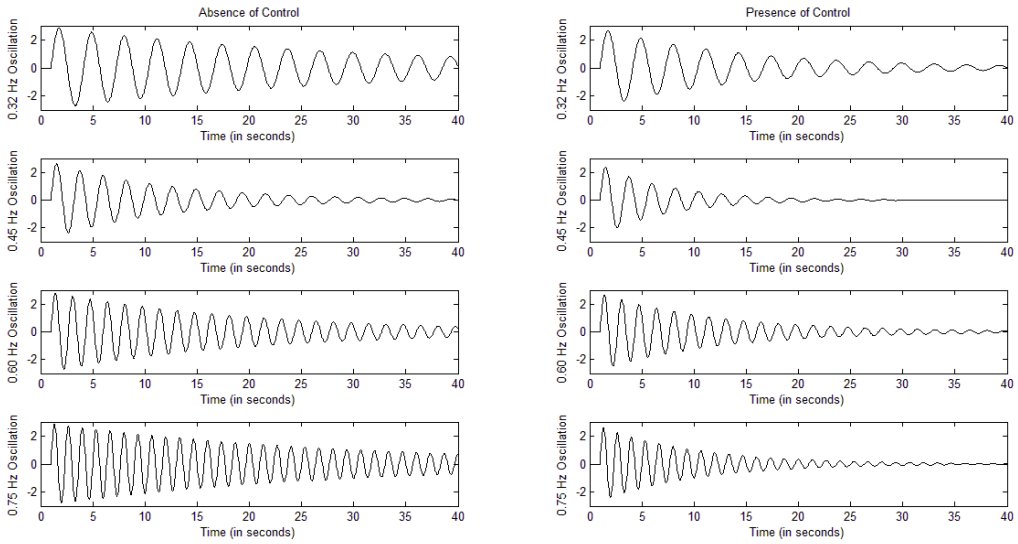

Fig. 5.9: Comparison of damping w.r.t. Dominant Modes for Third Case

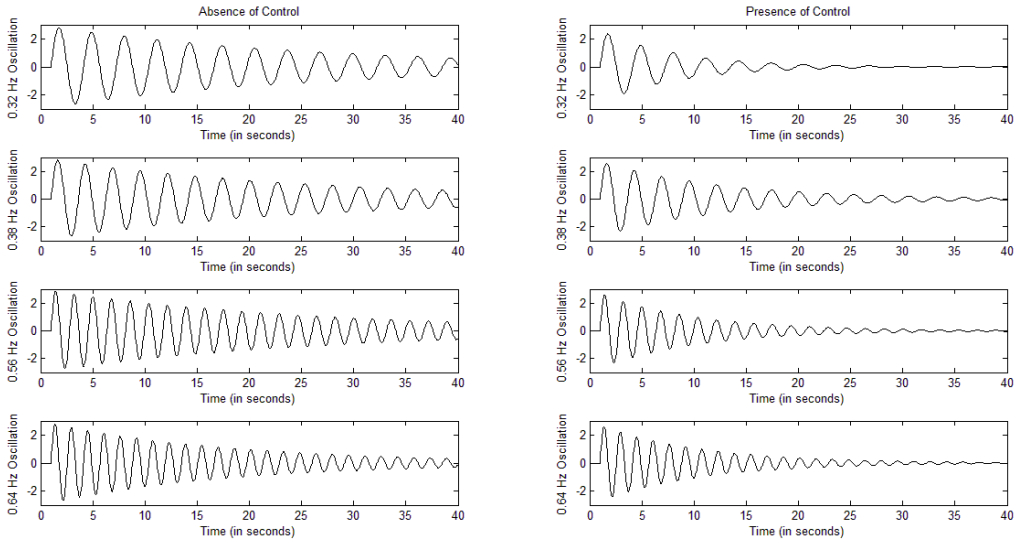

Fig. 5.10: Comparison of damping w.r.t. Dominant Modes for Fourth Case

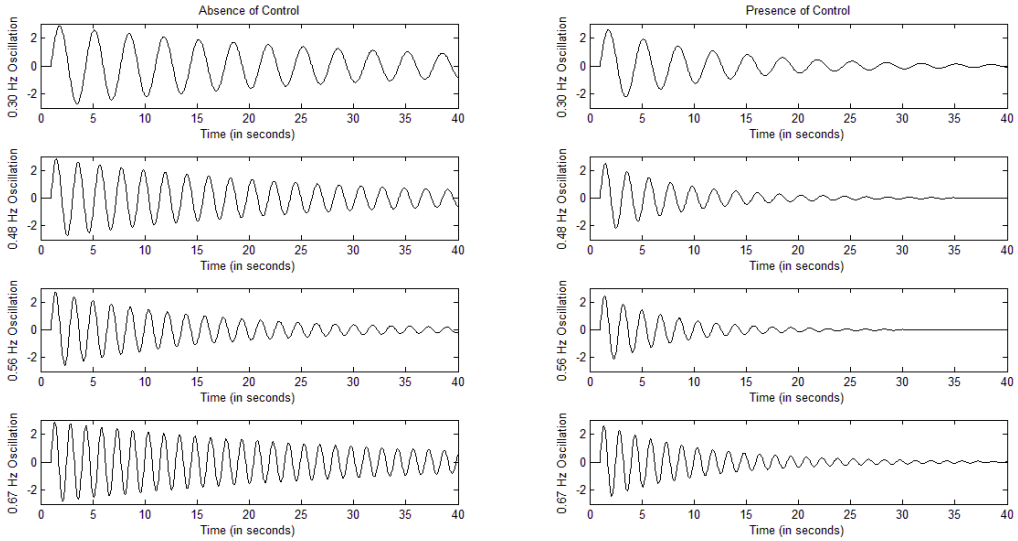

Fig. 5.11: Comparison of damping w.r.t. Dominant Modes for Fifth Case

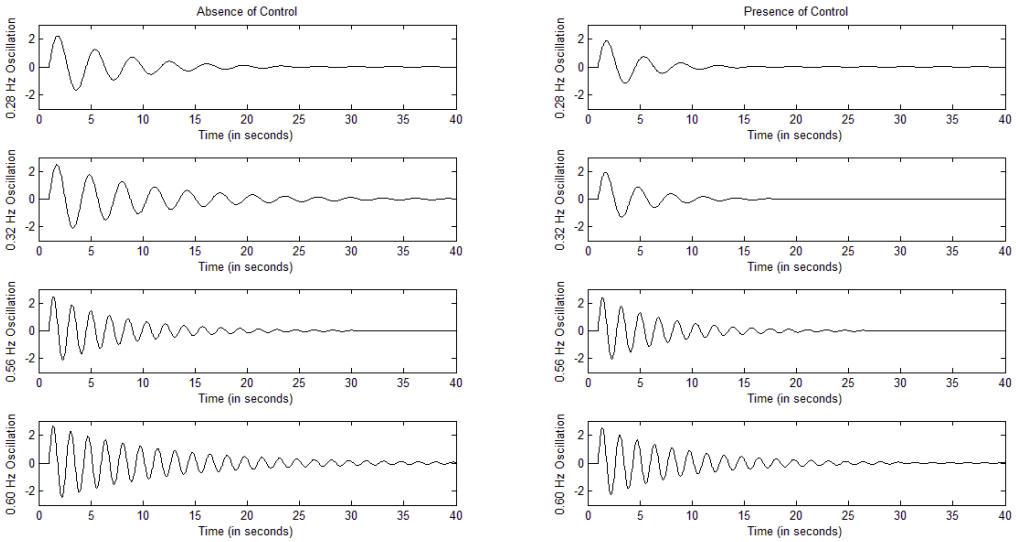

Fig. 5.12: Comparison of damping w.r.t. Dominant Modes for Sixth Case

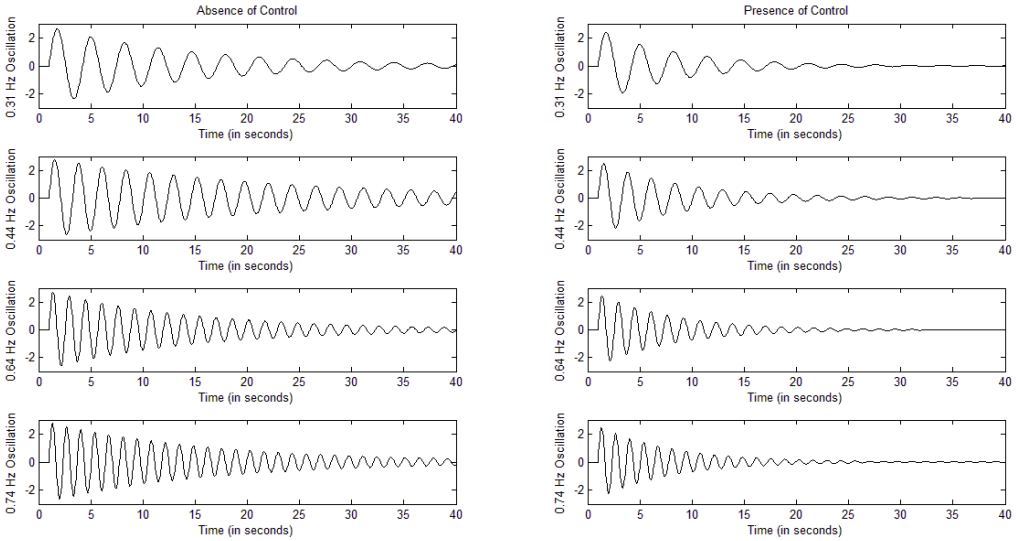

Fig. 5.13: Comparison of damping w.r.t. Dominant Modes for Seventh Case

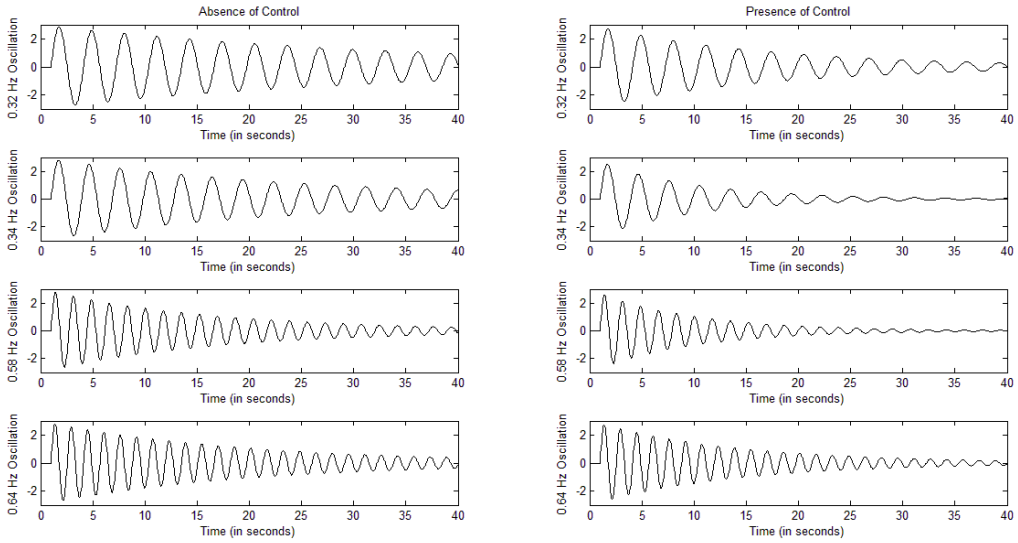

Fig. 5.14: Comparison of damping w.r.t. Dominant Modes for Eighth Case

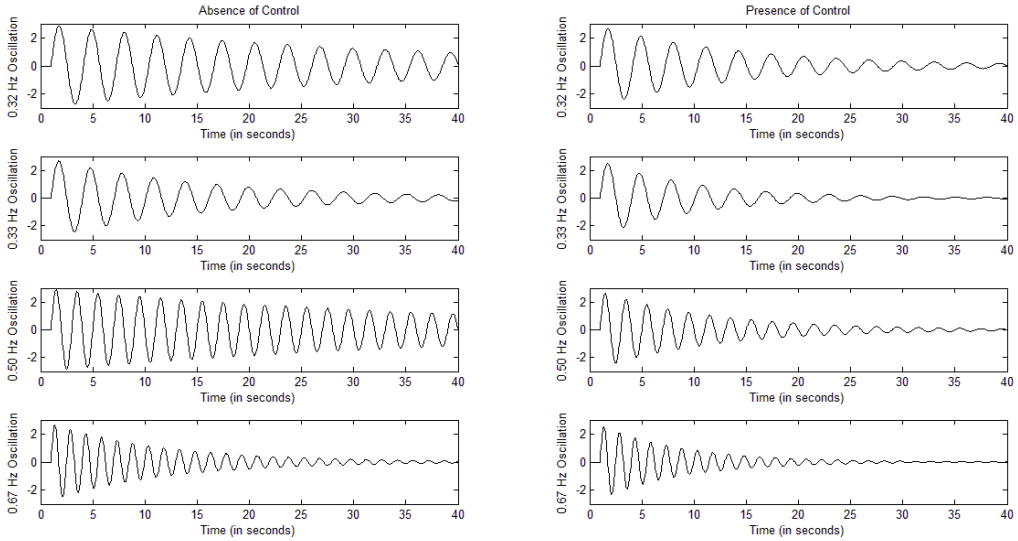

Based on analysis done previously on this system, a step change of 40% in the North-South HVDC Line extending from Celilo to Sylmar (Pacific DC Intertie), at time $t = 1\,second$ and lasting for 10 cycles was found to be a suitable contingency that would simultaneously excite all the inter-area modes of oscillations present in this model. Figure 5.15 shows the oscillations taking place in the seven tie-lines corresponding to this condition.

Fig. 5.15: Oscillations in the tie-lines due to a step input to the full-order model in absence of control

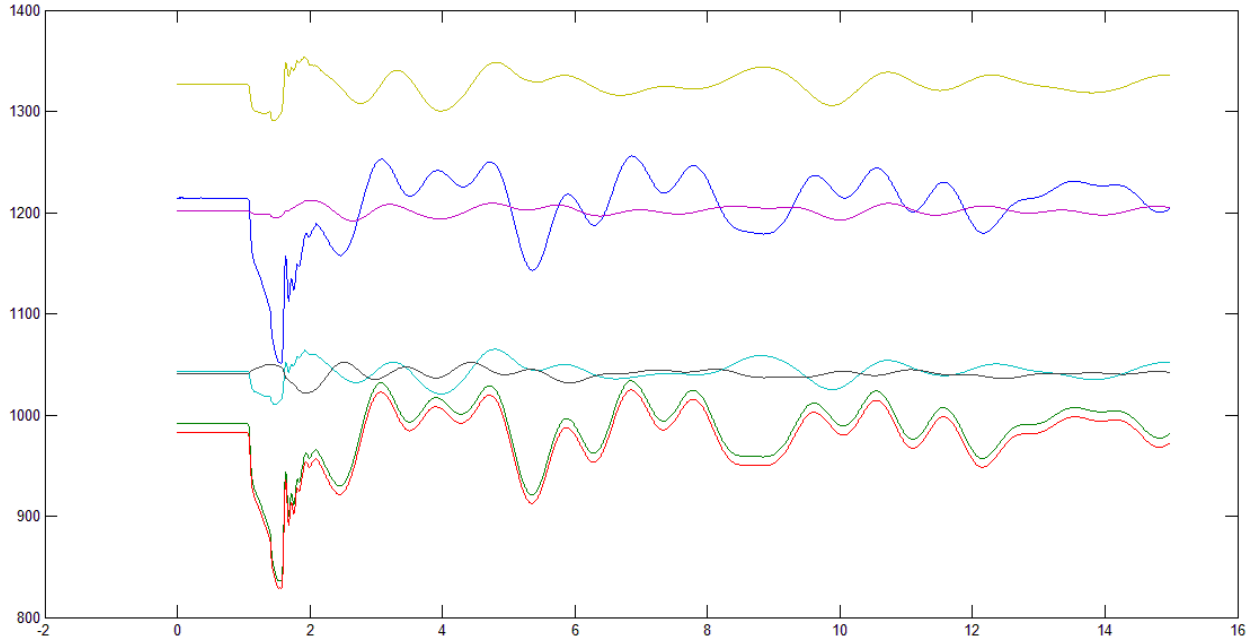

Figure 5.16 depicts the oscillations in the tie-lines when the control developed using the 127-bus reduced-order model is applied to this big system. In order to better examine the effect of the control on the inter-area modes, Prony Analysis was done on the uncontrolled and controlled waveforms. Table 5.2 summarizes the results obtained on performing Prony Analysis on the waveforms obtained on simulating the said contingency. In accordance with the FERC CEII Order No 702, the tie-lines have been represented by Line X, Line Y etc., where X and Y are natural numbers. The table confirms the fact that the proposed control is able to increase the damping of the dominant inter-area modes observed in the respective tie-lines. Based on this observation, Table 5.3 was created to compare the improvement in damping corresponding to the dominant inter-area modes present in the system.

Figures 5.17-5.21 depict the five prominent inter-area modes of oscillations present in this system as identified by Prony Analysis. The plot on the left depicts the damping of the modes in the absence of control whereas the ones on the right depict the improved damping obtained on applying the proposed algorithm. It is worthwhile to note here that the control logic developed on the basis of a small, equivalent system is able to improve the damping of all the inter-area modes of oscillations present in a much larger and complex system, that too for an untested contingency. This, if nothing else, clearly illustrates the huge advantage of using an LMI-based polytopic approach for the development of control for power system applications.

Fig. 5.16: Oscillations in the tie-lines due to a step input to the full-order model in presence of control

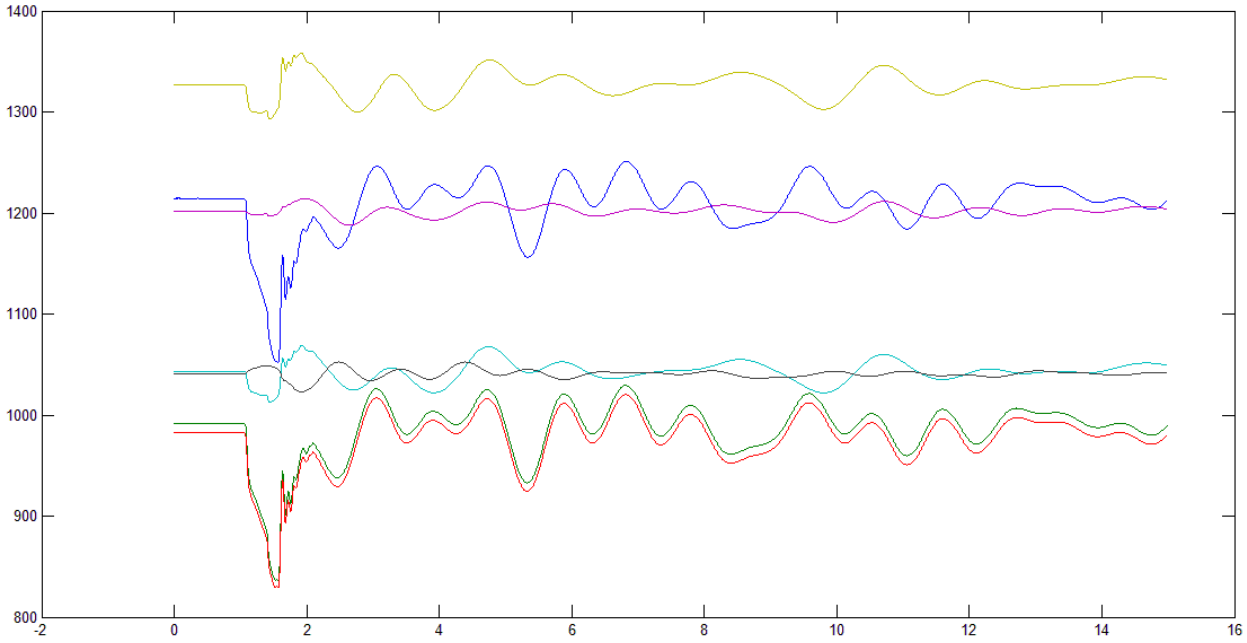

Table 5.2: Comparison of Damping with respect to Tie-lines

Names of Tie-lines	Observed Modes (Hz)	Damping Ratio	
		Without Control	With Control
Tie-line 1	0.30	0.019	0.045
	0.63	0.113	0.137
Tie-line 2	0.30	0.019	0.052
	0.64	0.128	0.149
Tie-line 3	0.30	0.025	0.040
	0.64	0.127	0.152
Tie-line 4	0.48	0.098	0.149
	0.78	0.056	0.064
Tie-line 5	0.52	0.092	0.139
	0.78	0.049	0.050
Tie-line 6	0.44	0.038	0.071
Tie-line 7	0.40	0.045	0.088

Table 5.3: Comparison of Damping with respect to Dominant Modes

Dominant Modes (Hz)	Damping Ratio (approximate)	
	Without Control	With Control
0.30	0.021	0.046
0.42	0.041	0.079
0.50	0.095	0.144
0.64	0.122	0.146
0.78	0.053	0.057

Fig. 5.17: Lowest inter-area mode of oscillation present in the full-order model of the WECC system

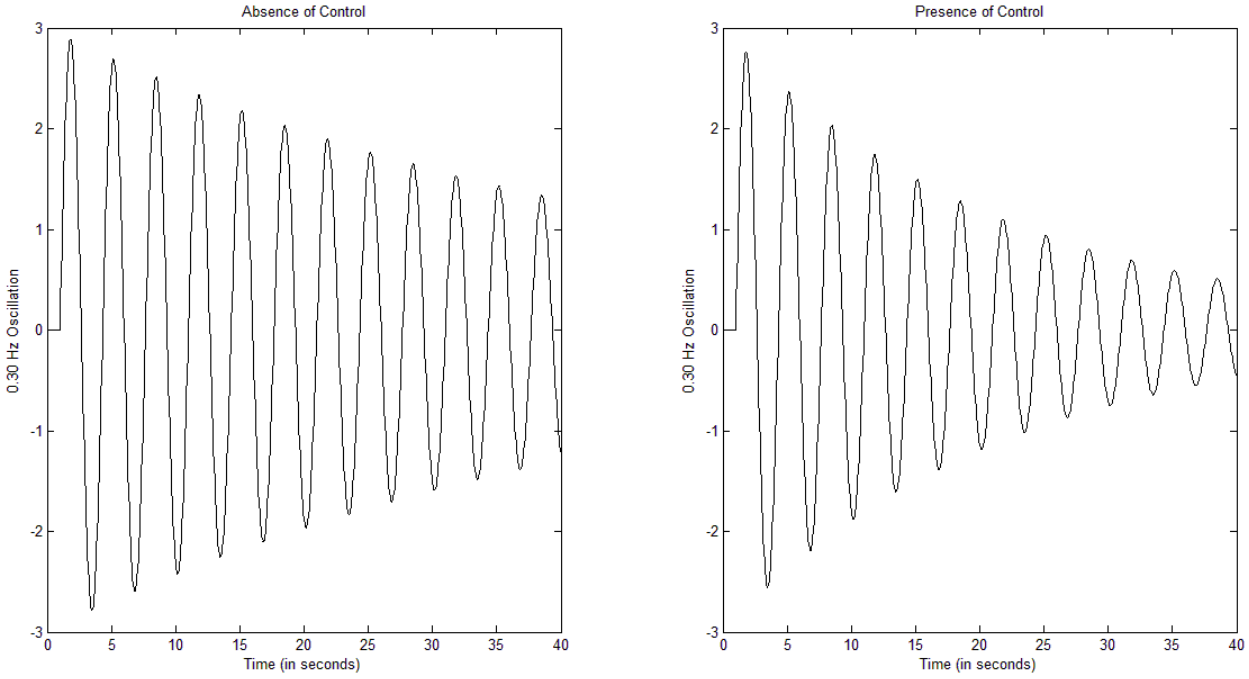

Fig. 5.18: Second lowest inter-area mode of oscillation present in the full-order model of the WECC system

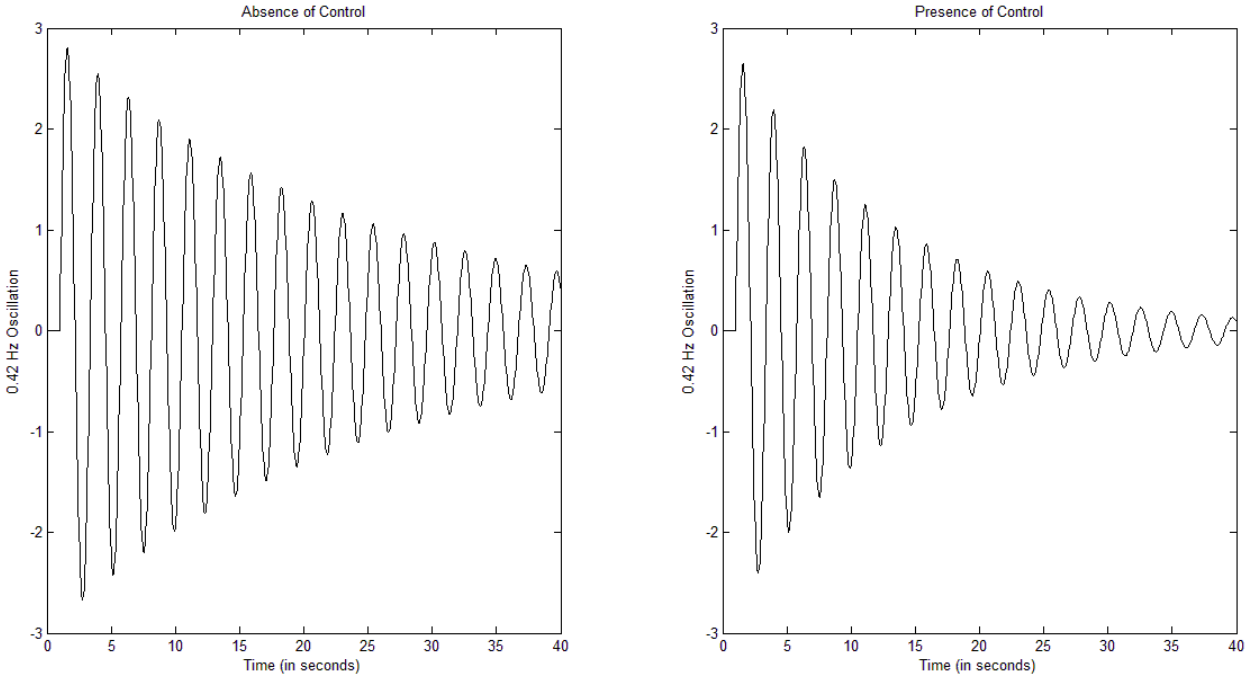

Fig. 5.19: Third lowest inter-area mode of oscillation present in the full-order model

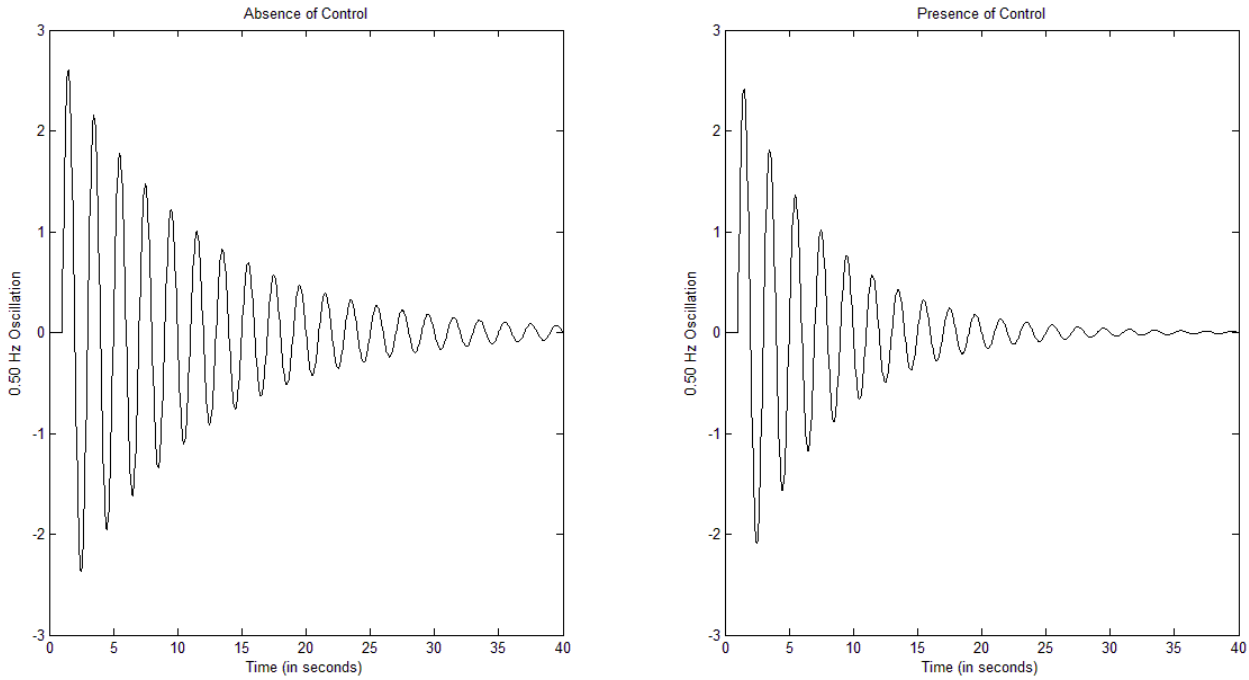

Fig. 5.20: Fourth lowest inter-area mode of oscillation present in the full-order model

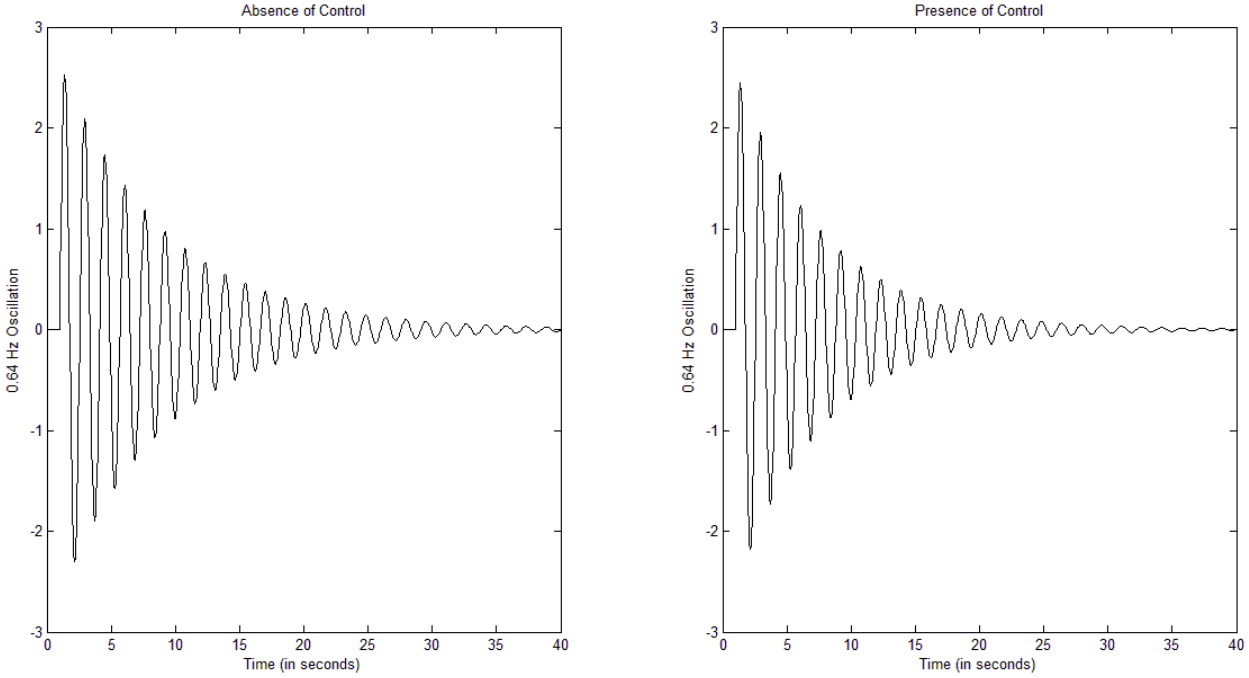

Fig. 5.21: Fifth lowest inter-area mode of oscillation present in the full-order model

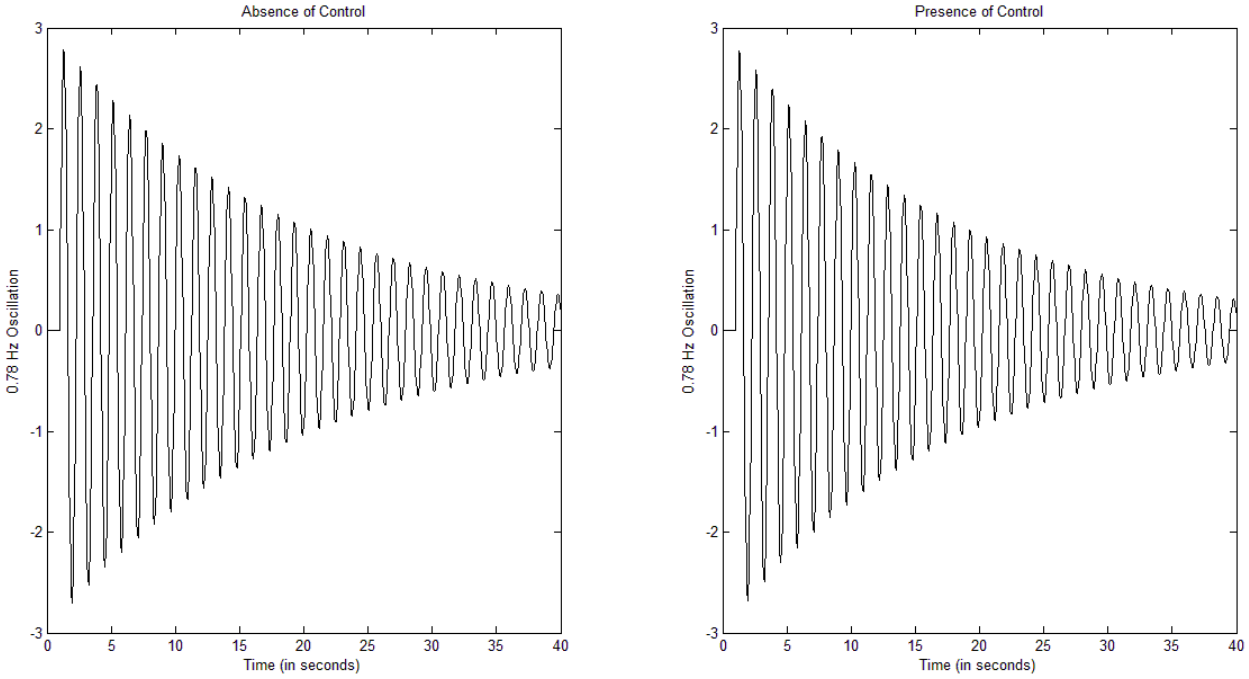

5.2.3 A Special Case

During all of our simulations, the assumption that was made was that the system was a stable one to start with. That is, all the vertices of the polytope had eigenvalues with negative real parts. This was done in accordance with our objective of improving the damping of the less damped inter-area mode of oscillations without making the other (local) modes unstable. But from a practical point of view, it is relevant to see the effect of the proposed control on an un-damped low frequency oscillation which would, if allowed to persist in the system, cause wide-spread havoc in it. In lieu with this realization, the following simulations were performed to test the performance of the coordinated control developed in this study on un-damped oscillations.

Case 1: 127 Bus equivalent model of the WECC System

There are two ways in which one could visualize the effect of the proposed control methodology on an un-damped oscillation – one method is to create a control from a polytope one of whose vertices would have an eigenvalue, corresponding to a low frequency inter-area mode, with positive real part. But since this would imply creating a polytopic system from scratch and as there is no guarantee that the LMI control developed from an unstable system would be feasible, this method was not used in the present scheme of things. The second approach is to tweak around with the parameters of the system, based on which the control has been developed, to create a single unstable inter-area mode and then try to use the control to damp it. The reason for choosing a single inter-area mode is that if a large number of inter-area modes get simultaneously excited, there is a higher probability that the operating region would move out of the polytopic region and there would be no guarantee that the proposed control would work. In accordance with this second method, the reactance of the line between Bus 1 and Bus 2 was increased from 0.002 to 0.005. This change resulted in the system becoming less tightly connected than what it was before and also made the 0.35 Hz oscillation more susceptible to contingencies. The step change that had been described previously (step change of 20% in the Celilo-Sylmar HVDC Line) was then applied on this system and the following waveforms were observed.

The waveforms shown in Fig. 5.22 below appear to have a superposition of higher harmonics; therefore to isolate the relevant mode of oscillation, Prony analysis was performed on the two waveforms. On doing so, the 0.35 Hz oscillation was indeed found to be the root cause behind the sustained oscillations and the effect of the proposed control on this un-damped oscillation also became prominent. The corresponding waveform is shown in Fig. 5.23. By doing this analysis it was ascertained that the proposed control was robust enough to damp even un-damped or slightly damped oscillations as long as the operating condition was within the polytopic region. In the next sub-section, a similar analysis is performed on the 4000+ bus model.

Fig. 5.22: Sustained oscillations produced due to a negatively damped 0.35 Hz oscillation

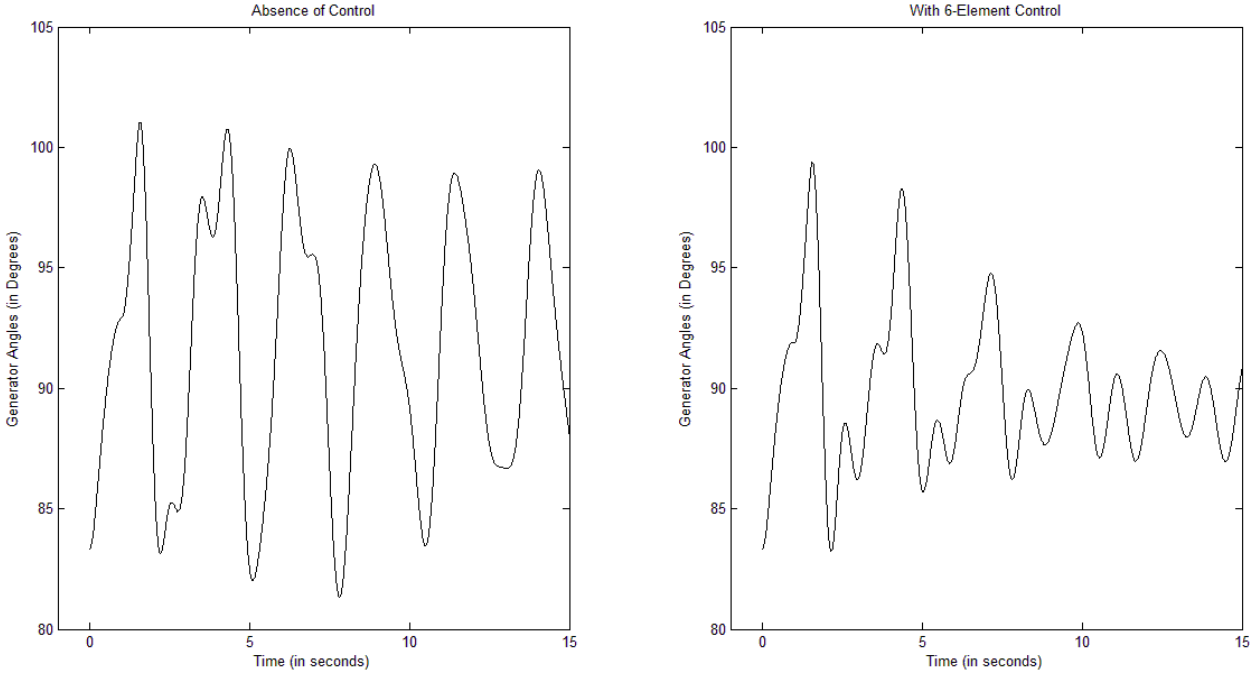

Fig. 5.23: Performance of proposed control on sustained oscillations (127 bus model)

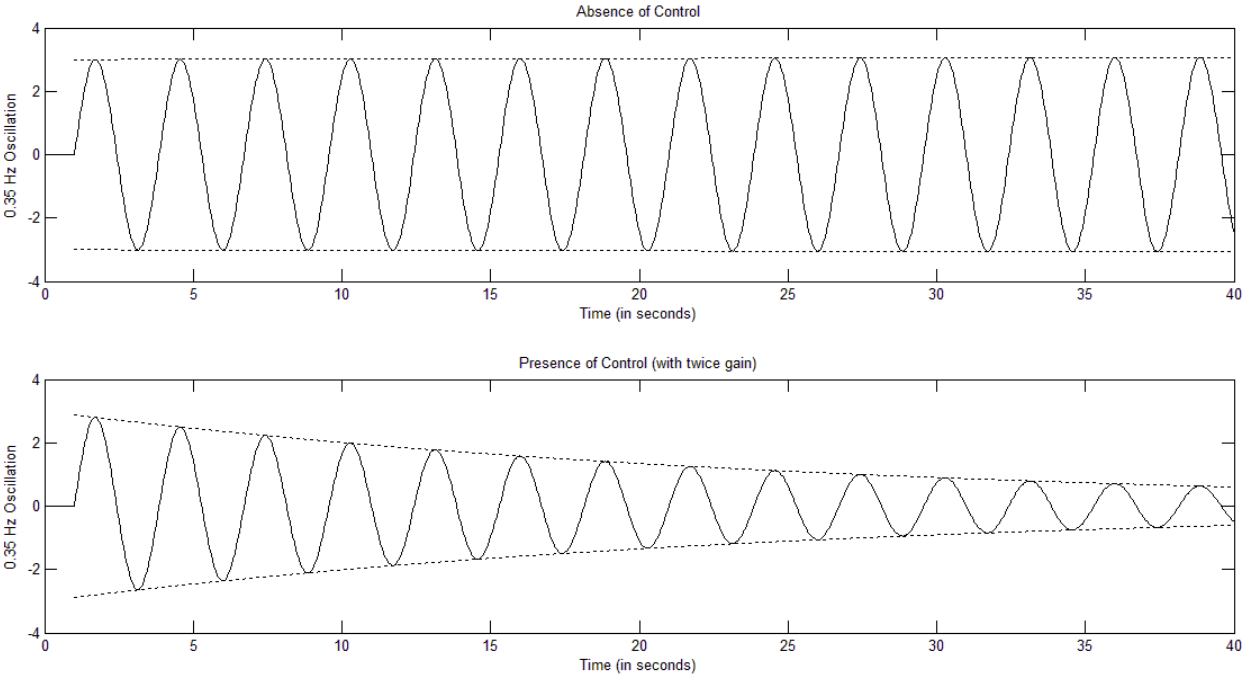

Case 2: 4000+ Bus model of the WECC System

In this system, it was realized that increasing the reactance of the line alone was not enough to excite the inter-area mode to the extent that we were interested in. If the reactance was increased by a small amount, the mode remained stable whereas if it was increased by a large amount, it caused transient stability problems. In order to overcome this dilemma, along with a slight increase in the reactance of the line, the duration of the step change was also increased from 0.16 seconds to 1.25 seconds. By doing this, we were able to create a negatively damped 0.3 Hz inter-area oscillation on which we could test the performance of the proposed control. On doing Prony analysis of the corresponding waveforms, Fig. 5.24 was obtained. It clearly illustrates the ability of the proposed technique in damping unstable oscillations of low frequency.

Fig. 5.24: Performance of proposed control on un-damped oscillations (4000+ bus model)

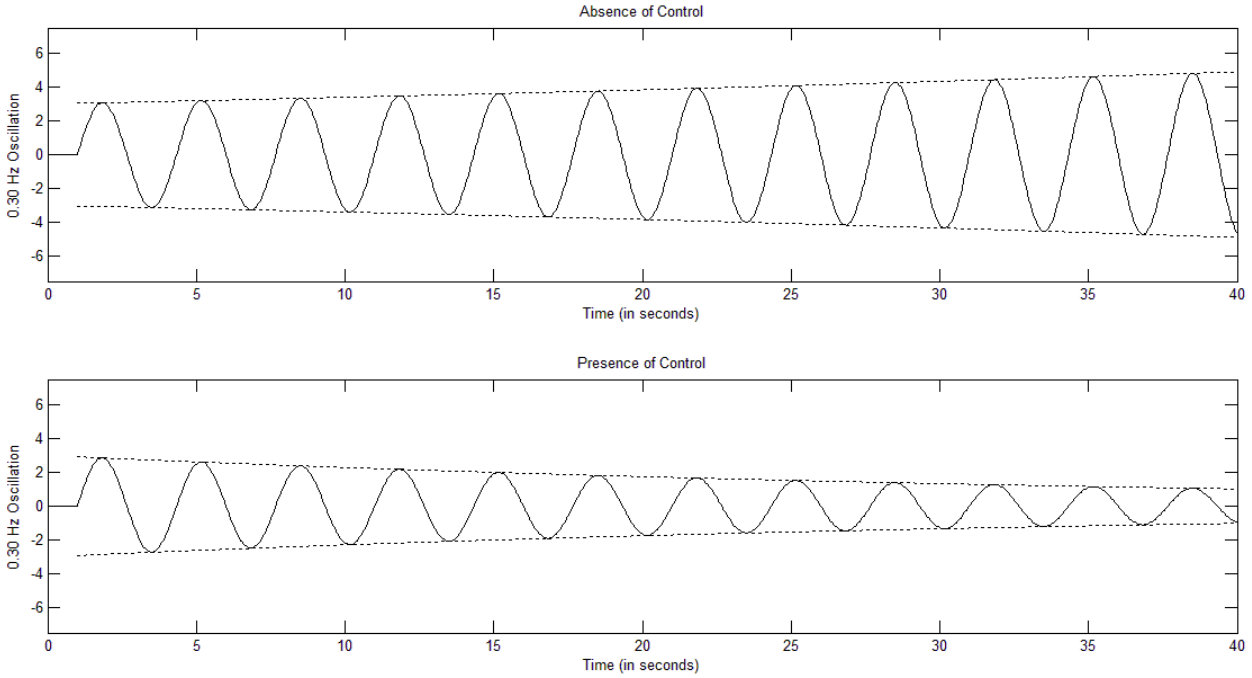

5.3 Conclusion

This chapter describes how the control law that was formulated in the Matlab suite PST can be applied to other standard power system simulators. The procedure to be followed for transferring the control for each of the three controllers used is explained in great details. An equivalent system, similar to the one in Matlab but more closer to the real-world system is created in PSLF to test the effectiveness of the control. A step input was provided to excite all the inter-area modes present in the system. On applying the control, it was observed that the inter-area modes were considerably damped without the local modes getting negatively affected. Considering the fact that the system which was used to come up with the

control was not the same on which it was applied, the performance of the control was found to be exemplary. The proposed control was then applied to the full-order model of the WECC system. The results indicated that the control performed reasonably well even on the full-order system without becoming computationally too complex. The conclusion made from this analysis was that, if the systems have good equivalence, then the proposed control technique developed in Matlab can be transferred to other power system simulators and even larger systems without significant loss in effectiveness.

Chapter 6 – Conclusion

6.1 Summary

This thesis presents an algorithm based on PMU measurements, Selective Modal Analysis (SMA) and Linear Matrix Inequalities (LMIs) to develop a robust damping controller capable of damping low frequency oscillations in general and the inter-area modes of oscillations in particular over a wide range of operating conditions. The advantage of the proposed technique being that it does not require frequent tuning/re-tuning of the controllers when the operating point undergoes small changes. Moreover, the design of the controller ensures that there is no negative interaction within the controls.

The proposed algorithm uses SMA to systematically reduce the size of the system to the relevant modes of oscillations. A polytopic system is created in Matlab by combining the reduced-order systems with LMIs being used for the design of the control. The control is tested on a 16 machine, 68 bus network depicting the New England – New York interconnected power system. DC lines and SVCs are used for the design of the control. The results indicate that the proposed technique is successful in providing sufficient damping to all the modes of oscillations with a special emphasis on the critical inter-area modes. It also reduced the complexity of the LMI optimization to such an extent that it could be applied to larger and more complex power systems.

The proposed control was then applied to a reduced-order model of the WECC system consisting of 29 machines and 127 buses. The controllers already present in the system were initially used for the development of the control. On doing so, it was observed that the number of controllers were not enough to provide the amount of damping that was required. More controllers in the form of ESDs were added into the system. The integrated form of control thus developed was found to provide adequate damping to the relevant modes of oscillations present in the system. Then, in order to test the versatility of the control developed herein and to make it more realistic, it was transferred from the Matlab environment to the environment of PSLF. However, since the two models were not identical, the gain of the control had to be adjusted to make it more effective. Although the control did not perform as well as it had in the Matlab environment because of the differences in the Matlab and PSLF models used, the fact that the logic of the control was sound was proved beyond doubt.

The proposed control was then transferred to the full-order model of the WECC system comprising of 4000+ buses and thousands of generators. In order to simulate the control, selective measurements were made corresponding to what was done in the 127-bus model. A step change in the loading of the Pacific DC Intertie was used as the contingency-under-test. The reason for using this particular case was that previous studies on this model had showed that this particular contingency excited all the low frequency

inter-area modes of oscillations present in the system. Moreover, since this was not one of the contingency cases used as the vertices of the polytope, it was a suitable case to test the robustness of the control. The control logic that was developed for the 127-bus model in PSLF was then applied to this system. The results indicate that the proposed methodology was successful in increasing the damping of all the low frequency inter-area modes present in the system. The implication of this was that the control technique developed in this thesis was sufficiently robust to damp oscillations in big systems without becoming computationally too complex. Thus, the thesis was successful in developing a robust coordinated form of control capable of damping low frequency inter-area oscillations over a wide variety of operating conditions. In other words, it had accomplished what it had set out to achieve.

6.2 Future Scope of Work

The control that we have developed in the course of this thesis is the first of its kind and therefore there is a possibility for further enhancements to be done in it. As an example of this, the proposed control had been able to provide more than 10% damping to all the inter-area modes present in the 127-bus model in the Matlab version whereas the damping percentage provided in the PSLF versions mainly ranged between 5 and 10. Although this difference was primarily because the two models were not identical, it also implied that there is scope for improvement in the development of the control itself. Similarly, the effect of the control on damping un-damped or very slightly damped oscillations can also be looked into.

In order to make the control more effective for future applications, the following areas can be considered good starting points –

a) Use of different cases to create the polytope,
b) Size of the Polytopic System,
c) Combination of Polytopes, and
d) Integrating PSSs into the control

These four topics are described in more details below.

Polytope composed of different cases: The eight cases that were the vertices of the polytope in this study were chosen so as to contain within them the relevant modes of oscillations that we wished to control. But they are not the only set of cases that will produce the desired result. A different choice of cases can be made to attain similar objective. Moreover, in future applications, one of the vertices can be made to contain an un-damped or very slightly damped inter-area mode of oscillation so that the control (if feasible) that is formed from such a polytope is guaranteed to damp un-stable oscillations. This can be one area in which research can be done in the near future.

Size of Polytopic System: For the design of the control developed in this thesis, the polytopic system had a dimension of 8, i.e. the LMI control came out of an eight-dimensional polytope. The eight cases that

had been used for the development of the polytope represented its eight vertices. The reason for choosing eight as the size of the polytope was that the version of Matlab that was being used for the development of the control was unable to process polytopes larger than eight. Recently it has been found that the latest versions of Matlab can work on polytopic systems having dimensions greater than eight. This implied that we could (in the near future) have more number of diverse cases combined together to create the polytope, thereby making the control more robust. However, the issue with having a large number of diverse cases is that the chances of the control becoming infeasible are also greatly increased. Therefore, there is a need to come up with an optimum size of the polytopic formulation which can satisfy all of our requirements and at the same time, be realistic. Research is currently being done to find this optimal size.

Combination of Polytopes: Before it was realized that the latest versions of Matlab could handle more than eight cases, the only way to increase the robustness of the control was to combine the gain matrices obtained from two or more eight-dimensional polytopes in an optimal manner. The logic to be used was that by combining m polytopes in an optimal fashion, one could handle $8 \times m$ cases at the same time. The control vector (u) would then look like,

$$u = -(\beta_1 K_1 + \beta_2 K_2 + \cdots + \beta_m K_m)x \tag{6.1}$$

Where,

$$\sum_{i=1}^{m} \beta_i = 1 \tag{6.2}$$

In the above equations, m denotes the number of polytopes being combined together and β_i represents the scalar multipliers denoting the percentage weight of the i^{th} polytope in the overall control design. It is expected that the concept of maximum-likelihood criterion will be used for computing the values of $\beta_i s$.

The advantage of combining the polytopes is that if the $\beta_i s$ are properly selected, then a very high number of diverse cases can be combined together to develop the control without having to face the problem of the control becoming infeasible. Moreover, this technique can be combined with the previous one (increasing size of individual polytopes) to generate a much more robust control. The only issue that has to be addressed in this method is the proper selection of the $\beta_i s$. If they are not selected correctly, then the control obtained from one polytope might work against the control obtained from another polytope, thereby failing the very purpose for which the control was developed. Research is currently ongoing for the correct selection of $\beta_i s$.

Integrating PSSs into the control: For the development of control in this thesis, DC lines, FACTS devices (SVCs) and ESDs had been used as the controllers. However, PSSs are the traditional units used to provide damping to the different oscillations present in the system and so they can also be made

a part of the integrated form of control that we have developed here. The primary reason for not including PSSs in the present control design was to alleviate the involved complexity associated with their inclusion in the iterations of SMA. This can be one topic on which research can be done in the near future.

References

[1] P. Kundur, *Power System Stability and Control*, New York: McGraw-Hill, 1994.

[2] Leonard L. Grigsby, *Power System Stability and Control*, 2nd Edition, CRC Press, 2008.

[3] P. Kundur; M. Klein, G. J. Rogers, and M. S. Zywno, "Application of power system stabilizers for enhancement of overall system stability," *Power Systems, IEEE Transactions on*, Vol. 4, No. 2, pp. 614-626, 1989.

[4] A. F. Snyder, "Inter-area Oscillation Damping by Power System Stabilizers with Synchronized Phasor Measurements," *Interim Research Report, Laboratoire d'Electrotechnique de Grenoble*, Grenoble, France, Sept. 1996.

[5] G. J. Rogers, "The Application of Power System Stabilizers to a Multi-generator Plant", *IEEE Trans. Power Syst.*, Vol. 15, No. 1, pp. 350-355, Feb. 2000.

[6] D. N. Kosterev, W. Taylor, and W. A. Mittelstadt, "Model validation for the August 10, 1996 WSCC system outage," IEEE Trans. on Power Syst., Vol. 14, No. 3, pp. 967-979, Aug. 1999.

[7] G. P. Liu, Z. Xu, Y. Huang, and W. L. Pan, "Analysis of inter-area oscillations in the South China interconnected power system," Electric Power Systems Research, Vol.70, pp. 38-45, June 2004.

[8] M. Q. Dong, D. J. Yang, and Y. Huang, "Analysis on the low frequency oscillation incidents measured by WAMS of Central China power grid during the 2008 ice hazard," Central China Electric Power, Vol. 21, No. 5, pp. 22-25, 2008.

[9] F. Zhu, Z. H. Liu, and L. Chu, "Achievement and experience of improving power system stability by PSS/excitation control in China," Power Engineering Society General Meeting, 2004. IEEE, Vol. 2, pp. 1767-1771, 2004.

[10] D. Hu, and V. Venkatasubramania, "New Wide-Area Algorithms for Detection and Mitigation of Angle Instabilities using Synchrophasors," *IEEE Power Engineering Society General Meeting*, pp.1-8, 2007.

[11] G. Q. Hu, R. M. He, H. C. Yang, P. Wang, and R. Ma, "Iterative Prony Method Based Power System Low Frequency Oscillation Mode Analysis and PSS Design," *Transmission and Distribution Conference and Exhibition: Asia and Pacific, 2005 IEEE/PES*, pp. 1-6, 2005.

[12] H. Ni, G. T. Heydt, and L. Mili, "Power system stability agents using robust wide area control," *IEEE Trans. Power Syst.*, Vol. 17, No. 9, pp. 1123-1131, Nov. 2002.

[13] Bikash Pal, and Balarko Chaudhuri, *Robust Control in Power Systems*, Springer Science + Business Media, Inc., 2005.

[14] J. Paserba, “Analysis and control of power system oscillation,” *CIGRE Special Publication 38.01.07*, Technical Brochure 111, 1996.

[15] M. Klein, G. J. Rogers, and P. Kundur, “A fundamental study of inter-area oscillations in power systems,” *Power Systems, IEEE Transactions on*, Vol. 6, No. 3, pp. 914-921, Aug. 1991.

[16] O. W. Hanson, C. J. Goodwin, and P. L. Dandeno, “Identification of Excitation and Speed Control Parameters in stabilizing inter-system oscillations,” *Power Apparatus and Systems, IEEE Transactions on*, Vol. PAS-87, No. 5, pp. 1306-1313, 1968.

[17] M. Klein, G. J. Rogers, S. Moorty, and P. Kundur, “Analytical investigation of factors influencing power system stabilizers performance,” *Energy Conversion, IEEE Transactions on*, Vol. 7, No. 3, pp. 382-390, Jan. 1992.

[18] D. K. Mugwanya, and J. E. Van Ness, “Mode coupling in power systems,” *Power Systems, IEEE Transactions on*, Vol. 2, No. 2, pp. 264-269, 1987.

[19] E. V. Larsen, and D. A. Swann. “Applying Power System Stabilizers Part II: Performance Objectives and Tuning Concepts,” *IEEE Transactions on Power Apparatus and Systems*, Vol. PAS-100, No. 6, pp. 3025-3033, June 1981.

[20] I. Kamwa, R. Grondin, and G. Trudel, “IEEE PSS2B versus PSS4B: The limits of Performance of Modern Power System Stabilizers” *IEEE Trans. Power Syst.*, Vol. 20, No. 2, pp. 903-915, May 2005.

[21] I. Kamwa, and L. Gerin-Lajoie, “State-Space System Identification-Towards MIMO Models for Modal Analysis and Optimization of Bulk Power Systems”, *IEEE Trans Power Syst.*, Vol. 15, No. 1, pp. 326-335, Feb. 2000.

[22] Y. Zhang, and A. Bose, “Design of Wide-Area Damping Controls for Inter-area Oscillations”, *IEEE Trans. Power Syst.*, Vol. 23, No. 3, pp.1136-1143, Aug. 2008.

[23] M. E. Aboul-Ela, A. A. Sallam, J. D. McCalley, and A. A. Fouad, “Damping controller design for power system oscillations using global signals”, *IEEE Trans. Power Syst.*, Vol. 11, No. 2, pp. 767-773, May 1996.

[24] D. R. Ostojic. “Stabilization of Multimodal Electromechanical Oscillations by Coordinated Application of Power System Stabilizers,” *IEEE Transactions on Power Systems*, Vol. 6, No. 4, pp. 1439-1445, Nov. 1991.

[25] X. Yang, and A. Feliachi. “Stabilization of Inter-Area Oscillation Modes through Excitation Systems,” *IEEE Transactions on Power Systems*, Vol. 9, No. 1, pp. 494-502, Feb. 1994.

[26] E. V. Larsen, and D. A. Swann. “Applying Power System Stabilizers Part I: General Concepts,” *IEEE Transactions on Power Apparatus and Systems*, Vol. PAS-100, No. 6, pp. 3017-3024, June 1981.

[27] E. V. Larsen, and D. A. Swann. “Applying Power System Stabilizers Part III: Practical Considerations,” *IEEE Transactions on Power Apparatus and Systems*, Vol. PAS-100, No. 6, pp. 3034-3041, June 1981.

[28] H. Bourles, S. Peres, T. Margotin, and M. P. Houry, “Analysis and design of a robust coordinated AVR/PSS,” *Power Systems, IEEE Transactions on*, Vol. 13, No. 2, pp. 568-575, 1998.

[29] L. Wang. “Damping Effects of Supplementary Excitation Control Signals on Stabilizing Generator Oscillations,” *International Journal of Electrical Power & Energy Systems*, Vol. 18, No. 1, pp. 47-53, Jan. 1996.

[30] A. J. A. Simoes Costa, F. D. Freitas, and A. S. e Silva, “Design of Decentralized Controllers for Large Power Systems Considering Sparsity,” *Power Systems, IEEE Transactions on*, Vol. 12, No. 1, pp. 144-152, 1997.

[31] M. Nambu and Y. Ohsawa. “Development of an Advanced Power System Stabilizer Using a Strict Linearization Approach,” *IEEE Transactions on Power Systems*, Vol. 11, No. 2, pp. 813-818, May 1996.

[32] IEEE Power Engineering Society System Oscillations Working Group, “Inter-Area Oscillations in Power Systems,” *IEEE #95-TP-101*, Oct. 1994.

[33] IEEE-PES and CIGRE, “FACTS Overview,” *IEEE Cat. #95TP108*, 1995.

[34] U. P. Mhaskar and A. M. Kulkarni, “Power oscillation damping using FACTS devices: Modal controllability, observability in local signals, and location of transfer function zeros,” *IEEE Trans. Power Syst.*, Vol. 21, No. 1, pp. 285-294, Feb. 2006.

[35] R. L. Cresap, W. A. Mittelstadt, D. N. Scott, and C. W. Taylor, "Operating Experience with Modulation of the Pacific HVDC Inter-tie", *IEEE Trans on Power Apparatus and Systems*, Vol. 97, No. 4, pp. 1053-1059, Apr. 1978.

[36] D. E. Martin, W. K. Wong, D. L. Dickmander, R. L. Lee, and D. J. Melvold, "Increasing WSCC power system performance with modulation controls on the Intermountain Power Project HVDC system", *IEEE Trans. on Power Delivery*, Vol. 7, No. 3, pp. 1634-1642, July 1992.

[37] P. S. Rao, and I. Sen, “Robust pole placement stabilizer design using linear matrix inequalities,” *IEEE Trans. Power Syst.*, Vol. 15, No. 1, pp. 313-319, 2000.

[38] M. Soliman, H. Emara, A. Elshafei, A. Bahgat, and O. P. Malik, “Robust output feedback power system stabilizer design: an LMI approach,” *IEEE Power and Energy Society General Meeting Conversion and Delivery of Electrical Energy in the 21st Century*, pp. 1-8, July 2008.

[39] V. A. F. De Campos, J. J. Da Cruz, and L. C. Zanetta, “Pole placement and robust adjustment of power systems stabilizers through linear matrix inequalities”, *Power Systems Conference and Exposition, PSCE*, pp. 2180-2187, 2006.

[40] A. Bensenouci, and A. M. Abdel Ghamy, “Mixed H_∞/H_2 with pole placement design of robust LMI-based Output feedback controllers for multi-area load frequency control”, *EUROCON 2007, Warsaw*, pp. 9-12, Sep. 2007.

[41] R. A. Jabr, B. C. Pal, and N. Martins, “A sequential Conic Programming Approach for the Coordinated and robust Design of Power System stabilizers”, *IEEE Trans Power Systems*, Vol. 25, No. 3, pp. 1627-1637, Aug. 2010.

[42] J. Ma, S. Garlapati, and J. Thorp, “Robust WAMS based control of inter area oscillations”, *Electric Power Components and Systems*, Vol. 39, No. 9, pp. 850-862, May 2011.

[43] G. C. Verghese, I. J. Perez-Arriaga, and F. C. Schweppe, “Selective modal analysis with applications to electric power systems, Part II: The Dynamic Stability Problem”, *IEEE Trans. PAS*, Vol. 101, No. 9, pp. 3126-3134, Sept. 1982.

[44] F. L. Pagola, Rouco, and I. J. Perez-Arriaga, “Analysis and Control of Small-Signal Stability in Electric Power Systems by Selective Modal Analysis,” *Eigenanalysis and Frequency Domain Methods for System Dynamic performance, IEEE publication 90TH0292-3-PWR*.

[45] J. J. Sinchez-Gasca, and J. H. Chow, “Power system reduction to simplify the design of damping controllers for inter-area oscillations,” *IEEE Trans. Power Syst.*, Vol. 11, No. 3, pp. 1342-1349, Aug. 1996.

[46] L. Wang, M. Klein, S. Yirga, and P. Kundur, “Dynamic Reduction of Large Power Systems for Stability Studies,” *IEEE Trans. on Power Systems*, Vol. 2, No. 2, pp. 889-895, May 1997.

[47] S. Boyd, L. El Ghaoui, E. Feron, and V. Balakrishnan, *Linear Matrix Inequalities in Systems and Control Theory*, SIAM books, Philadelphia, 1994.

[48] P. Gahinet, A. Nemirovski, A. J. Laub, and M. Chilali, *LMI Control Toolbox for use with MATLAB*, The Math Works, Inc., USA.

[49] J. I. Perez-Arriaga, *Selective Modal Analysis with applications to Power systems*, Ph. D. Dissertation, Department of Electrical Engineering and Computer Science, Massachusetts Institute of Technology, Massachusetts, June 1981.

[50] I. J. Perez-Arriaga, G. C. Verghese, and F. C. Schweppe, “Selective Modal Analysis with Applications to Electric Power Systems, Part I: Heuristic Introduction,” *IEEE Trans. PAS*, Vol. 101, No. 9, pp. 3117-3125, Sept. 1982.

[51] I. J. Perez-Arriaga, F. L. Pagola, G. C. Verghese, and F. C. Schweppe, “Selective Modal Analysis in Power Systems,” *American Control Conference*, pp. 650-655, 1983.

[52] J. F. Camino, J. W. Helton, and R. E. Skelton, “Solving matrix inequalities whose unknowns are matrices,” *43rd IEEE Conference on Decision and Control, 2004, CDC*, Vol. 3, pp. 3160-3166, 2004.

[53] G. Rogers, *Power System Oscillations*, Norwell, MA: Kluwer, 2000.

[54] DSA Tools, Dynamic Security Assessment Software, Powertech Labs Inc., http://www.dsatools.com/

[55] Electric Power Research Institute, “DC Multi-Infeed Study,” *EPRI, TR-TR-104586s, Projects 2675-04-05*, Final Report, Dec. 1994.

[56] Elizondo, David C., "A Methodology to Assess and Rank the Effects of Hidden Failures in Protection Schemes Based on Regions of Vulnerability and Index of Severity", Ph. D Dissertation, Bradley Department of Electrical and Computer Engineering, Virginia Polytechnic Institute and State University, Blacksburg, VA, 2003.

[57] P. F. Ribeiro, B. K. Johnson, M. L. Crow, A. Arsoy, and Y. Liu, "Energy Storage Systems for advanced power applications," *Proceedings of the IEEE*, Vol. 89, No. 12, pp. 1744-1756, 2001.

[58] W. Du, H. F. Wang, and R. Dunn, "Power system oscillation stability and control by FACTS and ESS–a survey," *International Conference on Sustainable Power Generation and Supply, SUPERGEN 2009*, pp. 1 – 13, 2009.

[59] M. H. Ali, B. Wu, and Roger A. Dougal, "An overview of SMES applications in power and energy systems," *IEEE Trans. on Sustainable Energy*, Vol. 1, No. 1, pp.38-47, Apr. 2010.

[60] P. Mercier, R. Cherkaoui, A. Oudalov, "Optimizing a battery energy storage system for frequency control application in an isolated power system," *IEEE Trans. on Power Syst.*, Vol. 24, No. 3, pp.1469-1477, Aug. 2009.

[61] S. M. Muyeen, R. Takahashi, M. H. Ali, T. Murata, and J. Tamura, "Transient stability augmentation of power system including wind farms by using ECS," *IEEE Trans. on Power Syst.*, Vol. 23, No. 3, pp.1179-1187, Aug. 2008.

[62] M. L. Lazarewicz, and A. Rojas, "Grid frequency regulation by recycling electrical energy in flywheels," *in Proc. 2004 IEEE Power Engineering Society General Meeting*, Vol. 2, pp. 2038-2042, 2004.

[63] S. Skogestad, and I. Postlethwaite, *Multivariable Feedback Control*, New York: Wiley, 2001.

[64] I. Kamwa, R. Grondin, and Y. Hébert, "Wide-Area measurement based stabilizing control of large power systems—a decentralized/hierarchical approach," *IEEE Trans. on Power Syst.*, Vol.16, No. 1, pp. 136-153, Feb. 2001.

[65] S. Ray and G. K. Venayagamoorthy, "Wide-area signal-based optimal neuron controller for a UPFC," *IEEE Trans. on Power Del.*, Vol. 23, No. 3, pp. 1597–1605, July 2008.

[66] B. Chaudhuri, B. C. Pal, "Robust damping of multiple swing modes employing global stabilizing signals with a TCSC," *IEEE Trans. on Power Syst.*, Vol. 19, No. 1, pp. 499-506, Feb. 2004.

[67] F. Okou, L.-A. Dessaint, and O. Akhrif, "Power systems stability enhancement using a wide-area signals based hierarchical controller," *IEEE Trans. on Power Syst.*, Vol. 20, No. 3, pp.1465-1477, Aug. 2005.

[68] Li Peng, Wu Xiaochen, Lu Chao, Shi Jinghai, Hu Jiong, He Jingbo, Zhao Yong, and Xu Aidong, "Implementation of CSG's wide-area damping control system: overview and experience," *Power Systems Conference and Exposition, 2009. PSCE '09*, pp. 1-9, 2009.

[69] GE Energy's Positive Sequence Load Flow (PSLF) Software and User Manual, http://site.ge-energy.com/prod_serv/products/utility_software/en/ge_pslf/index.htm

[70] Prony Toolbox in MATLAB, http://www.mathworks.com/matlabcentral/fileexchange/3955

[71] R. Prony, “Essai experimentale et analytique,” *J. l’ Ecole Polytechnique*, Vol. 1, pp. 24–76, 1795.

[72] J. F. Hauer, C. J. Demeure, and L. L. Scharf, “Initial results in Prony Analysis of Power System response signals,” *Power Systems, IEEE Transactions on*, Vol. 5, No. 1, pp. 80-89, 1990.

Appendix A: System Details

A.1 4-Machine 2-Area System

The 4-machine, 2-area system is a standard power system problem which was created for a research report commissioned from Ontario Hydro by the Canadian Electrical Association [15, 53] to exhibit the different types of oscillations that occur in both large and small interconnected power systems. The bus data, line data, transformer data, load data and generator data for this system are summarized below. The Base MVA for this system was 100 MVA.

Bus Data: Bus number is the unique number used to identify the bus, the base kV denotes the base voltage of the bus in kV, the magnitude of the bus voltage is expressed in p.u., the angle of the bus voltage is expressed in degrees, and the bus type denotes whether the particular bus is the swing bus, a generator bus or a load bus.

Bus Numbers	Base kV	Voltage Magnitude (p.u.)	Voltage Angle (degree)	Bus Type
1	22	1.0300	18.50	Gen Bus
2	22	1.0100	8.80	Gen Bus
3	500	1.0000	-6.10	Load Bus
4	115	0.9500	-10.00	Load Bus
5	115	1.0000	-10.00	Load Bus
10	230	1.0100	12.10	Load Bus
11	22	1.0300	-6.80	Gen Bus
12	22	1.0100	-16.90	Swing Bus
13	500	0.9900	-31.80	Load Bus
14	115	0.9500	-38.00	Load Bus
15	115	1.0000	-14.00	Load Bus
20	230	0.9900	2.10	Load Bus
101	500	1.0500	-19.30	Load Bus
110	230	1.0100	-13.40	Load Bus
120	230	0.9900	-23.60	Load Bus

Line Data: Line Number is the unique number used to identify the line, From Bus # represents the number of the From Bus, To Bus # represents the number of the To Bus, the resistance of the line is measured in p.u., the reactance of the line is measured in p.u., and the line charging susceptance is also measured in p.u.

Line Numbers	From Bus #	To Bus #	Resistance (p.u.)	Reactance (p.u.)	Line Charging (p.u.)
1	1	10	0.0002	0.0167	0.0100
2	2	20	0.0001	0.0167	0.0100
3	3	4	0.0001	0.0050	0.0100
4	3	5	0.0010	0.0070	0.0100
5	3	20	0.0010	0.0100	0.0175
6	3	101	0.0110	0.1100	0.1925
7	3	101	0.0110	0.1100	0.1925
8	10	20	0.0025	0.0250	0.0437
9	11	110	0.0010	0.0167	0.0000
10	12	120	0.0010	0.0167	0.0000
11	13	14	0.0001	0.0070	0.0000
12	13	15	0.0010	0.0100	0.0000
13	13	101	0.0110	0.1100	0.1925
14	13	101	0.0110	0.1100	0.1925
15	13	120	0.0010	0.0100	0.0175
16	110	120	0.0025	0.0250	0.0437

Load Data: Bus Number is the unique number used to identify the bus to which the load is connected, the base kV denotes the base voltage of the bus in kV, P_load denotes the real component of the load and is measured in p.u., while Q_load denotes the reactive component of the load and is also measured in p.u.

Bus Numbers	Base kV	P_load (p.u.)	Q_load (p.u.)
4	115	9.76	1
5	115	10.7	2.8
14	115	17.7	1
15	115	-10.4	2.7

Generator Data: Bus Number is the unique number used to identify the bus to which the generator is connected, MVA_base denotes the base MVA of the individual generators, P_gen denotes the real component of the power generated by the generator and is measured in p.u., Q_gen denotes the reactive component of the power generated by the generator and is also measured in p.u., X_l denotes the leakage reactance in p.u., X'_d denotes the unsaturated direct-axis transient reactance of the generator, H denotes the inertia constant of the turbine-governor set and is measured in seconds, and Qgen_max and Qgen_min denote the maximum and the minimum reactive power limits respectively.

Bus Numbers	MVA_base	P_gen (p.u.)	Q_gen (p.u.)	X_l (p.u.)	X'_d (p.u.)	H (sec)	Qgen_max (p.u.)	Qgen_min (p.u.)
1	1400	7.000	1.610	0.200	0.250	4.000	99	-99
2	1000	7.000	5.760	0.120	0.250	3.900	99	-99
11	700	7.160	1.490	0.200	0.250	3.500	99	-99
12	1000	7.000	1.390	0.120	0.250	6.500	99	-99

A.2 16-Machine System

The 16-machine, 68-bus system is an equivalent model of the New England-New York interconnected power system. The bus data, line data, transformer data, load data and generator data for this system are summarized below. The Base MVA for this system was 100 MVA.

Bus Data: Bus number is the unique number used to identify the bus, the magnitude of the bus voltage is expressed in p.u., the angle of the bus voltage is expressed in degrees, and the bus type denotes whether the particular bus is the swing bus, a generator bus or a load bus.

Bus Numbers	Voltage Magnitude (p.u.)	Voltage Angle (degree)	Bus Type
1	1.0600	6.57	Load Bus
2	1.0500	8.35	Load Bus
3	1.0300	5.39	Load Bus
4	1.0000	4.28	Load Bus
5	1.0000	5.22	Load Bus
6	1.0100	5.90	Load Bus
7	1.0000	3.64	Load Bus
8	1.0000	3.10	Load Bus
9	1.0300	2.55	Load Bus
10	1.0100	8.42	Load Bus
11	1.0100	7.56	Load Bus
12	1.0500	7.58	Load Bus
13	1.0100	7.75	Load Bus
14	1.0100	6.20	Load Bus
15	1.0100	6.11	Load Bus
16	1.0300	7.64	Load Bus
17	1.0300	6.55	Load Bus
18	1.0300	5.68	Load Bus
19	1.0500	12.24	Load Bus
20	0.9900	10.80	Load Bus
21	1.0300	10.28	Load Bus
22	1.0500	14.95	Load Bus
23	1.0400	14.67	Load Bus
24	1.0300	7.82	Load Bus
25	1.0600	9.67	Load Bus
26	1.0500	8.17	Load Bus
27	1.0400	6.29	Load Bus
28	1.0500	11.30	Load Bus

Bus Numbers	Voltage Magnitude (p.u.)	Voltage Angle (degree)	Bus Type
29	1.0500	13.94	Load Bus
30	1.0500	6.03	Load Bus
31	1.0500	8.56	Load Bus
32	1.0500	10.92	Load Bus
33	1.0500	7.44	Load Bus
34	1.0600	2.54	Load Bus
35	1.0100	2.55	Load Bus
36	1.0400	-0.85	Load Bus
37	1.0200	-6.80	Load Bus
38	1.0500	8.57	Load Bus
39	1.0000	-8.40	Load Bus
40	1.0600	15.24	Load Bus
41	0.9900	44.66	Load Bus
42	0.9900	39.19	Load Bus
43	1.0100	-7.58	Load Bus
44	1.0100	-7.61	Load Bus
45	1.0100	2.60	Load Bus
46	1.0200	9.42	Load Bus
47	1.0700	7.34	Load Bus
48	1.0700	9.27	Load Bus
49	1.0200	14.11	Load Bus
50	1.0100	19.56	Load Bus
51	1.0200	6.64	Load Bus
52	0.9900	38.96	Load Bus
53	1.0400	9.55	Gen Bus
54	0.9800	14.37	Gen Bus
55	0.9800	16.40	Gen Bus
56	0.9900	17.45	Gen Bus
57	1.0100	15.98	Gen Bus
58	1.0500	20.29	Gen Bus
59	1.0600	22.52	Gen Bus
60	1.0300	16.41	Gen Bus
61	1.0200	20.75	Gen Bus
62	1.0100	15.84	Gen Bus
63	1.0000	18.31	Gen Bus
64	1.0100	4.85	Gen Bus
65	1.0100	0.00	Swing Bus
66	1.0000	46.19	Gen Bus
67	1.0000	40.05	Gen Bus

Bus Numbers	Voltage Magnitude (p.u.)	Voltage Angle (degree)	Bus Type
68	1.0000	45.89	Gen Bus
98	1.0200	8.83	Load Bus
99	1.0200	14.71	Load Bus
198	1.0514	5.65	Load Bus
199	1.0553	8.08	Load Bus
298	1.0200	9.20	Load Bus
299	1.0000	8.08	Load Bus

Line Data: Line Number is the unique number used to identify the line, From Bus # represents the number of the From Bus, To Bus # represents the number of the To Bus, the resistance of the line is measured in p.u., the reactance of the line is measured in p.u., and the line charging susceptance is also measured in p.u.

Line Numbers	From Bus #	To Bus #	Resistance (p.u.)	Reactance (p.u.)	Line Charging (p.u.)
1	1	2	0.0035	0.0411	0.6987
2	1	30	0.0008	0.0074	0.4800
3	2	3	0.0013	0.0151	0.2572
4	2	25	0.0070	0.0086	0.1460
5	3	4	0.0013	0.0213	0.2214
6	3	18	0.0011	0.0133	0.2138
7	4	5	0.0008	0.0128	0.1342
8	4	14	0.0008	0.0129	0.1382
9	5	6	0.0002	0.0026	0.0434
10	5	8	0.0008	0.0112	0.1476
11	6	7	0.0006	0.0092	0.1130
12	6	11	0.0007	0.0082	0.1389
13	7	8	0.0004	0.0046	0.0780
14	8	9	0.0023	0.0363	0.3804
15	9	30	0.0019	0.0183	0.2900
16	10	11	0.0004	0.0043	0.0729
17	10	13	0.0004	0.0043	0.0729
18	13	14	0.0009	0.0101	0.1723
19	14	15	0.0018	0.0217	0.3660
20	15	16	0.0009	0.0094	0.1710
21	16	17	0.0007	0.0089	0.1342
22	16	19	0.0016	0.0195	0.3040
23	16	21	0.0008	0.0135	0.2548
24	16	24	0.0003	0.0059	0.0680
25	17	18	0.0007	0.0082	0.1319
26	17	27	0.0013	0.0173	0.3216
27	21	22	0.0008	0.0140	0.2565
28	22	23	0.0006	0.0096	0.1846
29	23	24	0.0022	0.0350	0.3610
30	23	59	0.0005	0.0272	0.0000
31	25	26	0.0032	0.0323	0.5310
32	26	27	0.0014	0.0147	0.2396
33	26	28	0.0043	0.0474	0.7802
34	26	29	0.0057	0.0625	1.0290

Line Numbers	From Bus #	To Bus #	Resistance (p.u.)	Reactance (p.u.)	Line Charging (p.u.)
35	28	29	0.0014	0.0151	0.2490
36	9	30	0.0019	0.0183	0.2900
37	9	36	0.0022	0.0196	0.3400
38	9	36	0.0022	0.0196	0.3400
39	36	37	0.0005	0.0045	0.3200
40	34	36	0.0033	0.0111	1.4500
41	33	34	0.0011	0.0157	0.2020
42	32	33	0.0008	0.0099	0.1680
43	30	31	0.0013	0.0187	0.3330
44	30	32	0.0024	0.0288	0.4880
45	1	31	0.0016	0.0163	0.2500
46	31	38	0.0011	0.0147	0.2470
47	33	38	0.0036	0.0444	0.6930
48	38	46	0.0022	0.0284	0.4300
49	46	49	0.0018	0.0274	0.2700
50	1	47	0.0013	0.0188	1.3100
51	47	48	0.0025	0.0268	0.4000
52	47	48	0.0025	0.0268	0.4000
53	48	40	0.0020	0.0220	1.2800
54	35	45	0.0007	0.0175	1.3900
55	37	43	0.0005	0.0276	0.0000
56	43	44	0.0001	0.0011	0.0000
57	44	45	0.0025	0.0730	0.0000
58	39	44	0.0000	0.0411	0.0000
59	39	45	0.0000	0.0839	0.0000
60	45	51	0.0004	0.0105	0.7200
61	50	52	0.0012	0.0900	2.0600
62	50	51	0.0009	0.0221	1.6200
63	49	52	0.0076	0.0077	1.1600
64	52	42	0.0040	0.0600	2.2500
65	42	41	0.0040	0.0600	2.2500
66	41	40	0.0060	0.0840	3.1500

Transformer Data: Transformer Number is the unique number used to identify the transformer, From Bus # represents the number of the From Bus, To Bus # represents the number of the To Bus, the resistance of the transformer is measured in p.u., the reactance of the transformer is measured in p.u., and the line charging susceptance (if present) is also measured in p.u. The tap-ratio is mentioned in the last column.

Transformer Numbers	From Bus #	To Bus #	Resistance (p.u.)	Reactance (p.u.)	Line Charging (p.u.)	Tap Ratio
1	1	27	0.0320	0.3200	0.41	1.00
2	2	53	0.0000	0.0091	0.00	1.03
3	6	54	0.0000	0.0250	0.00	1.07
4	10	55	0.0000	0.0200	0.00	1.07
5	12	11	0.0016	0.0435	0.00	1.06
6	12	13	0.0016	0.0435	0.00	1.06
7	19	20	0.0007	0.0138	0.00	1.06
8	19	56	0.0007	0.0142	0.00	1.07
9	20	57	0.0009	0.0180	0.00	1.01
10	22	58	0.0000	0.0143	0.00	1.03
11	25	60	0.0006	0.0232	0.00	1.03
12	29	61	0.0008	0.0156	0.00	1.03
13	31	62	0.0000	0.0260	0.00	1.04
14	32	63	0.0000	0.0130	0.00	1.04
15	35	34	0.0001	0.0074	0.00	0.95
16	36	64	0.0000	0.0075	0.00	1.04
17	37	65	0.0000	0.0033	0.00	1.04
18	41	66	0.0000	0.0015	0.00	1.00
19	41	98	0.0000	0.0100	0.00	1.00
20	42	67	0.0000	0.0015	0.00	1.00
21	42	99	0.0000	0.0100	0.00	1.00
22	42	198	0.0000	0.0100	0.00	1.00
23	46	298	0.0000	0.0100	0.00	1.00
24	49	299	0.0000	0.0100	0.00	1.00
25	52	68	0.0000	0.0030	0.00	1.00
26	52	199	0.0000	0.0100	0.00	1.00

Load Data: Bus Number is the unique number used to identify the bus to which the load is connected, P_load denotes the real component of the load and is measured in p.u., while Q_load denotes the reactive component of the load and is also measured in p.u.

Bus Numbers	P_load (p.u.)	Q_load (p.u.)
1	2.527	1.1856
2	0	0
3	3.22	0.02
4	5	1.84
5	0	0
6	0	0
7	2.34	0.84
8	5.22	1.77
9	1.04	1.25
10	0	0
11	0	0
12	0.09	0.88
13	0	0
14	0	0
15	3.2	1.53
16	3.29	0.32
17	0	0
18	1.58	0.3
19	0	0
20	6.8	1.03
21	2.74	1.15
22	0	0
23	2.48	0.85
24	3.09	-0.92
25	2.24	0.47
26	1.39	0.17
27	2.81	0.76
28	2.06	0.28
29	2.84	0.27
30	0	0
31	0	0
32	0	0
33	1.12	0
34	0	0
35	0	0

Bus Numbers	P_load (p.u.)	Q_load (p.u.)
36	1.02	-0.1946
37	60	3
38	0	0
39	2.67	0.126
40	0.6563	0.2353
41	10	2.5
42	11.5	2.5
43	0	0
44	2.6755	0.0484
45	2.08	0.21
46	1.507	0.285
47	2.0312	0.3259
48	2.412	0.022
49	1.64	0.29
50	1	-1.47
51	3.37	-1.22
52	24.7	1.23
53	0	0
54	0	0
55	0	0
56	0	0
57	0	0
58	0	0
59	0	0
60	0	0
61	0	0
62	0	0
63	0	0
64	0	0
65	0	0
66	0	0
67	0	0
68	0	0
98	1.09	0.36
99	-1.1	0.609
198	1.09	0.36
199	-1.1	0.609
298	1.09	0.36
299	-1.1	0.609

Generator Data: Bus Number is the unique number used to identify the bus to which the generator is connected, MVA_base denotes the base MVA of the individual generators, P_gen denotes the real component of the power generated by the generator and is measured in p.u., Q_gen denotes the reactive component of the power generated by the generator and is also measured in p.u., X_l denotes the leakage reactance in p.u., X'_d denotes the unsaturated direct-axis transient reactance of the generator, H denotes the inertia constant of the turbine-governor set and is measured in seconds, and Qgen_max and Qgen_min denote the maximum and the minimum reactive power limits respectively.

Bus Numbers	MVA_base	P_gen (p.u.)	Q_gen (p.u.)	X_l (p.u.)	X'_d (p.u.)	H (sec)	Qgen_max (p.u.)	Qgen_min (p.u.)
53	300	2.500	0.000	0.003	0.248	3.400	999	-999
54	800	5.450	0.000	0.035	0.425	4.949	999	-999
55	800	6.500	0.000	0.030	0.383	4.962	999	-999
56	800	6.320	0.000	0.030	0.300	4.163	999	-999
57	700	5.052	0.000	0.027	0.360	4.767	999	-999
58	900	7.000	0.000	0.022	0.354	4.911	999	-999
59	800	5.600	0.000	0.032	0.299	4.327	999	-999
60	800	5.400	0.000	0.028	0.354	3.915	999	-999
61	1000	8.000	0.000	0.030	0.487	4.037	999	-999
62	1200	5.000	0.000	0.020	0.487	2.911	999	-999
63	1600	10.000	0.000	0.010	0.253	2.005	999	-999
64	1900	13.500	0.000	0.022	0.552	5.179	999	-999
65	12000	35.910	0.000	0.003	0.334	4.078	0	0
66	10000	17.850	0.000	0.002	0.285	3.000	999	-999
67	10000	10.000	0.000	0.002	0.285	3.000	999	-999
68	11000	40.000	0.000	0.004	0.359	4.450	999	-999

A.3 29-Machine System

The 29-machine, 127-bus system is an equivalent model of the WECC system. The bus data, line data, transformer data, load data, generator data and shunt data for this system are summarized below. The Base MVA for this system was 100 MVA.

Bus Data: Bus number is the unique number used to identify the bus, the bus name is the unique name used to identify the bus, the base kV denotes the base voltage of the bus in kV, the magnitude of the bus voltage is expressed in p.u., the angle of the bus voltage is expressed in degrees, and the bus type denotes whether the particular bus is the swing bus, a generator bus or a load bus.

Bus Numbers	Bus Names	Base kV	Voltage Magnitude (p.u.)	Voltage Angle (degree)	Bus Type
1	CMAIN GM	20	1.0200	67.80	Gen Bus
2	CA230	230	1.0011	62.87	Load Bus
3	CA230TO	230	0.9786	53.83	Load Bus
4	CANALB	500	1.0786	49.24	Load Bus
5	CANAD G1	20	1.0000	24.74	Gen Bus
6	CANADA	500	1.0363	20.95	Load Bus
7	NORTH	500	1.0499	12.11	Load Bus
8	NORTH G3	20	1.0000	26.59	Gen Bus
9	HANFORD	500	1.0495	0.23	Load Bus
10	COULEE	500	1.0700	0.16	Load Bus
11	GARRISON	500	1.0371	-12.16	Load Bus
12	JOHN DAY	500	1.0828	-11.12	Load Bus
13	JOHN DAY	13.8	1.0000	0.00	Swing Bus
14	BIG EDDY	500	1.0892	-13.31	Load Bus
15	GRIZZLY	500	1.0674	-17.15	Load Bus
16	CELILOCA	500	1.0897	-13.42	Load Bus
17	BIG EDDY	230	1.0659	-14.57	Load Bus
18	CELILO	230	1.0616	-15.08	Load Bus
19	DALLES21	13.8	1.0550	-7.94	Gen Bus
20	BIG EDDY	115	1.0686	-16.93	Load Bus
21	SUMMER L	500	1.0582	-18.23	Load Bus
22	BURNS2	500	0.9844	-6.69	Load Bus
23	MALIN	500	1.0543	-23.34	Load Bus
24	MONTANA	500	1.0493	48.20	Load Bus
25	COLSTRP	500	1.0784	-1.36	Load Bus
26	MONTA G1	20	1.0000	56.59	Gen Bus
27	MIDPOINT	500	1.0619	-5.20	Load Bus
28	BRIDGER2	22	1.0090	2.46	Gen Bus

Bus Numbers	Bus Names	Base kV	Voltage Magnitude (p.u.)	Voltage Angle (degree)	Bus Type
29	MIDPOINT	345	0.9984	-1.57	Load Bus
30	BENLOMND	345	1.0446	-3.40	Load Bus
31	BENLOMND	230	1.0462	-3.96	Load Bus
32	NAUGHTON	230	1.0445	0.61	Load Bus
33	NAUGHT	20	1.0000	3.41	Gen Bus
34	TERMINAL	345	1.0391	-3.42	Load Bus
35	CAMP WIL	345	1.0429	-2.42	Load Bus
36	SPAN FRK	345	1.0351	-1.09	Load Bus
37	EMERY	345	1.0371	4.89	Load Bus
38	EMERY	20	1.0500	9.60	Gen Bus
39	SIGURD	345	1.0519	-0.55	Load Bus
40	PINTO	345	1.0404	-1.41	Load Bus
41	PINTO PS	345	1.0368	-2.44	Load Bus
42	MONA	345	1.0560	-2.01	Load Bus
43	INTERMT	345	1.0526	-4.37	Load Bus
44	INTERM1G	26	1.0500	0.28	Gen Bus
45	CRAIG	345	0.9752	16.27	Load Bus
46	CRAIG	22	0.9500	23.55	Gen Bus
47	HAYDEN	20	1.0000	33.73	Gen Bus
48	SAN JUAN	345	1.0356	-3.88	Load Bus
49	SJUAN G4	22	1.0000	-0.89	Gen Bus
50	FOURCORN	345	1.0091	-4.69	Load Bus
51	FOURCORN	500	1.0681	-7.91	Load Bus
52	FOURCORN	230	1.0073	-5.23	Load Bus
53	FCNGN4CC	22	1.0000	2.23	Gen Bus
54	CHOLLA	345	0.9774	-16.96	Load Bus
55	CORONADO	500	0.9795	-26.18	Load Bus
56	CORONADO	20	1.0400	-19.66	Gen Bus
57	MOENKOPI	500	1.0673	-24.86	Load Bus
58	WESTWING	500	1.0559	-29.59	Load Bus
59	PALOVRDE	500	1.0486	-29.64	Load Bus
60	PALOVRD2	24	0.9600	-21.72	Gen Bus
61	NAVAJO	500	1.0720	-23.94	Load Bus
62	NAVAJO 2	26	1.0000	-17.81	Gen Bus
63	ELDORADO	500	1.0512	-33.10	Load Bus
64	DEVERS	500	1.0354	-43.52	Load Bus
65	ELDORADO	20	1.0200	-25.98	Gen Bus
66	MOHAVE	500	1.0700	-29.36	Load Bus
67	MOHAV1CC	22	1.0500	-21.04	Gen Bus

Bus Numbers	Bus Names	Base kV	Voltage Magnitude (p.u.)	Voltage Angle (degree)	Bus Type
68	LUGO	500	1.0550	-46.09	Load Bus
69	SERRANO	500	1.0413	-50.08	Load Bus
70	VALLEY	500	1.0369	-47.76	Load Bus
71	MIRALOMA	500	1.0409	-49.68	Load Bus
72	MIRALOMA	20	1.0500	-45.44	Gen Bus
73	MIRALOMA	230	1.0382	-50.13	Load Bus
74	MESA CAL	230	1.0071	-55.06	Load Bus
75	LITEHIPE	230	1.0119	-55.78	Load Bus
76	LITEHIPE	20	1.0200	-49.63	Gen Bus
77	VINCENT	500	1.0612	-48.95	Load Bus
78	VINCENT	230	0.9949	-51.64	Load Bus
79	EAGLROCK	230	1.0101	-52.76	Load Bus
80	PARDEE	230	1.0060	-51.68	Load Bus
81	PARDEE	20	1.0100	-39.60	Gen Bus
82	SYLMAR S	230	1.0207	-48.26	Load Bus
83	MIDWAY	200	1.1670	-51.45	Load Bus
84	MIDWAY	500	1.0593	-48.61	Load Bus
85	LOSBANOS	500	1.0493	-49.53	Load Bus
86	MOSSLAND	500	1.0464	-49.80	Load Bus
87	DIABLO	500	1.0530	-46.13	Load Bus
88	DIABLO1	25	0.9800	-42.33	Gen Bus
89	GATES	500	1.0471	-47.68	Load Bus
90	TEVATR	500	0.9982	-39.00	Load Bus
91	TEVATR2	20	1.0000	-30.78	Gen Bus
92	OLINDA	500	1.0372	-31.07	Load Bus
93	ROUND MT	500	1.0346	-27.93	Load Bus
94	TABLE MT	500	1.0134	-32.07	Load Bus
95	ROUND MT	200	1.1239	-25.14	Load Bus
96	ROUND MT	20	1.0200	-15.08	Gen Bus
97	COTWDPGE	200	1.1361	-30.49	Load Bus
98	LOGAN CR	200	1.1402	-34.59	Load Bus
99	GLENN	200	1.1409	-34.20	Load Bus
100	CORTINA	200	1.1310	-34.98	Load Bus
101	TEVATR	200	1.1274	-39.64	Load Bus
102	TEVATR	20	1.0500	-35.69	Gen Bus
103	SYLMARLA	230	1.0383	-47.15	Load Bus
104	VICTORVL	500	1.0587	-42.48	Load Bus
105	VICTORVL	287	1.0521	-44.50	Load Bus
106	STA B2	287	1.0366	-50.72	Load Bus

Bus Numbers	Bus Names	Base kV	Voltage Magnitude (p.u.)	Voltage Angle (degree)	Bus Type
107	STA B1	287	1.0366	-50.72	Load Bus
108	STA B	138	1.0326	-51.90	Load Bus
109	STA BLD	230	1.0273	-52.11	Load Bus
110	STA F	230	1.0248	-51.88	Load Bus
111	RIVER	230	1.0236	-51.85	Load Bus
112	HAYNES	230	1.0313	-50.65	Load Bus
113	HAYNES3G	18	1.0000	-47.35	Gen Bus
114	STA G	230	1.0239	-51.18	Load Bus
115	GLENDAL	230	1.0234	-50.93	Load Bus
116	STA E	230	1.0252	-50.06	Load Bus
117	VALLEY	230	1.0293	-49.03	Load Bus
118	RINALDI	230	1.0340	-47.84	Load Bus
119	OWENS G	11.5	1.0200	-47.27	Gen Bus
120	STA E	500	1.0430	-47.67	Load Bus
121	ADELANTO	500	1.0603	-42.16	Load Bus
122	ADELAN&1	500	1.0809	-46.23	Load Bus
123	RINALDI	500	1.0721	-45.48	Load Bus
124	STA J	230	1.0311	-48.92	Load Bus
125	CASTAIC	230	1.0319	-47.29	Load Bus
126	CASTAI4G	18	1.0200	-45.98	Gen Bus
127	OLIVE	230	1.0348	-47.63	Load Bus

Line Data: Line Number is the unique number used to identify the line, From Bus # represents the number of the From Bus, To Bus # represents the number of the To Bus, the resistance of the line is measured in p.u., the reactance of the line is measured in p.u., and the line charging susceptance is also measured in p.u.

Line Numbers	From Bus #	To Bus #	Resistance (p.u.)	Reactance (p.u.)	Line Charging (p.u.)
1	2	3	0.0020	0.0200	0.8000
2	4	6	0.0035	0.0700	4.6060
3	6	7	0.0008	0.0239	3.3000
4	7	9	0.0002	0.0082	1.3000
5	7	9	0.0002	0.0082	1.3000
6	9	10	0.0011	0.0207	1.8553
7	9	11	0.0014	0.0226	1.8800
8	9	12	0.0012	0.0232	1.7152
9	9	12	0.0003	0.0200	3.6000
10	9	24	0.0007	0.0740	4.8700
11	11	12	0.0020	0.0330	1.8800
12	11	25	0.0018	0.0141	3.6800
13	12	14	0.0002	0.0045	0.3332
14	12	14	0.0002	0.0045	0.3050
15	12	15	0.0006	0.0141	1.0976
16	12	15	0.0011	0.0241	1.5554
17	12	15	0.0011	0.0241	1.5535
18	14	16	0.0000	0.0003	0.0143
19	14	16	0.0000	0.0003	0.0184
20	15	21	0.0010	0.0051	1.0513
21	15	23	0.0021	0.0166	2.9358
22	15	23	0.0021	0.0158	2.9538
23	17	18	0.0001	0.0013	0.0038
24	17	18	0.0001	0.0012	0.0033
25	21	22	0.0012	0.0237	2.2071
26	21	23	0.0008	0.0077	0.3273
27	22	27	0.0029	0.0025	23.9151
28	23	92	0.0011	0.0129	2.7575
29	23	93	0.0011	0.0091	1.2808
30	23	93	0.0010	0.0092	1.5715
31	29	30	0.0062	0.0673	1.1156
32	30	34	0.0016	0.0226	0.3810
33	30	35	0.0024	0.0332	0.5849
34	31	32	0.0108	0.0965	0.3296

Line Numbers	From Bus #	To Bus #	Resistance (p.u.)	Reactance (p.u.)	Line Charging (p.u.)
35	34	35	0.0008	0.0106	0.2039
36	35	36	0.0012	0.0172	0.2987
37	35	37	0.0052	0.0602	1.0100
38	35	37	0.0049	0.0537	0.8843
39	35	42	0.0017	0.0225	0.3992
40	35	42	0.0021	0.0238	0.3845
41	36	37	0.0034	0.0392	0.6524
42	37	39	0.0034	0.0374	0.6208
43	37	39	0.0034	0.0372	0.6182
44	37	40	0.0096	0.0878	1.4265
45	39	42	0.0038	0.0340	0.5824
46	39	42	0.0032	0.0349	0.5722
47	41	50	0.0048	0.0436	0.7078
48	42	43	0.0018	0.0245	0.4392
49	42	43	0.0018	0.0245	0.4392
50	42	45	0.0081	0.1369	2.4348
51	45	48	0.0098	0.1100	2.0000
52	48	50	0.0005	0.0053	0.0882
53	50	54	0.0018	0.0199	2.5760
54	51	57	0.0018	0.0323	3.1129
55	57	58	0.0018	0.0269	3.3453
56	57	61	0.0008	0.0055	1.3922
57	57	63	0.0022	0.0160	3.8163
58	58	59	0.0004	0.0096	0.9038
59	58	59	0.0004	0.0096	0.9038
60	58	61	0.0026	0.0376	4.7289
61	59	64	0.0026	0.0297	2.1530
62	59	64	0.0026	0.0297	2.1530
63	61	63	0.0028	0.0211	1.0194
64	63	66	0.0006	0.0142	1.0429
65	63	68	0.0019	0.0278	4.6712
66	63	104	0.0018	0.0252	0.5355
67	63	104	0.0018	0.0252	0.5355
68	64	70	0.0004	0.0091	0.6679
69	66	68	0.0019	0.0310	4.1402
70	68	69	0.0006	0.0128	0.9462
71	68	71	0.0003	0.0075	0.5174
72	68	71	0.0004	0.0075	0.5536
73	68	77	0.0004	0.0113	0.8292

Line Numbers	From Bus #	To Bus #	Resistance (p.u.)	Reactance (p.u.)	Line Charging (p.u.)
74	68	77	0.0004	0.0113	0.8292
75	68	104	0.0002	0.0041	0.2962
76	69	70	0.0004	0.0093	0.6856
77	69	71	0.0002	0.0046	0.3234
78	73	74	0.0014	0.0540	0.1525
79	74	75	0.0011	0.0127	0.0480
80	74	78	0.0032	0.0395	0.1440
81	74	79	0.0019	0.0258	0.0984
82	77	84	0.0013	0.0082	1.9687
83	77	84	0.0013	0.0082	1.9492
84	77	84	0.0011	0.0077	1.6015
85	78	80	0.0029	0.0365	0.1266
86	78	80	0.0014	0.0340	0.1125
87	79	80	0.0085	0.0703	0.1595
88	79	82	0.0014	0.0264	0.1020
89	80	82	0.0007	0.0119	0.0467
90	80	82	0.0007	0.0119	0.0467
91	84	85	0.0015	0.0147	0.0000
92	84	87	0.0009	0.0209	1.4571
93	84	87	0.0009	0.0209	1.4571
94	84	89	0.0007	0.0061	2.8240
95	84	90	0.0017	0.0376	2.0789
96	85	86	0.0005	0.0130	0.0000
97	85	89	0.0008	0.0199	0.0000
98	87	89	0.0008	0.0194	1.3285
99	89	90	0.0010	0.0257	0.7976
100	90	92	0.0016	0.0111	3.6348
101	90	94	0.0010	0.0104	0.9312
102	90	94	0.0016	0.0123	2.2819
103	93	94	0.0015	0.0069	0.7944
104	93	94	0.0015	0.0069	0.7944
105	95	97	0.0111	0.0668	0.0729
106	95	97	0.0105	0.0654	0.0686
107	95	97	0.0111	0.0664	0.0716
108	97	98	0.0167	0.1138	0.1361
109	97	99	0.0138	0.0927	0.1106
110	97	100	0.0248	0.1694	0.2023
111	97	101	0.0390	0.2740	0.3107
112	98	101	0.0224	0.1611	0.1834

Line Numbers	From Bus #	To Bus #	Resistance (p.u.)	Reactance (p.u.)	Line Charging (p.u.)
113	99	101	0.0306	0.2046	0.2447
114	100	101	0.0148	0.1010	0.1207
115	103	118	0.0003	0.0039	0.0092
116	103	118	0.0003	0.0039	0.0092
117	103	118	0.0003	0.0039	0.0092
118	103	125	0.0023	0.0342	0.0751
119	104	121	0.0000	0.0016	0.1200
120	104	121	0.0000	0.0016	0.1200
121	104	123	0.0008	0.0188	1.6667
122	105	106	0.0107	0.0791	0.3667
123	105	107	0.0107	0.0791	0.3667
124	109	110	0.0007	0.0103	0.0256
125	109	110	0.0007	0.0103	0.0256
126	110	111	0.0004	0.0037	0.0083
127	110	112	0.0020	0.0307	0.0689
128	110	114	0.0011	0.0119	0.0251
129	111	112	0.0022	0.0342	0.0772
130	111	112	0.0024	0.0367	0.0828
131	111	114	0.0006	0.0059	0.0125
132	112	114	0.0028	0.0430	0.0965
133	114	115	0.0004	0.0054	0.0120
134	114	116	0.0012	0.0124	0.0280
135	114	116	0.0012	0.0124	0.0280
136	115	116	0.0005	0.0072	0.0162
137	116	117	0.0013	0.0098	0.0212
138	116	118	0.0023	0.0158	0.0306
139	116	118	0.0023	0.0158	0.0306
140	117	118	0.0014	0.0112	0.0247
141	117	118	0.0014	0.0112	0.0247
142	118	124	0.0014	0.0097	0.0194
143	118	124	0.0014	0.0097	0.0194
144	118	124	0.0016	0.0097	0.0193
145	118	124	0.0016	0.0097	0.0193
146	118	125	0.0029	0.0380	0.0824
147	118	127	0.0003	0.0043	0.0095
148	120	121	0.0008	0.0167	1.1880
149	121	122	0.0007	0.0186	1.4026
150	124	125	0.0031	0.0468	0.1008
151	125	127	0.0022	0.0335	0.0734

Transformer Data: Transformer Number is the unique number used to identify the transformer, From Bus # represents the number of the From Bus, To Bus # represents the number of the To Bus, the resistance of the transformer is measured in p.u. and the reactance of the transformer is also measured in p.u. The tap-ratio is mentioned in the last column.

Transformer Numbers	From Bus #	To Bus #	Resistance (p.u.)	Reactance (p.u.)	Tap Ratio
1	1	2	0.0000	0.0020	1.0000
2	3	4	0.0000	0.0100	1.1000
3	5	6	0.0000	0.0015	1.0500
4	7	8	0.0000	0.0025	1.0660
5	12	13	0.0000	0.0038	1.0977
6	14	17	0.0002	0.0118	1.0238
7	14	17	0.0001	0.0074	1.0238
8	16	18	0.0000	0.0022	1.0234
9	17	19	0.0000	0.0103	1.0455
10	17	20	0.0009	0.0299	0.9873
11	24	26	0.0000	0.0050	1.0900
12	27	29	0.0000	0.0072	1.0500
13	28	29	0.0000	0.0046	1.0000
14	30	31	0.0003	0.0181	1.0000
15	32	33	0.0005	0.0141	1.0588
16	37	38	0.0002	0.0058	0.9855
17	40	41	0.0000	0.0195	1.0000
18	43	44	0.0000	0.0052	1.0250
19	45	46	0.0000	0.0124	1.0000
20	45	47	0.0000	0.0150	1.0000
21	48	49	0.0000	0.0060	1.0435
22	50	51	0.0000	0.0110	1.0630
23	50	51	0.0000	0.0110	1.0630
24	50	52	0.0003	0.0138	1.0000
25	50	52	0.0003	0.0139	1.0000
26	50	53	0.0000	0.0059	1.0000
27	54	55	0.0000	0.0146	1.0000
28	55	56	0.0000	0.0173	0.9545
29	59	60	0.0001	0.0050	1.1061
30	61	62	0.0000	0.0067	1.0800
31	63	65	0.0000	0.0151	0.9960
32	66	67	0.0000	0.0098	1.0500
33	71	72	0.0000	0.0052	0.9843
34	71	73	0.0000	0.0050	1.0000

Transformer Numbers	From Bus #	To Bus #	Resistance (p.u.)	Reactance (p.u.)	Tap Ratio
35	75	76	0.0000	0.0037	0.9787
36	77	78	0.0000	0.0115	1.0631
37	77	78	0.0000	0.0115	1.0631
38	77	78	0.0000	0.0115	1.0631
39	80	81	0.0000	0.0103	0.9871
40	82	103	0.0000	0.0012	1.0133
41	83	84	0.0003	0.0174	1.1190
42	83	84	0.0002	0.0119	1.1190
43	87	88	0.0000	0.0098	1.0500
44	90	91	0.0000	0.0045	0.9452
45	90	101	0.0002	0.0125	1.1190
46	93	95	0.0001	0.0174	1.1190
47	95	96	0.0000	0.0228	0.9174
48	101	102	0.0000	0.0182	0.9091
49	104	105	0.0002	0.0234	0.9789
50	106	108	0.0006	0.0149	1.0017
51	107	108	0.0006	0.0149	1.0017
52	108	109	0.0003	0.0133	1.0000
53	108	109	0.0003	0.0134	1.0000
54	112	113	0.0006	0.0254	1.0491
55	116	120	0.0001	0.0139	1.0106
56	116	120	0.0001	0.0139	1.0106
57	118	119	0.0050	0.1147	1.0478
58	118	122	0.0001	0.0069	1.0500
59	118	123	0.0003	0.0139	1.0500
60	125	126	0.0005	0.0238	1.0000

Load Data: Bus Number is the unique number used to identify the bus to which the load is connected, the bus name is the unique name used to identify the bus to which the load is connected, the base kV denotes the base voltage of the bus in kV, P_load denotes the real component of the load and is measured in p.u., while Q_load denotes the reactive component of the load and is also measured in p.u.

Bus Numbers	Bus Names	Base kV	P_load (p.u.)	Q_load (p.u.)
1	CMAIN GM	20	1.000	0.000
2	CA230	230	36.000	7.000
5	CANAD G1	20	1.000	0.000
6	CANADA	500	44.000	10.000
7	NORTH	500	50.000	4.000
8	NORTH G3	20	1.000	0.000
9	HANFORD	500	35.000	5.000
11	GARRISON	500	25.840	3.940
12	JOHN DAY	500	32.000	11.000
13	JOHN DAY	13.8	1.000	0.000
14	BIG EDDY	500	-0.442	0.220
15	GRIZZLY	500	-0.666	-0.970
17	BIG EDDY	230	-0.675	1.600
18	CELILO	230	31.370	16.810
19	DALLES21	13.8	1.000	0.000
20	BIG EDDY	115	1.600	0.313
23	MALIN	500	-3.390	-1.190
24	MONTANA	500	17.000	3.000
25	COLSTRP	500	-15.250	-0.500
26	MONTA G1	20	1.000	0.000
28	BRIDGER2	22	1.000	0.000
29	MIDPOINT	345	6.100	-4.140
30	BENLOMND	345	0.339	0.119
31	BENLOMND	230	1.480	-0.079
32	NAUGHTON	230	2.550	1.000
33	NAUGHT	20	1.000	0.000
34	TERMINAL	345	1.850	0.785
35	CAMP WIL	345	4.577	0.817
36	SPAN FRK	345	1.412	0.714
37	EMERY	345	1.161	0.384
38	EMERY	20	1.000	0.000
39	SIGURD	345	3.790	-0.430
40	PINTO	345	0.316	0.115
42	MONA	345	-0.620	0.128

Bus Numbers	Bus Names	Base kV	P_load (p.u.)	Q_load (p.u.)
43	INTERMT	345	20.530	9.071
44	INTERM1G	26	1.000	0.000
45	CRAIG	345	23.500	-1.270
46	CRAIG	22	1.000	0.000
47	HAYDEN	20	1.000	0.000
48	SAN JUAN	345	8.400	0.050
49	SJUAN G4	22	1.000	0.000
50	FOURCORN	345	2.390	-0.560
52	FOURCORN	230	1.397	0.238
53	FCNGN4CC	22	1.000	0.000
55	CORONADO	500	17.500	-0.560
56	CORONADO	20	**1.000**	**0.000**
58	WESTWING	500	6.170	-0.690
59	PALOVRDE	500	7.934	2.070
60	PALOVRD2	24	1.000	0.000
61	NAVAJO	500	0.900	0.700
62	NAVAJO 2	26	1.000	0.000
63	ELDORADO	500	9.023	-0.114
64	DEVERS	500	8.560	0.196
65	ELDORADO	20	1.000	0.000
67	MOHAV1CC	22	1.000	0.000
68	LUGO	500	2.042	-0.282
69	SERRANO	500	12.300	0.728
70	VALLEY	500	4.060	0.410
71	MIRALOMA	500	30.980	11.890
72	MIRALOMA	20	1.000	0.000
74	MESA CAL	230	3.774	0.645
75	LITEHIPE	230	31.910	6.300
76	LITEHIPE	20	1.000	0.000
78	VINCENT	230	10.660	-0.108
79	EAGLROCK	230	1.750	0.180
80	PARDEE	230	31.180	0.780
81	PARDEE	20	1.000	0.000
82	SYLMAR S	230	4.010	0.806
83	MIDWAY	200	7.776	0.326
84	MIDWAY	500	0.556	-3.290
85	LOSBANOS	500	2.650	0.140
86	MOSSLAND	500	0.400	0.215
87	DIABLO	500	0.500	0.250

Bus Numbers	Bus Names	Base kV	P_load (p.u.)	Q_load (p.u.)
88	DIABLO1	25	1.000	0.000
89	GATES	500	3.050	-0.076
90	TEVATR	500	56.610	34.910
91	TEVATR2	20	1.000	0.000
92	OLINDA	500	-1.890	0.615
94	TABLE MT	500	-0.007	1.185
95	ROUND MT	200	1.480	0.000
96	ROUND MT	20	1.000	0.000
97	COTWDPGE	200	2.104	-0.770
98	LOGAN CR	200	0.080	0.000
99	GLENN	200	0.275	-0.001
100	CORTINA	200	-0.433	0.200
101	TEVATR	200	8.840	0.548
102	TEVATR	20	1.000	0.000
103	SYLMARLA	230	-27.710	16.540
105	VICTORVL	287	-1.290	0.322
108	STA B	138	2.372	-0.632
109	STA BLD	230	1.380	0.280
110	STA F	230	1.170	0.240
111	RIVER	230	3.200	0.650
113	HAYNES3G	18	1.000	0.000
114	STA G	230	1.210	0.250
115	GLENDAL	230	1.350	0.270
116	STA E	230	8.078	1.321
117	VALLEY	230	2.052	0.176
118	RINALDI	230	1.210	0.250
119	OWENS G	11.5	1.000	0.000
121	ADELANTO	500	-18.620	9.710
124	STA J	230	8.877	-0.062
126	CASTAI4G	230	1.000	0.000
127	OLIVE	20	-0.728	-0.170

Generator Data: Bus Number is the unique number used to identify the bus to which the generator is connected, the bus name is the unique name used to identify the bus to which the generator is connected, MVA_base denotes the base MVA of the individual generators, P_gen denotes the real component of the power generated by the generator and is measured in p.u., Q_gen denotes the reactive component of the power generated by the generator and is also measured in p.u., X_l denotes the leakage reactance in p.u., X'_d denotes the unsaturated direct-axis transient reactance of the generator, X'_q denotes the unsaturated quadrature-axis transient reactance of the generator, and H denotes the inertia constant of the turbine-governor set and is measured in seconds.

Bus Numbers	Bus Names	MVA_base	P_gen (p.u.)	Q_gen (p.u.)	X_l (p.u.)	X'_d (p.u.)	X'_q (p.u.)	H (sec)
1	CMAIN GM	6100	44.800	11.502	0.250	0.291	0.440	2.950
5	CANAD G1	9004	44.500	10.111	0.150	0.250	0.600	4.340
8	NORTH G3	13000	99.500	18.540	0.161	0.228	0.424	3.460
13	JOHN DAY	5421	51.748	8.552	0.248	0.357	0.651	3.670
19	DALLES21	1199	13.010	4.315	0.287	0.370	0.500	3.000
26	MONTA G1	3085	29.100	9.533	0.178	0.220	0.348	3.380
28	BRIDGER2	1770	16.400	2.857	0.215	0.280	0.490	2.320
33	NAUGHT	832	4.450	0.917	0.260	0.324	0.450	3.010
38	EMERY	2229	16.650	-0.314	0.185	0.240	0.430	2.820
44	INTERM1G	1982	17.800	5.346	0.200	0.245	0.420	2.880
46	CRAIG	1488	10.480	-1.329	0.190	0.245	0.510	2.610
47	HAYDEN	3000	20.500	4.648	0.190	0.250	0.500	2.450
49	SJUAN G4	2054	9.620	1.488	0.205	0.260	0.453	2.630
53	FCNGN4CC	2458	21.600	-0.305	0.205	0.285	0.485	3.420
56	CORONADO	914	8.000	1.230	0.195	0.250	0.453	2.640
60	PALOVRD2	3117	26.400	3.781	0.285	0.375	0.567	3.830
62	NAVAJO 2	3540	16.900	1.955	0.175	0.220	0.400	3.590
65	ELDORADO	2104	9.827	-1.288	0.300	0.320	0.530	6.070
67	MOHAV1CC	1818	16.800	4.466	0.205	0.285	0.485	3.490
72	MIRALOMA	3000	16.900	5.938	0.290	0.340	1.000	2.750
76	LITEHIPE	9000	31.950	10.325	0.175	0.245	0.376	2.820
81	PARDEE	2500	22.000	3.937	0.180	0.220	0.440	3.030
88	DIABLO1	1685	7.650	-2.062	0.311	0.467	1.270	3.460
91	TEVATR2	6840	34.670	16.546	0.190	0.250	0.500	3.820
96	ROUND MT	1022	10.570	0.256	0.263	0.320	0.670	4.390
102	TEVATR	895	5.940	1.924	0.300	0.320	0.530	4.160
113	HAYNES3G	540	3.250	0.683	0.185	0.256	0.410	4.130
119	OWENS G	113	1.100	0.291	0.150	0.238	0.365	3.800
126	CASTAI4G	500	2.000	-0.522	0.155	0.195	0.568	6.410

Shunt Data: Bus Number is the unique number used to identify the bus to which the shunt element is connected, the bus name is the unique name used to identify the bus to which the shunt element is connected, the base kV denotes the base voltage of the bus in kV, G_shunt represents the conductance of the shunt element in p.u., and B_shunt represents the susceptance of the shunt element also in p.u.

Bus Numbers	Bus Names	Base kV	G_shunt (p.u.)	B_shunt (p.u.)
7	NORTH	500	0.0000	12.0000
9	HANFORD	500	0.0000	5.5000
12	JOHN DAY	500	0.0000	10.1935
15	GRIZZLY	500	-0.0929	-5.6029
16	CELILOCA	500	0.0000	4.6200
17	BIG EDDY	230	0.0000	5.7685
18	CELILO	230	0.0000	7.9200
21	SUMMER L	500	0.0028	1.1638
22	BURNS2	500	11.5674	-23.7541
23	MALIN	500	0.0799	-0.8631
27	MIDPOINT	500	-10.9334	-2.2000
29	MIDPOINT	345	0.0000	-8.7000
35	CAMP WIL	345	0.0000	-0.6000
37	EMERY	345	0.0000	-2.2000
39	SIGURD	345	0.0000	-0.5000
40	PINTO	345	0.0000	-0.1800
43	INTERMT	345	0.0000	4.3000
48	SAN JUAN	345	0.0000	3.9000
50	FOURCORN	345	0.0000	-1.5500
51	FOURCORN	500	0.0058	-1.1300
57	MOENKOPI	500	-0.0058	-3.7070
58	WESTWING	500	0.0000	-4.2700
59	PALOVRDE	500	0.0000	-1.4600
61	NAVAJO	500	0.0000	-1.9000
63	ELDORADO	500	0.0000	-3.1900
66	MOHAVE	500	0.0000	-1.9600
71	MIRALOMA	500	0.0000	4.0000
77	VINCENT	500	0.0179	0.0000
78	VINCENT	230	0.0000	-1.9000
83	MIDWAY	200	0.0000	-1.3000
84	MIDWAY	500	-0.1346	-2.6639
89	GATES	500	0.1196	-2.6538
90	TEVATR	500	0.0321	15.5844
92	OLINDA	500	-0.0096	0.1388

Bus Numbers	Bus Names	Base kV	G_shunt (p.u.)	B_shunt (p.u.)
93	ROUND MT	500	-0.1282	0.4316
94	TABLE MT	500	0.1197	-0.4221
95	ROUND MT	200	0.0000	-1.2800
101	TEVATR	200	0.0000	-0.3200
103	SYLMARLA	230	0.0000	21.4600
105	VICTORVL	287	0.0000	-1.0800
121	ADELANTO	500	0.0000	9.1200
123	RINALDI	500	0.0000	-0.8000

Appendix B: Program Codes

B.1 MATLAB Programs

The Matlab programs for performing LMI and SMA computations are divided into three parts. The first program called “Postpro” does post-processing on the system matrices obtained out of PST. It reorders the matrices in the desired format required for performing iterations of SMA. The second program called “SMA” performs the actual SMA iterations and to check for its convergence in accordance with the proposed algorithm. The third program “Simplepp” does the polytopic formulation and comes up with a single *gain* matrix capable of optimizing all cases lying inside the polytope in accordance with the LMI concept. The programs summarized below are for the 29 machine, 127 bus equivalent model of the WECC system having six controls.

Program 1: Postpro

```
%%%%%%%%%%%%%%%%%%%%%%%%%%%%%%%%%%%%%%%%%%%%%%%%%%%%%%%%%%%%%%%%%%%%%%%%%%%%%%%%
%                                                                               %
% Program Name: Postpro                                                         %
%                                                                               %
% Description: Performs post-processing on the matrices obtained out of PST     %
%                                                                               %
% Author: Anamitra Pal                                                          %
%         Virginia Tech.                                                        %
%                                                                               %
% Last Modified: 10/13/2011                                                     %
%                                                                               %
%%%%%%%%%%%%%%%%%%%%%%%%%%%%%%%%%%%%%%%%%%%%%%%%%%%%%%%%%%%%%%%%%%%%%%%%%%%%%%%%

% a_mat is the system matrix obtained out of PST
nn = size(a_mat)*[1 0]'; % nn = Size of System
nc = 12; % Number of original Controls; four for each DC line, one each for
SVC and ESD
n4 = nn - nc;
r1 = find(mac_state(:,2)==1); % Corresponds to the generator angles
r2 = find(mac_state(:,2)==2); % Corresponds to the generator speeds
r3 = find(mac_state(:,2)>2); % Corresponds to the remaining machine states
r4 = n4+1:nn; % Corresponds to the states associated with the Controls
r = [r1' r2' r3' r4];
A = 0*eye(nn); % Initializing the A-matrix
BB = 0*ones(nn,nc); % Initializing the B-matrix
A(1:nn,1:nn) = a_mat(r,r);

% Corresponds to the control action performed by the SVC
BB(:,1) = b_svc(r,1);

% Corresponds to the control action performed by the ESDs
BB(:,2:4) = b_lmod(r,5:7);
```

```
% Corresponds to the control action performed by the DC lines
BB(:,5:8) = b_lmod(r,1:4);
BB(:,9:12) = b_rlmod(r,1:4);

C1S = c_ang(1,r); % Corresponding to the H_inf optimization
C2S = c_spd(1:28,r); % Corresponding to the H_2 optimization

% Transformation matrix to reduce the number of controls
gamma = [ 1 0 0 0 0 0 0 0 0 0 0 0 ;
          0 1 0 0 0 0 0 0 0 0 0 0 ;
          0 0 1 0 0 0 0 0 0 0 0 0 ;
          0 0 0 1 0 0 0 0 0 0 0 0 ;
          0 0 0 0 1 -1 0 0 .3 .3 0 0;
          0 0 0 0 0 0 1 -1 0 0 .3 .3; ];

nnc = size(gamma)*[1 0]'; % Number of reduced controls

% Transforming the A-matrix
An(1:n4,1:n4) = A(1:n4,1:n4);
An(1:n4,n4+1:n4+nnc) = A(1:n4,n4+1:n4+nc)*gamma';
An(n4+1:n4+nnc,1:n4) = gamma*A(n4+1:n4+nc,1:n4);
An(n4+1:n4+nnc,n4+1:n4+nnc) = gamma*A(n4+1:n4+nc,n4+1:n4+nc)*gamma';
AA = An;

% Transforming the B-matrix
Bnn = gamma*BB(n4+1:nn,1:nc)*gamma';
Bn = [ 0*ones(nnc,n4) Bnn ]';
BB = [ Bn Bn ];

% Transforming the C-matrix
C1 = C1S(:,1:n4+nnc);
C2 = C2S(1:28,1:n4+nnc);
CC = [ C1 ; C2 ];

% Initializing the D-matrix in accordance with the size of the other matrices
DD = 0*ones(29,nnc*2);
DD(1,1) = 1;
DD(2:7,7:12) = eye(nnc);

% Creating the LTI system
S127_6controls = ltisys(AA,BB,CC,DD,eye(n4+nnc));
save num127_6controls S127_6controls % Storing the LTI system in a .MAT file
for future use
```

In accordance with the proposed algorithm, the system matrix obtained as the output of "Postpro" is re-ordered so that the relevant dynamics of the system is governed by its top-left portion (A_1 matrix). The following program reads this file and tests the convergence of SMA on it. It also performs the rudimentary control check in the form of an LQR optimization as suggested in Step 4 of the proposed technique.

Program 2: SMA

```
%%%%%%%%%%%%%%%%%%%%%%%%%%%%%%%%%%%%%%%%%%%%%%%%%%%%%%%%%%%%%%%%%%%%%%%%%%%%%%%%
%                                                                               %
% Program Name: SMA                                                             %
%                                                                               %
% Description: Performs iterations of SMA to check for its convergence          %
%                                                                               %
% Author: Anamitra Pal                                                          %
%         Virginia Tech.                                                        %
%                                                                               %
% Last Modified: 10/13/2011                                                     %
%                                                                               %
%%%%%%%%%%%%%%%%%%%%%%%%%%%%%%%%%%%%%%%%%%%%%%%%%%%%%%%%%%%%%%%%%%%%%%%%%%%%%%%%

clc
clear

m = 21; % Size of the system to be tested
n = 2*m;

% Reading system matrix from the Excel File obtained after re-arranging it
using the Frequency-Participation factor based table obtained using DSA Tools
[NUMERIC,TXT,RAW] = XLSREAD('21Gen.xlsx');

% Storing the relevant partitions of the system matrix
n_A = 174; % The number of rows/columns in A matrix
nnc = 6; % The number of reduced controls
for i=1:n_A
    for j=1:n_A
        A(i,j) = NUMERIC(i,j);
    end
end
for i=1:n
    for j=1:n
        A1(i,j) = NUMERIC(i,j);
    end
end
for i=1:n
    for j=n+1:n_A
        A2(i,j-n) = NUMERIC(i,j);
    end
end
for i=n+1:n_A
    for j=1:n
        A3(i-n,j) = NUMERIC(i,j);
    end
end
```

```
for i=n+1:n_A
    for j=n+1:n_A
        A4(i-n,j-n) = NUMERIC(i,j);
    end
end
for i=1:n
    for j=n_A+1:n_A+nnc
        B1(i,j-n_A) = NUMERIC(i,j);
    end
end
for i=n+1:n_A
    for j= n_A+1:n_A+nnc
        B2(i-n,j-n_A) = NUMERIC(i,j);
    end
end

% The new Control Matrix
B = [ B1 ; B2 ];

N0 = zeros(n_A-n,nnc);

% First Iteration of SMA
[V,D] = eig(A1);
W = 0*eye(n);
WW = 0*ones(n,nnc);
s = ones(n,1);
U = inv(V);
for i=1:n
    s = D(i,i);
    v = V(:,i);
    u = U(i,:);
    W(:,i) = A2/(s*eye(n_A-n)-A4)*A3*v;
    WW(i,:) = (u*A2/(s*eye(n_A-n)-A4))*B2;
end
M = real(W/V);
N = real(V*WW);

% Second Iteration of SMA
[V1,D1] = eig(A1+M);
U1 = inv(V1);
for i=1:n
    s = D1(i,i);
    v = V1(:,i);
    u = U1(i,:);
    W1(:,i) = A2/(s*eye(n_A-n)-A4)*A3*v;
    WW1(i,:) = (u*A2/(s*eye(n_A-n)-A4))*B2;
end
M1 = real(W1/V1);
N1 = real(V1*WW1);

% Third Iteration of SMA
[V2,D2] = eig(A1+M1);
U2 = inv(V2);
for i=1:n
    s = D2(i,i);
    v = V2(:,i);
```

```
    u = U2(i,:);
    W2(:,i) = A2/(s*eye(n_A-n)-A4)*A3*v;
    WW2(i,:) = (u*A2/(s*eye(n_A-n)-A4))*B2;
end
M2 = real(W2/V2);
N2 = real(V2*WW2);

% Fourth Iteration of SMA
[V3,D3] = eig(A1+M2);
U3 = inv(V3);
for i=1:n
    s = D3(i,i);
    v = V3(:,i);
    u = U3(i,:);
    W3(:,i) = A2/(s*eye(n_A-n)-A4)*A3*v;
    WW3(i,:) = (u*A2/(s*eye(n_A-n)-A4))*B2;
end
M3 = real(W3/V3);
N3 = real(V3*WW3);

% SMA was found to converge at the end of the fourth iteration, the next
% two iterations were done to ensure that the system did not digress from
% the converged points

% Fifth Iteration of SMA
[V4,D4] = eig(A1+M3);
U4 = inv(V4);
for i=1:n
    s = D4(i,i);
    v = V4(:,i);
    u = U4(i,:);
    W4(:,i) = A2/(s*eye(n_A-n)-A4)*A3*v;
    WW4(i,:) = (u*A2/(s*eye(n_A-n)-A4))*B2;
end
M4 = real(W4/V4);
N4 = real(V4*WW4);

% Sixth Iteration of SMA
[V5,D5] = eig(A1+M4);
U5 = inv(V5);
for i=1:n
    s = D5(i,i);
    v = V5(:,i);
    u = U5(i,:);
    W5(:,i) = A2/(s*eye(n_A-n)-A4)*A3*v;
    WW5(i,:) = (u*A2/(s*eye(n_A-n)-A4))*B2;
end
M5 = real(W5/V5);
N5 = real(V5*WW5);

% Generates the plots showing the convergence of SMA by the fourth iteration
plot(eig(A1),'go')
hold on
plot(eig(A1+M),'co')
plot(eig(A1+M1),'bo')
plot(eig(A1+M2),'mo')
```

```
plot(eig(A1+M3),'ro')
plot(eig(A),'k.')
axis([-2 0.1 -15 15])

% Generates the plots showing the transition of the eigenvalues with increase
in gain
figure
plot(eig(A),'ks')
hold on
plot(eig(A1+M5),'bs')
Anew = A1 + M5;
[K,S,E] = lqr(Anew,N5,eye(n),eye(nnc)); % Performs LQR optimization
Nnew5 = [ K' ; N0 ];
for i=1:11
    g1 = 1*(i-1)*.1;
    plot(eig(A1+M5-g1*N5*K),'r.')
    plot(eig(A-g1*B*Nnew5'),'go')
end
axis([-2 0.1 -15 15])

% Storing the reduced system as an input for the LMI control program
AA = real(A1+M5);
BS = 0*eye(n,nnc);
BS(:,1:nnc) = N5;
BB = real([BS BS]);
for i=n_A+1:n_A+m+1
    for j=1:n
        CC(i-n_A,j) = real(NUMERIC(i,j));
    end
end
DD = 0*ones(m+1,12);
DD(1,1) = 1;
DD(2:7,7:12) = eye(nnc);
SS1_21_6controls = ltisys(AA,BB,CC,DD,eye(n));
save num1_21_6controls SS1_21_6controls
```

The set of reduced systems obtained through “SMA” in the previous program are combined together to form the polytope. A suitable LMI region is specified to perform the optimization. The output of “Simplepp” is the desired gain of the state feedback, denoted by the matrix K.

Program 3: Simplepp

```
%%%%%%%%%%%%%%%%%%%%%%%%%%%%%%%%%%%%%%%%%%%%%%%%%%%%%%%%%%%%%%%%%%%%%%%%%
%                                                                       %
% Program Name: Simplepp                                                %
%                                                                       %
% Description: Performs LMI optimization of the reduced-order systems  %
%                                                                       %
% Author: Anamitra Pal                                                  %
%         Virginia Tech.                                                %
%                                                                       %
% Last Modified: 10/13/2011                                             %
%                                                                       %
%%%%%%%%%%%%%%%%%%%%%%%%%%%%%%%%%%%%%%%%%%%%%%%%%%%%%%%%%%%%%%%%%%%%%%%%%

clc
clear

tic

% Loads the reduced-order system obtained as an output of SMA
load num1_21_6controls
load num2_21_6controls
load num3_21_6controls
load num4_21_6controls
load num5_21_6controls
load num6_21_6controls
load num7_21_6controls
load num8_21_6controls

% Defining individual cases of the polytopic system
SS1 = SS1_21_6controls;
SS2 = SS2_21_6controls;
SS3 = SS3_21_6controls;
SS4 = SS4_21_6controls;
SS5 = SS5_21_6controls;
SS6 = SS6_21_6controls;
SS7 = SS7_21_6controls;
SS8 = SS8_21_6controls;

% Defining the polytopic system
Pols = psys([SS1,SS2,SS3,SS4,SS5,SS6,SS7,SS8]);

% Defining the LMI region
region = [ 0.6000 + 1.0000i         0                    0               1.0000
0                  0
                 0                  0 + 2.0000i          0                    0
0.9986             -0.0523
                 0                  0                    0                    0
0.0523             0.9986 ]; % 7.5% Damping with Half Plane at -0.30
```

```
% Computing the multi-objective state feedback control
[gopt,h2opt,K,Pcl] = msfsyn(Pols,[21 6],[0 0 .5 .5],region);

% Defining the closed loop system
SP1 = psinfo(Pcl,'sys',1);
SP2 = psinfo(Pcl,'sys',2);
SP3 = psinfo(Pcl,'sys',3);
SP4 = psinfo(Pcl,'sys',4);
SP5 = psinfo(Pcl,'sys',5);
SP6 = psinfo(Pcl,'sys',6);
SP7 = psinfo(Pcl,'sys',7);
SP8 = psinfo(Pcl,'sys',8);

% Plots the eigenvalues of the closed loop system
plot(eig(SP1(1:42,1:42)),'ko')
hold on
plot(eig(SP2(1:42,1:42)),'ko')
plot(eig(SP3(1:42,1:42)),'ko')
plot(eig(SP4(1:42,1:42)),'ko')
plot(eig(SP5(1:42,1:42)),'ko')
plot(eig(SP6(1:42,1:42)),'ko')
plot(eig(SP7(1:42,1:42)),'ko')
plot(eig(SP8(1:42,1:42)),'ko')

% For plotting the line denoting 7.5% and 15% Damping Ratios and a Half-plane
at -0.30
x = -9:1:0;
y1 = -16.3499*x;
y2 = 16.3499*x;
y3 = -7.5958*x;
y4 = 7.5958*x;
plot(x,y1,'k')
hold on
plot(x,y2,'k')
plot(x,y3,'k')
plot(x,y4,'k')
y = -15:0.1:15;
x0 = -0.30;
plot(x0,y,'k')
axis([-2 0 -15 15])

% Stores the gain matrix in a .MAT File
save K_opt21_6controls K

toc
```

B.2 EPCL Programs

The EPCL programs for performing the dynamic simulations in PSLF are divided into two parts. The first program called “Sample_main” states all the initial quantities. It specifies the details of the contingency to be tested and calls for an in-run program at every time-step to apply the control and generate the output. The second program called “Sample_in” specifies the control actions to be performed and creates a text file containing the values of the desired output at every time-step. The programs summarized below are for the 29 machine, 127 bus equivalent model of the WECC system having six controls.

Program 1: Sample_main

```
/*%%%%%%%%%%%%%%%%%%%%%%%%%%%%%%%%%%%%%%%%%%%%%%%%%%%%%%%%%%%%%%%%%%%%%%%%*/
/*                                                                          */
/* Program Name: Sample_main                                                */
/*                                                                          */
/* Description: Performing Dynamic Simulations in PSLF                      */
/*                                                                          */
/* Author: Anamitra Pal                                                     */
/*         Virginia Tech.                                                   */
/*                                                                          */
/* Last Modified: 10/13/2011                                                */
/*                                                                          */
/*%%%%%%%%%%%%%%%%%%%%%%%%%%%%%%%%%%%%%%%%%%%%%%%%%%%%%%%%%%%%%%%%%%%%%%%%*/

/*-------------------------------------*/
/* Initializing and loading base case */
/*-------------------------------------*/

$base = "127bus.sav"          /* Load-Flow Data in PSLF format */
$basedy = "127bus.dyd"        /* Dynamic Data in PSLF format   */
$outchan = "pslf.chf"         /* Output Channel                */
$initrep = "pslf.rep"         /* Init Report                   */
$dynrep = "pslf2.rep"         /* Dynamic Report                */
$inrun = "Sample_in.p"        /* Inrun EPCL to output data     */

/*-----------------------------------------*/
/* Specifying Dynamic Simulation Variables */
/*-----------------------------------------*/
@tinit = 1           /* Time at which contingency starts */
@tstep = 1.16        /* Time at which contingency ends   */
@tend = 40           /* Time to end simulation           */

/* Retrieving Saved Case */
@ret = getf($base)
dispar[0].noprint = 0

/* Retrieving Dynamic Data */
@ret = psds()                                  /* MUST be included to setup
modlib */
@ret = rdyd($basedy,$dynrep,1,1,1)             /* All flags 1
*/
```

```
/* Setting In-RUN -> MUST BE BEFORE INIT */
dypar[0].run_epcl = $inrun                    /* Name of the EPCL to In-Run */

/* Initialize Dynamic Simulation */
@ret = init($outchan,$initrep,"1","0")        /* Output Channel: pslf.chf */
                                              /* "1" Fix Bad Data, "0" don't
turn off unused models */

/* Setting Parameters for Run */              /* Run to @tinit, apply
contingency, run to @tstep, remove contingency, run to @tend */
dypar[0].tpause = @tinit
dypar[0].nscreen = 999999                     /* Don't Print to Screen (makes
simulation run faster) */
@ret = run()

/* 20% increase in load across Celilo-Sylmar HVDC Line */
load[13].p = load[13].p + 2*320
load[87].p = load[87].p - 2*280

dypar[0].tpause = @tstep
dypar[0].nscreen = 999999                     /* Don't Print to Screen (makes
simulation run faster) */
@ret = run()

load[13].p = load[13].p - 2*320
load[87].p = load[87].p + 2*280

dypar[0].tpause = @tend
dypar[0].nscreen = 1                          /* Don't Print to Screen (makes
simulation run faster) */
@ret = run()

@ret = dsst()                                 /* Stop dynamic simulation */
end
```

Program 2: Sample_in

```
/*%%%%%%%%%%%%%%%%%%%%%%%%%%%%%%%%%%%%%%%%%%%%%*/
/*                                               */
/* Program Name: Sample_in                       */
/*                                               */
/* Description: Outputs results to a text file */
/*                                               */
/* Author: Anamitra Pal                          */
/*         Virginia Tech.                        */
/*                                               */
/* Last Modified: 10/13/2011                     */
/*                                               */
/*%%%%%%%%%%%%%%%%%%%%%%%%%%%%%%%%%%%%%%%%%%%%%*/

/*--------------------------------------*/
/* In-RUN EPCL                          */
/*--------------------------------------*/
@onetime = -0.008                           /* Time before initialization */
dim #delta[50]                              /* Specifying an array of size 50
*/

/*-------------------------------------------------*/
/*Monitoring the Supervisory Boundary (in-run EPCL)*/
/*-------------------------------------------------*/

$output = "127bus.txt"                      /* Output file*/

@ret = setlog($output)
logprint($output, "<",dypar[0].time, ">")   /* Prints the time step */

if(dypar[0].time < @onetime)

/* Initializing global variables */
mailbox[0].number[1] = genbc[0].angle       /* genbc[x].angle denotes the
angle of the generator whose internal number is x */
mailbox[0].number[2] = genbc[4].angle
mailbox[0].number[3] = genbc[5].angle
mailbox[0].number[4] = genbc[8].angle
mailbox[0].number[5] = genbc[9].angle
mailbox[0].number[6] = genbc[12].angle
mailbox[0].number[7] = genbc[13].angle
mailbox[0].number[8] = genbc[14].angle
mailbox[0].number[9] = genbc[15].angle
mailbox[0].number[10] = genbc[16].angle
mailbox[0].number[11] = genbc[17].angle
mailbox[0].number[12] = genbc[18].angle
mailbox[0].number[13] = genbc[20].angle
mailbox[0].number[14] = genbc[23].angle
mailbox[0].number[15] = genbc[25].angle
mailbox[0].number[16] = genbc[27].angle
mailbox[0].number[17] = genbc[28].angle
mailbox[0].number[18] = genbc[29].angle
mailbox[0].number[19] = genbc[30].angle
mailbox[0].number[20] = genbc[31].angle
```

```
mailbox[0].number[21] = genbc[32].angle
mailbox[0].number[22] = genbc[0].speed      /* genbc[x].speed denotes the
speed of the generator whose internal number is x */
mailbox[0].number[23] = genbc[4].speed
mailbox[0].number[24] = genbc[5].speed
mailbox[0].number[25] = genbc[8].speed
mailbox[0].number[26] = genbc[9].speed
mailbox[0].number[27] = genbc[12].speed
mailbox[0].number[28] = genbc[13].speed
mailbox[0].number[29] = genbc[14].speed
mailbox[0].number[30] = genbc[15].speed
mailbox[0].number[31] = genbc[16].speed
mailbox[0].number[32] = genbc[17].speed
mailbox[0].number[33] = genbc[18].speed
mailbox[0].number[34] = genbc[20].speed
mailbox[0].number[35] = genbc[23].speed
mailbox[0].number[36] = genbc[25].speed
mailbox[0].number[37] = genbc[27].speed
mailbox[0].number[38] = genbc[28].speed
mailbox[0].number[39] = genbc[29].speed
mailbox[0].number[40] = genbc[30].speed
mailbox[0].number[41] = genbc[31].speed
mailbox[0].number[42] = genbc[32].speed
else

/* Computing increment in respective generator angles and speeds */
@delta1 = genbc[0].angle - mailbox[0].number[1]
@delta2 = genbc[4].angle - mailbox[0].number[2]
@delta3 = genbc[5].angle - mailbox[0].number[3]
@delta4 = genbc[8].angle - mailbox[0].number[4]
@delta5 = genbc[9].angle - mailbox[0].number[5]
@delta6 = genbc[12].angle - mailbox[0].number[6]
@delta7 = genbc[13].angle - mailbox[0].number[7]
@delta8 = genbc[14].angle - mailbox[0].number[8]
@delta9 = genbc[15].angle - mailbox[0].number[9]
@delta10 = genbc[16].angle - mailbox[0].number[10]
@delta11 = genbc[17].angle - mailbox[0].number[11]
@delta12 = genbc[18].angle - mailbox[0].number[12]
@delta13 = genbc[20].angle - mailbox[0].number[13]
@delta14 = genbc[23].angle - mailbox[0].number[14]
@delta15 = genbc[25].angle - mailbox[0].number[15]
@delta16 = genbc[27].angle - mailbox[0].number[16]
@delta17 = genbc[28].angle - mailbox[0].number[17]
@delta18 = genbc[29].angle - mailbox[0].number[18]
@delta19 = genbc[30].angle - mailbox[0].number[19]
@delta20 = genbc[31].angle - mailbox[0].number[20]
@delta21 = genbc[32].angle - mailbox[0].number[21]
@delta22 = genbc[0].speed - mailbox[0].number[22]
@delta23 = genbc[4].speed - mailbox[0].number[23]
@delta24 = genbc[5].speed - mailbox[0].number[24]
@delta25 = genbc[8].speed - mailbox[0].number[25]
@delta26 = genbc[9].speed - mailbox[0].number[26]
@delta27 = genbc[12].speed - mailbox[0].number[27]
@delta28 = genbc[13].speed - mailbox[0].number[28]
@delta29 = genbc[14].speed - mailbox[0].number[29]
@delta30 = genbc[15].speed - mailbox[0].number[30]
@delta31 = genbc[16].speed - mailbox[0].number[31]
```

```
@delta32 = genbc[17].speed - mailbox[0].number[32]
@delta33 = genbc[18].speed - mailbox[0].number[33]
@delta34 = genbc[20].speed - mailbox[0].number[34]
@delta35 = genbc[23].speed - mailbox[0].number[35]
@delta36 = genbc[25].speed - mailbox[0].number[36]
@delta37 = genbc[27].speed - mailbox[0].number[37]
@delta38 = genbc[28].speed - mailbox[0].number[38]
@delta39 = genbc[29].speed - mailbox[0].number[39]
@delta40 = genbc[30].speed - mailbox[0].number[40]
@delta41 = genbc[31].speed - mailbox[0].number[41]
@delta42 = genbc[32].speed - mailbox[0].number[42]

/* Providing State-feedback obtained out of the LMI control Program */
/* Feed backing for the generator angles */
@temp1a =  K(1,1)*(@delta1) + K(1,2)*(@delta2) + K(1,3)*(@delta3) +
K(1,4)*(@delta4) + K(1,5)*(@delta5) + K(1,6)*(@delta6) + K(1,7)*(@delta7) +
K(1,8)*(@delta8) + K(1,9)*(@delta9) + K(1,10)*(@delta10) + K(1,11)*(@delta11)
@temp1b = K(1,12)*(@delta12) + K(1,13)*(@delta13) + K(1,14)*(@delta14) +
K(1,15)*(@delta15) + K(1,16)*(@delta16) + K(1,17)*(@delta17) +
K(1,18)*(@delta18) + K(1,19)*(@delta19) + K(1,20)*(@delta20) +
K(1,21)*(@delta21)
@temp1 = @temp1a + @temp1b
@temp2a = K(2,1)*(@delta1) + K(2,2)*(@delta2) + K(2,3)*(@delta3) +
K(2,4)*(@delta4) + K(2,5)*(@delta5) + K(2,6)*(@delta6) + K(2,7)*(@delta7) +
K(2,8)*(@delta8) + K(2,9)*(@delta9) + K(2,10)*(@delta10) + K(2,11)*(@delta11)
@temp2b = K(2,12)*(@delta12) + K(2,13)*(@delta13) + K(2,14)*(@delta14) +
K(2,15)*(@delta15) + K(2,16)*(@delta16) + K(2,17)*(@delta17) +
K(2,18)*(@delta18) + K(2,19)*(@delta19) + K(2,20)*(@delta20) +
K(2,21)*(@delta21)
@temp2 = @temp2a + @temp2b
@temp3a = K(3,1)*(@delta1) + K(3,2)*(@delta2) + K(3,3)*(@delta3) +
K(3,4)*(@delta4) + K(3,5)*(@delta5) + K(3,6)*(@delta6) + K(3,7)*(@delta7) +
K(3,8)*(@delta8) + K(3,9)*(@delta9) + K(3,10)*(@delta10) + K(3,11)*(@delta11)
@temp3b = K(3,12)*(@delta12) + K(3,13)*(@delta13) + K(3,14)*(@delta14) +
K(3,15)*(@delta15) + K(3,16)*(@delta16) + K(3,17)*(@delta17) +
K(3,18)*(@delta18) + K(3,19)*(@delta19) + K(3,20)*(@delta20) +
K(3,21)*(@delta21)
@temp3 = @temp3a + @temp3b
@temp4a = K(4,1)*(@delta1) + K(4,2)*(@delta2) + K(4,3)*(@delta3) +
K(4,4)*(@delta4) + K(4,5)*(@delta5) + K(4,6)*(@delta6) + K(4,7)*(@delta7) +
K(4,8)*(@delta8) + K(4,9)*(@delta9) + K(4,10)*(@delta10) + K(4,11)*(@delta11)
@temp4b = K(4,12)*(@delta12) + K(4,13)*(@delta13) + K(4,14)*(@delta14) +
K(4,15)*(@delta15) + K(4,16)*(@delta16) + K(4,17)*(@delta17) +
K(4,18)*(@delta18) + K(4,19)*(@delta19) + K(4,20)*(@delta20) +
K(4,21)*(@delta21)
@temp4 = @temp4a + @temp4b
@temp5a = K(5,1)*(@delta1) + K(5,2)*(@delta2) + K(5,3)*(@delta3) +
K(5,4)*(@delta4) + K(5,5)*(@delta5) + K(5,6)*(@delta6) + K(5,7)*(@delta7) +
K(5,8)*(@delta8) + K(5,9)*(@delta9) + K(5,10)*(@delta10) + K(5,11)*(@delta11)
@temp5b = K(5,12)*(@delta12) + K(5,13)*(@delta13) + K(5,14)*(@delta14) +
K(5,15)*(@delta15) + K(5,16)*(@delta16) + K(5,17)*(@delta17) +
K(5,18)*(@delta18) + K(5,19)*(@delta19) + K(5,20)*(@delta20) +
K(5,21)*(@delta21)
@temp5 = @temp5a + @temp5b
@temp6a = K(6,1)*(@delta1) + K(6,2)*(@delta2) + K(6,3)*(@delta3) +
K(6,4)*(@delta4) + K(6,5)*(@delta5) + K(6,6)*(@delta6) + K(6,7)*(@delta7) +
K(6,8)*(@delta8) + K(6,9)*(@delta9) + K(6,10)*(@delta10) + K(6,11)*(@delta11)
```

```
@temp6b = K(6,12)*(@delta12) + K(6,13)*(@delta13) + K(6,14)*(@delta14) +
K(6,15)*(@delta15) + K(6,16)*(@delta16) + K(6,17)*(@delta17) +
K(6,18)*(@delta18) + K(6,19)*(@delta19) + K(6,20)*(@delta20) +
K(6,21)*(@delta21)
@temp6 = @temp6a+@temp6b

/* Feed backing for the generator speeds */
@temp7a =  K(1,22)*(@delta22) + K(1,23)*(@delta23) + K(1,24)*(@delta24) +
K(1,25)*(@delta25) + K(1,26)*(@delta26) + K(1,27)*(@delta27) +
K(1,28)*(@delta28) + K(1,29)*(@delta29) + K(1,30)*(@delta30) +
K(1,31)*(@delta31) + K(1,32)*(@delta32)
@temp7b = K(1,33)*(@delta33) + K(1,34)*(@delta34) + K(1,35)*(@delta35) +
K(1,36)*(@delta36) + K(1,37)*(@delta37) + K(1,38)*(@delta38) +
K(1,39)*(@delta39) + K(1,40)*(@delta40) + K(1,41)*(@delta41) +
K(1,42)*(@delta42)
@temp7 = @temp7a + @temp7b
@temp8a = K(2,22)*(@delta22) + K(2,23)*(@delta23) + K(2,24)*(@delta24) +
K(2,25)*(@delta25) + K(2,26)*(@delta26) + K(2,27)*(@delta27) +
K(2,28)*(@delta28) + K(2,29)*(@delta29) + K(2,30)*(@delta30) +
K(2,31)*(@delta31) + K(2,32)*(@delta32)
@temp8b = K(2,33)*(@delta33) + K(2,34)*(@delta34) + K(2,35)*(@delta35) +
K(2,36)*(@delta36) + K(2,37)*(@delta37) + K(2,38)*(@delta38) +
K(2,39)*(@delta39) + K(2,40)*(@delta40) + K(2,41)*(@delta41) +
K(2,42)*(@delta42)
@temp8 = @temp8a + @temp8b
@temp9a = K(3,22)*(@delta22) + K(3,23)*(@delta23) + K(3,24)*(@delta24) +
K(3,25)*(@delta25) + K(3,26)*(@delta26) + K(3,27)*(@delta27) +
K(3,28)*(@delta28) + K(3,29)*(@delta29) + K(3,30)*(@delta30) +
K(3,31)*(@delta31) + K(3,32)*(@delta32)
@temp9b = K(3,33)*(@delta33) + K(3,34)*(@delta34) + K(3,35)*(@delta35) +
K(3,36)*(@delta36) + K(3,37)*(@delta37) + K(3,38)*(@delta38) +
K(3,39)*(@delta39) + K(3,40)*(@delta40) + K(3,41)*(@delta41) +
K(3,42)*(@delta42)
@temp9 = @temp9a + @temp9b
@temp10a = K(4,22)*(@delta22) + K(4,23)*(@delta23) + K(4,24)*(@delta24) +
K(4,25)*(@delta25) + K(4,26)*(@delta26) + K(4,27)*(@delta27) +
K(4,28)*(@delta28) + K(4,29)*(@delta29) + K(4,30)*(@delta30) +
K(4,31)*(@delta31) + K(4,32)*(@delta32)
@temp10b = K(4,33)*(@delta33) + K(4,34)*(@delta34) + K(4,35)*(@delta35) +
K(4,36)*(@delta36) + K(4,37)*(@delta37) + K(4,38)*(@delta38) +
K(4,39)*(@delta39) + K(4,40)*(@delta40) + K(4,41)*(@delta41) +
K(4,42)*(@delta42)
@temp10 = @temp10a + @temp10b
@temp11a = K(5,22)*(@delta22) + K(5,23)*(@delta23) + K(5,24)*(@delta24) +
K(5,25)*(@delta25) + K(5,26)*(@delta26) + K(5,27)*(@delta27) +
K(5,28)*(@delta28) + K(5,29)*(@delta29) + K(5,30)*(@delta30) +
K(5,31)*(@delta31) + K(5,32)*(@delta32)
@temp11b = K(5,33)*(@delta33) + K(5,34)*(@delta34) + K(5,35)*(@delta35) +
K(5,36)*(@delta36) + K(5,37)*(@delta37) + K(5,38)*(@delta38) +
K(5,39)*(@delta39) + K(5,40)*(@delta40) + K(5,41)*(@delta41) +
K(5,42)*(@delta42)
@temp11 = @temp11a + @temp11b
@temp12a = K(6,22)*(@delta22) + K(6,23)*(@delta23) + K(6,24)*(@delta24) +
K(6,25)*(@delta25) + K(6,26)*(@delta26) + K(6,27)*(@delta27) +
K(6,28)*(@delta28) + K(6,29)*(@delta29) + K(6,30)*(@delta30) +
K(6,31)*(@delta31) + K(6,32)*(@delta32)
```

```
@temp12b = K(6,33)*(@delta33) + K(6,34)*(@delta34) + K(6,35)*(@delta35) +
K(6,36)*(@delta36) + K(6,37)*(@delta37) + K(6,38)*(@delta38) +
K(6,39)*(@delta39) + K(6,40)*(@delta40) + K(6,41)*(@delta41) +
K(6,42)*(@delta42)
@temp12 = @temp12a+@temp12b

/* Provision for adjusting the gain of the control */
N = 2 /* Factor by which the gains are adjusted */
@temp11 = N*(@temp1)
@temp21 = N*(@temp2)
@temp31 = N*(@temp3)
@temp41 = N*(@temp4)
@temp51 = N*(@temp5)
@temp61 = N*(@temp6)
@temp71 = N*(@temp7)
@temp81 = N*(@temp8)
@temp91 = N*(@temp9)
@temp101 = N*(@temp10)
@temp111 = N*(@temp11)
@temp121 = N*(@temp12)

/* Computing new loads in accordance with the control */
/* Corresponding to the SVC */
load[100].q = load[100].q - @temp11 - @temp71           /* load[x].q denotes
reactive power of the load having internal number x */

/* Corresponding to the ESD */
load[0].p = load[0].p - @temp21 - @temp81               /* load[x].p denotes
real power of the load having internal number x */
load[2].p = load[2].p - @temp31 - @temp91
load[62].p = load[62].p - @temp41 - @temp101

/* Corresponding to the DC lines */
load[13].p = load[13].p - @temp51 - @temp111
load[13].q = load[13].q - 0.3*(@temp51) - 0.3*(@temp111)
load[87].p = load[87].p + @temp51 + @temp111
load[87].q = load[87].q - 0.3*(@temp51) - 0.3*(@temp111)
load[34].p = load[34].p - @temp61 - @temp121
load[34].q = load[34].q - 0.3*(@temp61) - 0.3*(@temp121)
load[100].p = load[100].p + @temp61 + @temp121
load[100].q = load[100].q - 0.3*(@temp61) - 0.3*(@temp121)

/* Updating the global variables */
mailbox[0].number[1] = genbc[0].angle
mailbox[0].number[2] = genbc[4].angle
mailbox[0].number[3] = genbc[5].angle
mailbox[0].number[4] = genbc[8].angle
mailbox[0].number[5] = genbc[9].angle
mailbox[0].number[6] = genbc[12].angle
mailbox[0].number[7] = genbc[13].angle
mailbox[0].number[8] = genbc[14].angle
mailbox[0].number[9] = genbc[15].angle
mailbox[0].number[10] = genbc[16].angle
mailbox[0].number[11] = genbc[17].angle
mailbox[0].number[12] = genbc[18].angle
mailbox[0].number[13] = genbc[20].angle
```

```
mailbox[0].number[14] = genbc[23].angle
mailbox[0].number[15] = genbc[25].angle
mailbox[0].number[16] = genbc[27].angle
mailbox[0].number[17] = genbc[28].angle
mailbox[0].number[18] = genbc[29].angle
mailbox[0].number[19] = genbc[30].angle
mailbox[0].number[20] = genbc[31].angle
mailbox[0].number[21] = genbc[32].angle
mailbox[0].number[22] = genbc[0].speed
mailbox[0].number[23] = genbc[4].speed
mailbox[0].number[24] = genbc[5].speed
mailbox[0].number[25] = genbc[8].speed
mailbox[0].number[26] = genbc[9].speed
mailbox[0].number[27] = genbc[12].speed
mailbox[0].number[28] = genbc[13].speed
mailbox[0].number[29] = genbc[14].speed
mailbox[0].number[30] = genbc[15].speed
mailbox[0].number[31] = genbc[16].speed
mailbox[0].number[32] = genbc[17].speed
mailbox[0].number[33] = genbc[18].speed
mailbox[0].number[34] = genbc[20].speed
mailbox[0].number[35] = genbc[23].speed
mailbox[0].number[36] = genbc[25].speed
mailbox[0].number[37] = genbc[27].speed
mailbox[0].number[38] = genbc[28].speed
mailbox[0].number[39] = genbc[29].speed
mailbox[0].number[40] = genbc[30].speed
mailbox[0].number[41] = genbc[31].speed
mailbox[0].number[42] = genbc[32].speed
endif

/* Printing the Generator angles */
for @i=0 to casepar[0].ngen - 1
     @x = genbc[@i].angle                                    /* Retrieving the
Generator angle at bus i */
     logprint($output, @x,">")
next

@ret = close ( $output )
```